Ice nucleation by feldspars and carbon nanomaterials

by

Thomas Francis Whale

Submitted in accordance with the requirements for the degree of Doctor of Philosophy

University of Leeds

School of Earth and Environment

April 2016

The candidate confirms that the work submitted is his own, except where work which has formed part of jointly-authored publications has been included. The contribution of the candidate and the other authors to this work has been explicitly indicated below. The candidate confirms that appropriate credit has been given within the thesis where reference has been made to the work of others. The work in chapters two to six of the thesis has appeared in the following publications:

Whale, T. F., Murray, B. J., O'Sullivan, D., Wilson, T. W., Umo, N. S., Baustian, K. J., Atkinson, J. D., Workneh, D. A., and Morris, G. J. 'A technique for quantifying heterogeneous ice nucleation in microlitre supercooled water droplets', published in Atmospheric Measurement Techniques (2015). This publication forms chapter two. The technique described was conceived by myself and BJM. I conducted the majority of developmental and experimental work. Experimental design and development was assisted by all the co-authors. TWW and DAW conducted some experiments on NX illite. GJM, my industrial supervisor, provided expertise relating to the use of the EF600 Stirling cryocooler used in the µl-NIPI. I wrote the paper with BJM which was commented on by all co-authors.

Whale, T. F., Rosillo-Lopez, M., Murray, B. J., and Salzmann, C. G. 'Ice nucleation properties of oxidized carbon nanomaterials', published in the Journal of Physical Chemistry Letters (2015). This publication forms chapter three. I conceived the work described and conducted all ice nucleation experiments. MR-L synthesised and characterised the carbon nanomaterials. BJM and CGS supervised myself and Martin respectively and helped with experimental design. I wrote the paper, with the assistance of all the coauthors.

Harrison, A. D., Whale, T. F., Carpenter, M. A., Holden, M. A., Neve, L., O'Sullivan, D., Vergara Temprado, J., and Murray, B. J. 'Not all feldspar is equal: A survey of ice nucleating properties across the feldspar group of minerals' submitted for review in Atmospheric Chemistry and Physics Discussions (2016). This publication makes up chapter four. ADH and myself are joint first authors on this paper. I designed the study in conjunction with BJM. I sourced the samples with the intention of conducting a survey of ice nucleation by feldspars. Together with BJM, I supervised ADH who conducted many of the experiments together with me during an undergrad summer placement. MJC supplied samples and expertise relating to feldspar mineralogy. MAH conducted experiments on one feldspar sample. LN performed powder X-ray diffraction analysis of some samples. JVT

wrote the computer program used for calculating error bars. I wrote the paper in conjunction with BJM and ADH.

Whale, T. F., Holden M. A., O'Sullivan, D., Wilson, T.W., Harrison A. D., Murray B. J. 'The microtexture of alkali feldspar is important for its ice nucleating ability' in preparation for submission to Physical Chemistry Chemical Physics. The manuscript for this submission forms Chapter five. I designed and performed all experiments. All co-authors contributed to the ideas in the paper. I wrote the paper with the assistance of BJM. Professor Mark Hodson kindly supplied most of the feldspar samples used in this study.

Whale, T. F., Wilson, T.W., Murray B. J. 'The enhancement and suppression of immersion mode heterogeneous ice nucleation by solutes' in preparation for submission to Chemical Communications. The manuscript for this submission forms chapter six. The enhancement and suppression of immersion mode heterogeneous ice nucleation by solutes' by Thomas F. Whale, Theo W. Wilson and Benjamin J. Murray. I conceived and designed the experiments with assistance from TWW. I performed all experiments. I wrote the paper with the assistance of BJM.

Acknowledgements

I would like to thank my supervisors, Benjamin Murray, Stephen Dobbie and John Morris for their guidance, support and patience during this project. I also express my gratitude to all those who have been part of the Murray research group throughout my studies for their help and company: Theo Wilson, Daniel O'Sullivan, Mark Holden, Ross Herbert, Tamsin Malkin, Jim Atkinson, Kelly Baustian, Hannah Price, Nsikanabasi Umo, Alex Harrison and Blue Jenkins.

I thank all the many friends and family who have helped me through this project. In particular I thank my parents, Michael and Victoria Whale, for their love and support.

Finally, I gratefully acknowledge financial assistance provided by the National Environmental Research Council and Asymptote Ltd.

Abstract

Immersion mode heterogeneous ice nucleation is the crucial first step in the glaciation of mixed-phase clouds, which have an important but poorly understood influence on global climate. Additionally, immersion mode ice nucleation plays an important role in the cryopreservation of biological material. At present, this important process is not well understood, hindering progress in these fields. In particular, it is not clear what physical and chemical properties cause a substance to nucleate ice well. The first section of this project describes the development and testing of a new droplet 1 µL volume droplet freezing assay. This instrument is a fast and effective tool for evaluating the ice nucleating efficacy of relatively large quantities of a given nucleator compared to instruments that use droplets of a size that are typically present in clouds. The rest of the thesis describes the characterisation of a series of nucleators using this instrument, with the aim of improving understanding of immersion mode ice nucleation.

Four types of carbon nanomaterial were investigated; all were found to nucleate ice in the immersion mode. This included graphene nanoflakes, which are among the smallest entities that have been found to nucleate ice. Surprisingly, more oxidised nanomaterials did not nucleate ice more efficiently than less oxidised ones.

Following on from previous work which found that feldspars nucleate ice more efficiently than other minerals, it was shown that alkali feldspars nucleate ice much more efficiently than plagioclase feldspars. The structures of alkali and plagioclase feldspars are similar so the large difference observed is surprising. In order to probe the reasons behind these observations we tested a range of alkali feldspar of known microtexture. It was found that those lacking microtexture nucleate ice similarly to plagioclase feldspars showing that a feature associated with microtexture (and therefore not directly related to the chemical or crystallographic structure of alkali feldspar) plays an important role in ice nucleation.

Finally, it was shown that ice nucleation by feldspars and quartz is significantly enhanced by the presence of ammonium salts and deactivated by several alkali halides. Some other nucleators were found to be unaffected. This provides a possible route for learning more about the mechanism of ice nucleation by different nucleators.

Table of Contents

List of Tables

List of Figures

List of Abbreviations

ATD	Arizona Test Dust
BET	Brunauer–Emmett–Teller surface area
CCN	Cloud Condensation Nuclei
cx-GNF	Carboxylated Graphene Nanoflakes
CFDC	Continuous Flow Diffusion Chamber
CNT	Classical Nucleation Theory
CPA	Cryoprotectant agent
FROST	Framework for Reconciling Observable Stochastic Time-dependence
GO	Graphene Oxide
INP	Ice Nucleating Particle
IPCC	Intergovernmental Panel on Climate Change
LDN	Leaf Derived Nuclei
MCSM	Multiple Component Stochastic model
o-MWCNTS	Oxidized Multiwall Carbon Nanotubes
o-SWCNTs	Nxidized singlewall Carbon Nanotubes
XPS	X-ray photoelectron spectroscopy
µl-NIPI	microlitre Nucleation by Immersed Particle Instrument

1. Introduction

1.1. The importance of ice nucleation

At atmospheric pressure ice I_h is the thermodynamically stable form of water below 0°C. Pure water does not freeze at 0°C because the stable phase must nucleate before crystal growth can occur. Liquid water can supercool to temperatures below -35°C (Riechers et al., 2013;Herbert et al., 2015) before ice nucleation occurs homogenously. In most real-world situations ice nucleation is induced by a heterogeneous ice nucleating particle (INP). Ice nucleation is an important process in the atmosphere and in biological cryopreservation processes. Despite decades of research heterogeneous ice nucleation remains poorly understood. Given the importance and ubiquity of the water-ice phase transition, a greater understanding of the process is of both practical and fundamental interest. It is primarily this lack of understanding which this project seeks to address. This introduction starts with a description of the modes of heterogeneous ice nucleation followed by a discussion of the impact that heterogeneous ice nucleation has on the atmosphere and cryobiology, aiming to provide background and motivation for the work contained in later chapters.

1.1.1. Modes of heterogeneous ice nucleation

There are multiple conceivable pathways by which ice can form on a heterogeneous INP, known as modes. There has been some controversy about the terminology used to describe modes of ice nucleation. In particular, the definitions of Vali (1985) and Pruppacher and Klett (1997) were subtly different, leading to some confusion. Vali et al. (2014) have led an online discussion by the community on ice nucleation terminology and published the outcome (Vali et al., 2015). It is these definitions that are outlined here and used throughout this work.

The two overarching modes of ice nucleation are deposition and freezing. Deposition ice nucleation is defined as ‘Ice nucleation from supersaturated vapor on an INP or equivalent without prior formation of liquid’ (a gas to solid phase transition). Freezing nucleation is defined as ‘Ice nucleation within a body of supercooled liquid ascribed to the presence of an INP, or equivalent’ (a liquid to solid phase transition). Freezing nucleation is further subdivided into immersion freezing, where the INP is immersed in liquid water, contact freezing, where freezing is initiated at the air-water interface as the INP comes into contact with supercooled liquid water and condensation freezing, where freezing takes

place concurrently with formation of liquid water. It is difficult to differentiate condensation freezing from both deposition nucleation and immersion freezing as the microscopic mechanism of ice formation is not known in most cases. It is quite possible that many, most or all cases of deposition nucleation are preceded by formation of microscopic quantities of water which then freezes, followed by depositional growth (Marcolli, 2014). It is known that this sort of mechanism occurs for organic vapours (e.g (Campbell et al., 2013;Kovács et al., 2012)). Equally, it is not clear how condensation freezing should be differentiated from immersion freezing in cases where liquid water does form prior to freezing (which may be most or all cases). This project is solely concerned with immersion mode ice nucleation where particles are clearly immersed in water. The following sections describe the relevance of immersion mode ice nucleation to the atmosphere and cryobiology.

1.1.2. Atmospheric Ice nucleation

Clouds consist of water droplets or ice crystals, or a mixture of both, suspended in the atmosphere. They play a key role in climate. By interacting with incoming shortwave radiation and outgoing longwave radiation they can impact the energy budget of the earth. They also play a key role in the earth's hydrological cycle by controlling water transport and precipitation (Hartmann et al., 1992). The magnitude of the effect of clouds on the global energy budget is highly uncertain (Lohmann and Feichter, 2005) although the latest Intergovernmental Panel on Climate Change (IPCC) report suggests a net cooling effect from clouds of -20 W m^{-2} (Boucher et al., 2013).

Much of this uncertainty stems from the poorly understood nature of interactions between atmospheric aerosol and clouds (Field et al., 2014). Atmospheric aerosol consists of solid or liquid particles suspended in the air. There are many different types of aerosol in the atmosphere. Primary aerosol is emitted directly from both natural and anthropogenic sources as particles and includes mineral dust, sea salt, black carbon and primary biological particles. Secondary aerosol forms from gaseous precursors which are often emitted by plants and oceanic processes. Clouds form when moist air rises through the atmosphere and cools down. Typically, water droplets form on aerosol particles called cloud condensation nuclei (CCN), although there may be situations in cirrus clouds where ice apparently forms directly onto INPs via deposition mode ice nucleation (Pruppacher and Klett, 1997).

As the majority of clouds are formed via processes involving aerosol particles cloud properties such as lifetime, composition and size are highly dependent on the properties of the aerosol particles with which the cloud interacts. These effects are known as aerosol indirect effects (Denman et al., 2007). Cloud glaciation, which is dependent on the ice nucleation properties of the aerosol in clouds (Denman et al., 2007) is one of these effects. In the latest IPCC report these effects have been grouped together, and confidence in the assessment of the impact of aerosol-cloud interactions is rated as 'low'. The potential scale of the impact ranges from a very slight warming effect to cooling of 2 Wm^{-2} (Field et al., 2014).

There are two overarching categories of tropospheric clouds in which ice nucleation is most relevant. These are cirrus clouds and mixed-phase clouds. Cirrus clouds form in the upper troposphere at temperatures below -38°C, and consist of concentrated solution droplets, which can be frozen via immersion mode ice nucleation, or ice formed by deposition nucleation. Mixed-phase clouds form lower down in the troposphere between 0°C and about -38°C. Ice formation in these clouds is generally thought to be controlled by immersion mode ice nucleation (de Boer et al., 2011;Cui et al., 2006) although contact mode may also play a role (Ansmann et al., 2005).

Ice nucleation processes have the potential to alter mixed-phase cloud properties in several ways. Mixed-phase clouds occasionally supercool to temperatures where homogenous freezing is important, below about -35°C (Herbert et al., 2015) but generally glaciate at warmer temperatures (Ansmann et al., 2009;Kanitz et al., 2011). This indicates heterogeneous ice nucleation controls mixed-phase cloud glaciation in many cases. At -20°C about half of mixed-phase clouds globally are glaciated (Choi et al., 2010).

The presence of ice crystals in a cloud can change its radiative properties significantly compared to a liquid cloud and the size and concentration of ice crystals are also important (Lohmann and Feichter, 2005). Cloud thickness, spatial extent and lifetime can alter radiative forcing also and can potentially depend on INP concentration. Precipitation processes are closely linked to ice formation as ice I is more stable than liquid water below 0 °C. As such, ice particles in mixed-phase clouds tend to grow at the expense of supercooled liquid water droplets. This process is known as the Wegener-Bergeron-Findeisen process and is thought most important route for precipitation from mixed-phase clouds as larger particles will fall faster than smaller ones (Pruppacher and Klett, 1997). Clouds which contain relatively small ice crystal concentrations and more supercooled water are more likely to precipitate as the ice crystals can grow to larger sizes than they

might have if ice crystal concentrations were higher, as a result lifetime of these clouds might be shorter than it would otherwise have been. Additionally, ice multiplication processes can result from the fragmentation of ice formed through primary ice nucleation processes and increase the concentration of ice crystals in clouds by several orders of magnitude (Phillips et al., 2003). The best understood of these is the Hallett-Mossop process which occurs from -3 °C to -8 °C (Hallett and Mossop, 1974) although other processes have also been posited (Yano and Phillips, 2011). All these various processes, and others, interact in complex and generally poorly understood ways, contributing the large uncertainty on the radiative forcing due to aerosol-cloud interactions (Field et al., 2014). These interactions between aerosol, clouds and liquid in mixed phase clouds need to be understood quantitatively to properly understand and assess the impact of clouds on climate and weather. However, the current lack of fundamental understanding of the heterogeneous ice nucleation process is a severe impediment to improving understanding of this important uncertainty (Slater et al., 2015).

1.1.3. Cryopreservation

Cryopreservation is a process where biological material, cells or tissues, are preserved by cooling to temperatures lower than those at which normal biological function takes place. Sufficiently low temperatures can prevent cell damage by stopping or slowing enzymatic and chemical activity thereby allowing samples to be stored for long periods and used when desired. Temperatures below -100°C are generally regarded as being low enough to prevent damage in the practical long term (Fuller et al., 2004). There are a great many routine applications of cryopreservation techniques including biobanking (De Souza and Greenspan, 2013), preservation of gametes for reproductive medicine (Fuller and Paynter, 2004) and preservation of animal gametes for farming (Barbas and Mascarenhas, 2008) and also many emerging fields where cryopreservation is of vital importance such as regenerative medicine (Asghar et al., 2014). There are two main methods of cryopreservation, controlled rate freezing and vitrification. Ice nucleation is an important process in both methods.

Controlled rate freezing procedures preserve cells and tissues by cooling at a ‘slow’ rate in the vicinity of 1°C min^{-1} from biological temperatures to around -20°C, sometimes with a plateau in cooling to allow for nucleation to take place. Once a temperature of -20°C or so is reached cooling is accelerated to colder temperatures, usually either -80°C in a freezer or -196°C in liquid nitrogen, depending upon the method being used for long term storage.

The principle on which such controlled rate freezing procedures are based is the ‘two factor hypothesis of freezing injury’ proposed by Mazur et al. (1972). This says that if cells are cooled too quickly nucleation tends to take place inside the cells being frozen. The needle-like growth habit of crystalline ice means that intra-cellular ice formation is almost invariably fatal to the cell (Mazur et al., 2005;Morris and Acton, 2013). If cooling is conducted slowly and ice is present externally to the cells the cell interiors can dry out by osmosis and eventually solidify into a survivable, non-crystalline state. However, if cooling is conducted too slowly, injury due to other factors can occur. It is generally thought that if cells dry out too much, high concentrations of internal and external electrolytes can cause fatal damage (Lovelock, 1953;Fuller and Paynter, 2004).

In the ideal situation ice is nucleated externally to the cells undergoing cryopreservation at a temperature as close to the melting point of the cryopreservation medium used as possible. This maximises the amount of time available for the interior of the cell to dry out during the rest of the slow cooling procedure, while still allowing solidification to proceed quickly enough to avoid cell damage. Very often, controlled rate freezing is conducted without any effort to encourage freezing externally to cells. As such ice will nucleate on whatever is the most efficient nucleator in the cryopreservation system, which may well be inside cells. It may also be that this nucleation occurs at relatively low temperatures, leading to slow, inadequate diffusion of water out of cells. It has been demonstrated that in many cases, although not all, deliberate nucleation of extra-cellular ice can improve cell survival rates substantially (Morris and Acton, 2013).

Cryoprotectant agents (CPAs) are soluble molecules such as glycerol, dimethyl sulfoxide, polyols, sugars and salts that are added to cryopreservation systems to improve outcomes. CPAs are known to be beneficial in the vast majority of cases (Fuller et al., 2004), but it is not always clear by what mechanism they work. All CPAs interact strongly with water and tend to increase viscosity. This may help to insulate membranes from high concentrations of electrolytes (Fuller et al., 2004;Fuller, 2004). It is also thought that certain CPAs may inhibit intracellular ice formation (Towey and Dougan, 2012).

Much is still unknown about ice nucleation in these systems. A better understanding of what causes ice nucleation inside and outside cells would allow for design of superior cryopreservation systems. From a practical perspective, efficient ice nucleators are of use in ensuring that ice nucleation in media surrounding cells takes place at warmer temperatures (Morris and Acton, 2013).

An alternative cryopreservation procedure is vitrification. Vitrifcation procedures rely on using very high cooling rates (ideally thousands of degrees per minute) and very high concentrations of cryoprotectants to completely avoid ice nucleation in and around the cells undergoing cryopreservation (Rall and Fahy, 1985;Fahy et al., 1984). Instead of crystalline ice forming, viscosity of the cell contents and the cell surroundings increases to the point that a glassy solid is formed before ice nucleation has the opportunity to take place. This state is very often survivable for cells and the method is routinely used to freeze humans eggs and embryos (Kuleshova, 2009). Again, the key point of the procedure is avoidance of ice nucleation (Fuller et al., 2004) , so improved knowledge of the mechanism and causes of heterogeneous ice nucleation is also important here.

Freeze drying (also known as lyophilisation) is used in the preparation and preservation of a wide range of substances. This includes drug molecules (Tang and Pikal, 2004), vaccines (Hansen et al., 2015) and various types of living cells (Fuller et al., 2004). Freeze drying is conducted by freezing a liquid sample and subliming off the vast majority of the ice content of the sample under vacuum. This stabilises the product left behind allowing for long term storage. A key determinant of the drying rate is the size of subliming ice crystals, which is controlled by the temperature of ice nucleation (Searles et al., 2001). It is thought that this is because nucleation at the bottom of the vials used for freeze-drying, prior to the supercooling of liquid higher up the vial, promotes the formation of large columnar ice crystals which sublime more quickly than smaller ice crystals that form when nucleation takes place from a deeper state of supercooling. As such, improved control of nucleation temperature has the potential to improve broth the quality of freeze-dried products and the rate at which they can be produced (Kasper and Friess, 2011;Searles et al., 2001).

1.2. Experimental methods for examining ice nucleation

The majority of quantitative studies of how efficiently a particular material nucleates ice have been conducted with the goal of determining what species nucleate ice in the atmosphere. The atmospheric community has employed a wide variety of techniques. There are two overarching families of techniques for determining the immersion mode ice nucleating efficiency of nucleators. These are wet dispersion methods and dry dispersion methods (Hiranuma et al., 2015). Wet dispersion methods involve dispersion of INPs into water which is then frozen. Dry dispersion methods involve the dispersion

of aerosol particles into air, where they are then activated into water droplets before freezing. Techniques have also been divided into those which use droplets supported on surface or suspended in oil and those which use droplets suspended in gas (Murray et al., 2012) which are largely synonymous with wet and dry dispersion techniques, respectively. Almost invariably, ice nucleation data takes the form of a fraction of droplets frozen under a given set of conditions. Typical variables are temperature, cooling rate, droplet size, and nucleator identity and concentration in droplets.

1.2.1. Wet dispersion methods

Most wet dispersion techniques are droplet freezing experiments, also known as droplet freezing assays. These involve dividing a sample of water into multiple sub-samples and cooling these individual samples down until they freeze. For studies of heterogeneous ice nucleation a nucleator is suspended in the water prior to sub-division, or pure water droplets are placed onto a nucleating surface. The temperature at which droplets freeze is recorded, typically by simultaneous video and temperature logging. Different droplet volumes have been used, ranging from millilitres to picolitres (Vali, 1995;Murray et al., 2012). Droplets are typically either placed on hydrophobic surfaces (e.g (Murray et al., 2010;Lindow et al., 1982)) or in wells or vials (e.g (Hill et al., 2014)). In these cases freezing is usually observed visually, often through a microscope. Emulsions of water droplets in oil can also be frozen, and freezing events recorded via microscope (e.g. (Zolles et al., 2015)) or using a calorimeter (Michelmore and Franks, 1982). Recently, microfluidic devices have been used to create mono-disperse droplets for studying ice nucleation (Stan et al., 2009;Riechers et al., 2013).

Droplet freezing techniques typically use linear cooling rates, although isothermal experiments have also been conducted (Herbert et al., 2014;Broadley et al., 2012;Sear, 2014). Larger droplets up to millilitre volumes have typically been used for investigations of biological ice nucleators while the smallest droplets have been used for studies of homogeneous ice nucleation. The majority of studies of atmospherically relevant INPs have been conducted using smaller, nano- to picolitre sized droplets (Murray et al., 2012).

Other techniques that use wet dispersion to produce droplets include those that freeze single droplets repeatedly many times in order to establish the variation in freezing temperature in that single droplet (Barlow and Haymet, 1995;Fu et al., 2015). Wind tunnels are similar in that they support single suspended droplets in an upward flow of air of known temperature (Pitter and Pruppacher, 1973;Diehl et al., 2002). Freezing probabilities are determined by conducting multiple experiments. Droplets are typically

prepared by wet dispersion then introduced into the airflow but could also be dry dispersed. Similarly, droplets can be suspended by electrodynamic levitation (Krämer et al., 1999).

Gurganus et al. (2014;2013,2011) have developed a technique that seeks to identify the spatial location of nucleation events on a surface or object placed in a water droplet using high speed cameras with the object of determining if nucleation occurs preferentially at the triple point of contact between a surface, air and water. While this is not a wet dispersion technique as such it does freeze a single water droplet in a manner very similar to typical droplet freezing assays.

1.2.2. Dry dispersion methods

Cloud expansion chambers are large vessels in which temperature, humidity and aerosol contents are controlled, usually with the goal of simulating clouds (Niemand et al., 2012;Connolly et al., 2009;Emersic et al., 2015). Experiments involve pumping the chamber out to reduce temperature thereby inducing ice nucleation in the chamber. The ice nucleation efficiency of aerosols in the chamber can be determined from the appearance of ice crystals. In order to conduct experiments in the immersion mode the INPs must activate as CCN before ice nucleation occurs.

Continuous Flow Thermal Gradient Diffusion Chambers (CFDCs) flow air containing aerosols through a space where temperature and humidity are controlled using two plates coated in ice (Garimella et al., 2016;Stetzer et al., 2008;Rogers, 1988). Typically, aerosol size distributions and concentrations are characterised going into the area of controlled supersaturation with respect to ice and the number of ice crystals coming out the other end it also determined. In this way a droplet fraction frozen can be determined. Alternatively, a pre-conditioning section can be used to ensure that all aerosol particles prior are activated as CCN prior to entry to the ice nucleation section of the instrument, thereby ensuring that all freezing is immersion mode (Lüönd et al., 2010).

1.3. Nucleation theory

While there is no satisfactory overarching theory for nucleation phenomena (Sear, 2012) there are various theories and descriptions used to describe ice nucleation. This section describes theories and descriptions used for describing immersion mode ice nucleation data.

1.3.1. Homogeneous ice nucleation

Homogenous nucleation is nucleation which does not involve a heterogeneous nucleator. In the atmosphere cloud water droplets can supercool to temperatures below -35°C. While heterogeneous ice nucleation is probably more common in most mixed-phase clouds homogeneous nucleation is also thought to be a factor (Sassen and Dodd, 1988) and mixed phase clouds have been observed at sufficiently cold temperatures to support this (Choi et al., 2010;Kanitz et al., 2011). Given the great difficulty of avoiding heterogeneous nucleation of ice (Langham and Mason, 1958) it seems very unlikely that homogenous nucleation is a factor in other systems where ice nucleation has relevance (e.g. cryobiological). Many laboratory experiments have also investigated homogenous nucleation (Riechers et al., 2013;Murray et al., 2010;Stan et al., 2009) and it has been shown that classical nucleation theory (CNT) can describe laboratory data for homogenous nucleation well (Riechers et al., 2013).

1.3.1.1. Classical description of homogenous ice nucleation

The following is a derivation of CNT adapted from work by Pruppacher and Klett (1997), Mullin (2001), Debenedetti (1996) Murray et al. (2010) and Vali et al. (2015). Supercooling occurs because of a kinetic barrier to the formation of solid clusters large enough for spontaneous growth. This stems from the increasing energy cost of forming interface between ice and supercooled water as the size of a cluster grows. At the cluster size where the energy gain of adding a water molecule exceeds the energy cost of forming an interface between the ice and supercooled water spontaneous growth will occur. This can be expressed as:

$$\Delta \boldsymbol{G} = \Delta \boldsymbol{G_s} + \Delta \boldsymbol{G_V} \qquad 1.1$$

Where ΔG is the overall change in Gibbs free energy of the ice cluster, ΔG_s is the surface free energy between surface of the particle and the bulk of the supercooled water and ΔG_V is volume excess free energy. ΔG_s and ΔG_V are competing terms, ΔG_V being negative while ΔG_s is positive. G_s can be expressed as:

$$\boldsymbol{G_s = 4\pi r^2 \gamma} \qquad 1.2$$

Where r is the radius of the solid cluster and γ is the interfacial energy between ice and water. G_v can be expressed as:

$$\boldsymbol{G_v = \frac{4\pi r^3}{3v} k_B T \ln S} \qquad 1.3$$

Where v is the volume of a water molecule in ice, k_B is the Boltzmann constant, T is the temperature, and S is the saturation ratio with respect to ice. Adding equations 1.2 and 1.3 gives the total Gibbs free energy of the barrier to nucleation:

$$\Delta G = -\frac{4\pi r^3}{3v} k_B T \ln S + 4\pi r^2 \gamma \qquad 1.4$$

The two terms of equation 1.4 are opposing so the free energy of ice formation passes through a maximum, as shown in Figure 1.1. The maximum value corresponds to the size of the critical nucleus, r_i^*.

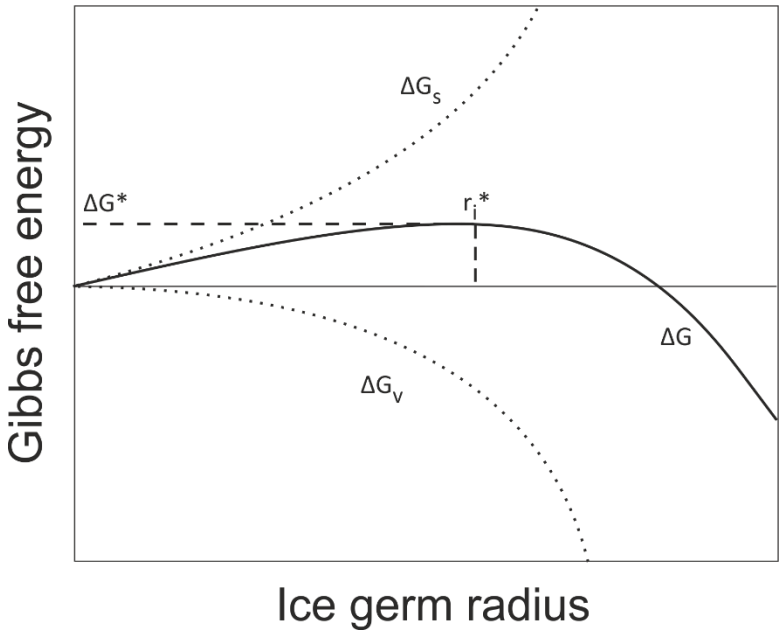

Figure 1.1 Schematic of ice germ radius against Gibbs free energy.

Critical nucleus size can be calculated by differentiating equation 1.4 with respect to r_i^* and setting $d\Delta G/dr_i=0$ before rearranging for r_i yields:

$$r_i^* = \frac{-2\gamma v}{k_B T \ln S \Delta G_v} \qquad 1.5$$

Equation 1.5 can be used to calculate the temperature dependence of critical radius size. S can be calculated using parameterisations from Murphy and Koop (2005) along with the value for γ from Murray et al. (2010). It can be seen that the size of the critical nucleus increases sharply with rising temperature in Figure 1.2.

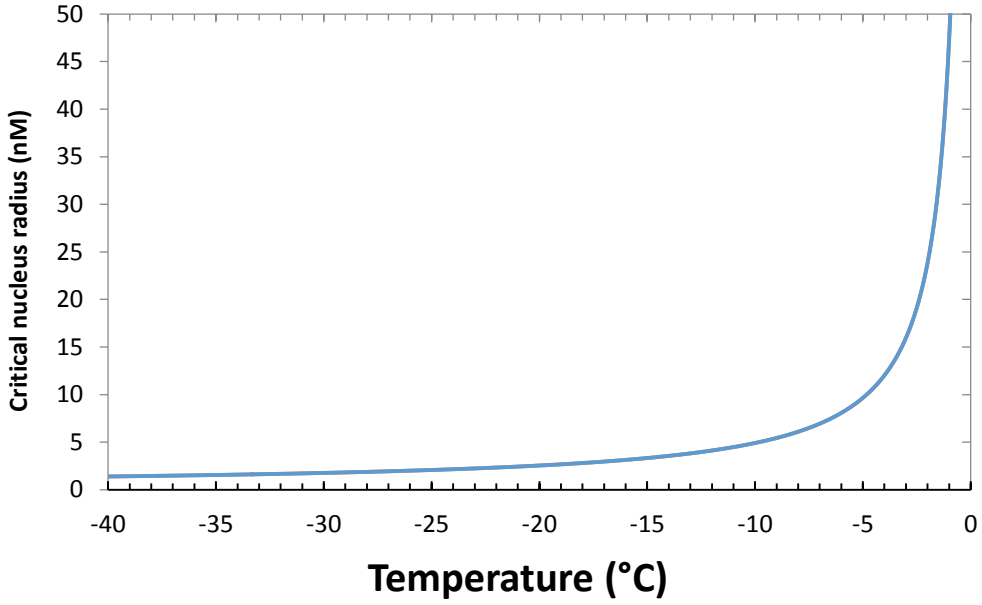

Figure 1.2: Critical radius size for Ice I_{sd} as a function of temperature.

By substituting back into equation 1.4, ΔG^* at temperature T can be calculated:

$$\Delta G^* = \frac{16\pi\gamma^3 v^2}{3(k_b T \ln S)^2} \qquad 1.6$$

To determine nucleation rate, the Arrhenius style equation 1.7 can be applied.

$$J_{hom} = A \exp(-\frac{\Delta G^*(T)}{kT}) \qquad 1.7$$

J_{hom} is the nucleation rate, A is the pre-exponential factor and k the Boltzmann constant. Combining equations 1.6 and 1.7 equation 1.8 can be written down.

$$\ln J_{hom} = \ln A - \frac{16\pi\gamma^3 v^2}{3k^3 T^3 (\ln S)^2} \qquad 1.8$$

Hence, a plot of $\ln J_{hom}$ against $T^{-3}(\ln S)^{-2}$ will be linear with an intercept of ln A and, over a narrow temperature range, slope:

$$m = -\frac{16\pi\gamma^3 v^2}{3k^3} \qquad 1.9$$

Since v is known this allows γ to be determined from experiments determining J_{hom}.

J_{hom} has units of nucleation events cm^{-3} s^{-1}. In larger volumes of water nucleation is therefore more probable. In an experiment looking at a large number of identical droplets held a constant temperature where a single nucleation event within a droplet is assumed to lead to crystallisation of that droplet a freezing rate *R(t)* can be determined. *R(t)* is a purely experimental value that has units of events s^{-1}. It can be determined for any droplet freezing experiment, heterogeneous or homogeneous. Application to heterogeneous experiments is discussed in section 1.3.2. *R(t)* can be calculated using:

$$R(t) = \frac{1}{N_0 - N_F}\frac{\mathrm{d}N_F}{\mathrm{d}t} \qquad 1.10$$

Where N_F is the total number of frozen droplets at time t and N_0 is the total number of droplets present, frozen or unfrozen. If V is the volume of the droplets equation 1.11 can be written down.

$$J_v = \frac{R(t)}{V} \qquad 1.11$$

Where J_v is the volume nucleation rate. if the droplets are free of impurities so that nucleation is via the homogenous mechanism then:

$$J_{hom} = J_v = \frac{R(t)}{V} \qquad 1.12$$

Following on from this, for constant temperature the fraction of droplets N_L that remains unfrozen at time *t* can therefore be calculated using:

$$N_L = N_0 \exp(-J_{hom} V t) \qquad 1.13$$

Experimental data from droplet freezing experiments can therefore be used to calculate interfacial tension using equations 9 and 10. In cases where droplets are constantly cooled, rather than being held at a steady temperature to small increments of it is necessary to apply equation 1.13 to small time intervals over which changes in temperature are small. In this way $J_{hom}(T)$ can be determined.

1.3.2. Heterogeneous ice nucleation

Heterogeneous ice nucleation takes place when an external entity lowers the energy barrier preventing ice nucleation. As a result the probability of a nucleation event occurring at any given supercooled temperature or supersaturation with respect to ice becomes higher. The observed outcome is that heterogeneous ice nucleation takes place at higher temperatures than homogenous ice nucleation in otherwise equivalent systems. Different nucleators nucleate ice with varying efficiency (Murray et al., 2012;Hoose and

Möhler, 2012). It is also important to note that there are different modes of heterogeneous ice nucleation as discussed in section 1.1.1. The following sections detail methods for describing immersion mode heterogeneous ice nucleation efficiency.

1.3.2.1. Application of CNT to Heterogeneous Nucleation

In classical nucleation theory the temperature dependent heterogeneous nucleation rate coefficient can be related to the energy difference by:

$$J_{het}(T) = A_{het}\exp(-\frac{\Delta G^{*}\varphi}{kT}) \qquad 1.14$$

Where A_{het} is a constant and φ the factor by which the heterogeneous energy barrier to nucleation is lower than the homogenous barrier. This equation is identical to equation 1.7, except that the height of the energy barrier is lowered by a factor φ calculated using:

$$\varphi = \frac{(2+\cos\theta)(1-\cos\theta)^2}{4} \qquad 1.15$$

Where θ is the contact angle between a spherical ice nucleus and a flat surface of the nucleator. It is possible to calculate contact angles if $J_{het}(T)$ is known therefore. It is not clear what contact angles mean physically although they give an indication of a material's ice nucleating ability

1.3.2.2. Single Component Stochastic Models

The simplest CNT based models are a type of single component stochastic (SCS) model. $J_{het}(T)$ is usually measured per surface area of nucleator meaning it has units of events cm^{-2} s^{-1}. These models use a single nucleation rate (J_{het}) to describe a nucleator's behaviour. J_{het} is in principle calculated in the same way as J_{hom} from equation 1.10 except that a rate per surface area of nucleator, J_s is used:

$$J_{het} = J_s = \frac{R(t)}{A} \qquad 1.16$$

J_{het} can be related to CNT as described as in section 1.3.2.1 (e.g (Chen et al., 2008)) to account for temperature dependence of J_{het} but a simple linear temperature dependence can also be used (e.g. (Murray et al., 2011)).

These models are not usually appropriate as they assume that all droplets in an experiment nucleate ice with the same rate. Although there are examples of nucleators which show good agreement with a single component model, notably KGa-1b kaolinite (Herbert et al., 2014;Murray et al., 2011) it is clear that this is not the case for many materials. J_{het}

often does not equal *R/A* (Herbert et al., 2014;Vali, 2014, 2008). As a result, various other models of ice nucleation have been developed. Multiple component stochastic models are an extension of single component models.

1.3.2.3. Multiple component stochastic models

Multiple stochastic models (MCSMs) have been developed to describe the observed variation in nucleation rates between droplets. These models divide a population of droplets, or sites, into sub-populations with different single component rates. There are a number of different variations on this theme. Some use distributions of efficiencies described by CNT (Lüönd et al., 2010;Marcolli et al., 2007;Niedermeier et al., 2011;Niedermeier et al., 2014), while others use linear dependences (Broadley et al., 2012). All use multiple different curves, representing different sites, droplets or particles and sum the freezing probabilities of all these to generate a total nucleation rate at a given temperature. Such descriptions therefore retain time dependence as well as accounting for variability between droplets.

1.3.2.4. Singular models

Singular models of ice nucleation assume that each droplet in an ice nucleation experiment contains a site that induces it to freeze at a specific 'characteristic' temperature (Vali and Stansbury, 1966).The justification for this approach is that it is typically observed that variability in freezing temperature for a single droplet frozen and thawed multiple times is generally much smaller than the range in freezing temperature of a population of droplets with identical nucleator content (Vali, 2008;Vali and Stansbury, 1966). The concept was originally put forward by Levine (1950).Typically, concentration of sites is related to either droplet volume or surface area of nucleator. The 'differential nucleus spectrum', $k(T)$, which can be calculated from the output of ice nucleation experiments using:

$$k(T) = \frac{1}{V.(N_0 - N_F(T))} . \frac{dN_F(T)}{dT} \qquad 1.17$$

Where V is the droplet volume used in the experiment, N_0 is the total number of droplets in the experiment and $N_f(T)$ is the number of droplets frozen at temperature T. By integrating this expression the cumulative nucleus spectrum, $K(T)$ can be derived:

$$K(T) = -\frac{1}{V} . \ln\left(1 - \frac{N_F(T)}{N_0}\right) \qquad 1.18$$

$K(T)$ has dimensions of sites per volume. Recently, it has become common to determine the surface area of nucleator contained in each droplet in order to calculate the ice active

site density $n_s(T)$, which is a measure of the number of sites per unit surface area of nucleator (Connolly et al., 2009). $n_s(T)$ is related to $K(T)$ by:

$$n_s(T) = \frac{K(T)}{A} \quad 1.19$$

Where A is the surface area of nucleator per droplet. To calculate $n_s(T)$ directly from droplet experimental data the following expression can be used:

$$n_s(T) = -\frac{1}{A}\ln(1 - \frac{N_F(T)}{N_0}) \quad 1.20$$

Site specific models of ice nucleation can also conceivably use other units besides nucleator surface area and droplet volume, for instance, number of nucleation sites per cell or per particle can be calculated, if the number of these entities per droplet is known.

Singular models ignore time dependence. According to a site-specific model at constant temperature no freezing will take place. This is generally not the case but it is often true that freezing does not follow the sort of exponential decay that would be predicted by a single component model (Sear, 2014).

1.3.2.5. The Framework for Reconciling Observable Stochastic Time-dependence (FROST)

To overcome the difficulty that simple site-specific models do not account for time dependence 'modified singular' models can be used (Vali, 2008;Vali, 1994). If two identical sets of droplets (identical meaning that the two sets contain the same surface area of nucleator) are cooled at different rates a greater fraction of the droplets that are cooled more slowly will be frozen at a given relevant temperature. This is because time dependence of ice nucleation will mean that every droplet has a greater probability of freezing in the longer time interval allowed to it by the slower cooling rate, compared to the faster cooling rate. Modified singular models incorporate a factor that accounts for shifts induced by differing cooling rates into typical site-specific expressions for ice nucleation. The Framework for Reconciling Observable Stochastic Time-dependence (FROST) derived by Herbert et al. (2014) is similar to the modified singular approach which allows ice nucleation data obtained from experiments conducted at different ramp rates, or in isothermal conditions to be reconciled. The shift in freezing temperature between two experiments conducted at cooling rates r_1 and r_2 can be calculated using:

$$\Delta T_f = \beta = \frac{1}{\lambda}\ln\left(\frac{r_1}{r_2}\right) \qquad 1.23$$

Where β is the shift in freezing temperature caused by the change in cooling rate and λ is the slope, –dln(J)/dT , of the individual components in the MCSM of Broadley et al. (Broadley et al., 2012) and Herbert et al. (2014). This equation can be used to calculate λ from experimental fraction frozen data. A similar quantity, ω, is defined as the gradient –dln(R/A)/dT. Herbert et al. (2014) showed using computer simulations that when $\omega = \lambda$ a single component stochastic model can be applied. When $\omega \neq \lambda$ there is variation in the nucleating ability of droplets in the experiment and a MCSM must be used to account for data. Figure 1.3 shows why this is. λ can be regarded as a fundamental property of a nucleator.

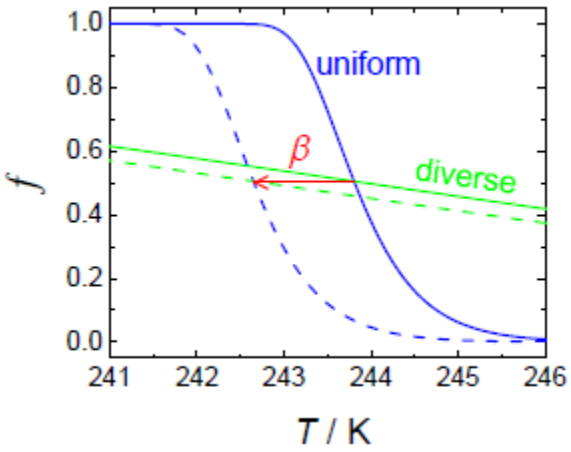

Figure 1.3: Comparison between diverse and uniform nucleators. The shift in freezing temperature, β, depends on λ, the slope of single components that make up the total nucleation rate for the experiment (Equation 1.23). In the diverse case, where there are many particles with different nucleating efficiencies the shallow slope of the fraction frozen curve means that little change in the value of fraction frozen is observed even though β is the same as in the uniform, single component case. Figure from Herbert et al. (2014).

FROST can be used to reconcile $n_s(T)$ from experiments conducted at different ramp rates by substituting fraction frozen values calculated using equation 1.23 into equation 1.20. If a standard r_1 value of 1 °C min^{-1} it can be shown that:

$$\frac{N_F(T,r)}{N_0} = 1 - \exp\left(-n_s\left(T - \frac{\ln r}{-\lambda}\right).A\right) \qquad 1.24$$

Where $N_F(T,r)$ is the number of droplets frozen at temperature T for an experiment conducted at ramp rate r. This equation is compatible with the modified singular model

of Vali (1994). Typical modified singular approaches use an empirical shift from experimental data in temperature instead of λ.

By performing multiple experiments Herbert et al. (2014) showed that FROST could account for experimental data. Four sets of experiments conducted at four different ramp rates could be reconciled with single λ value for two different nucleators. For KGa-1b kaolinite this λ was equal to its ω value while for BCS 376 microcline this was not the case, meaning that a single component model could be used to describe ice nucleation by KGa-1b but not BCS 376.

1.3.2.6. Comparison and summary of models of heterogeneous nucleation

Heterogeneous ice nucleation is, in the majority of cases, a phenomenon with both site-specific and time dependent characteristics. For most experiemnts it is likely that individual droplets in freezing experiments contain many sites which nucleate ice more efficiently than the majority of the nucleator surface area, one which may nucleate ice more efficiently that all others sites in the droplet, as assumed by the site-specific model. Ice nucleation at sites is likely to be stochastic, and may be well described by a single component stochastic model, possibly by classical nucleation theory with a suitably reduced free energy barrier height. As the specific mechanism of heterogeneous ice nucleation is not known it cannot be said that this is the case.

There is little reason to suppose that classical nucleation theory as applied to heterogeneous nucleation is valid for the nucleation of ice. It is generally acknowledged that the contact angle used in equations 1.14 and 1.15 has no physical meaning and serves as a proxy for lowering the height of the free energy barrier calculated by CNT at a given temperature. Clearly, site-specific models are also unphysical insofar as ice nucleation is to some extent stochastic. No experiment has found that droplets repeatedly freeze at the exact same temperature.

Site-specific models account for the strong temperature dependence observed in nucleation by most nucleators while single component stochastic models account for the time dependence. They ignore time dependence and droplet to droplet variability in nucleation efficiency respectively. The various multiple component stochastic models and time dependent site-specific models seek to add the facet of the problem that the simple models do not account for.

Ultimately, none of these models of ice nucleation offer real insight into the underlying mechanism of ice nucleation (Vali, 2014). Multiple component stochastic models generally provide the best fit to experimental data, which is not surprising as they have the most degrees of freedom. They are, in a sense, fitting routines. That said, they are probably also the most physically realistic model of ice nucleation. Generally, it is convenient to use site specific models as temperature dependence is the overriding determinant of freezing rate. Many, recent studies have tended to determine n_s as a means of comparing ice nucleating species. Agreement is not universal however, for instance efforts have been made to explain the variation in freezing rate between the individual droplets in experiments as a product of variations in the amount of material between different droplets (Alpert and Knopf, 2016).

1.4. What makes a good heterogeneous ice nucleator?

This section deals with the question of what causes a nucleator to nucleate ice well. Why should one substance nucleate ice more efficiently than another? There is no clear answer to this question at this time. To start to address the question the next section consists of a summary of those substances that are known to nucleate ice.

1.4.1. What is known to nucleate ice?

The majority of studies of immersion mode heterogeneous ice nucleation have been conducted with the aim of understanding and quantifying ice nucleation by substances that might nucleate ice in the atmosphere. Extensive reviews are available (Murray et al., 2012;Hoose and Möhler, 2012). The following section details these substances.

Large amounts of mineral dusts are emitted to into the atmosphere, mostly from arid regions in Africa and Asia (Prospero et al., 2002). It has, for many years, been known that snow crystals contain mineral dust residues (Kumai, 1961). and more recent work has found that mineral dusts make up a large proportion of ice crystal residues in certain cloud types (Pratt et al., 2009;Murray et al., 2012). There is a volume of older work on ice nucleation by mineral dusts (Pruppacher and Klett, 1997). In many of these cases only onset freezing temperatures are recorded and it is therefore difficult to assess the relative efficiency of freezing. Recently, n_s values for a range of natural mixed dusts have been calculated (Niemand et al., 2012;Connolly et al., 2009) as well as for proxies of natural

dusts such as NX illite and Arizona test dust (ATD) (Broadley et al., 2012;Connolly et al., 2009;Marcolli et al., 2007).

Until recently it had been thought that clay minerals were responsible for the ice nucleation activity of mineral dusts (Lüönd et al., 2010;Pinti et al., 2012;Pruppacher and Klett, 1997), partially on the basis of kaolinite's lattice match to hexagonal ice (see 1.4.2.3 for a discussion of lattice matching) (Pruppacher and Klett, 1997). Atkinson et al. (2013) have recently shown that feldspars nucleate ice far more efficiently than the other major components of mineral dusts and that they are likely to be responsible for much of the ice nucleation observed in mixed phase clouds in various regions of the world.

The ice nucleation activities of a wide range of biological entities has been investigated in the past. The starting point for much of this work was the discovery by Schnell and Vali (1972) that decomposing leaf matter induced freezing at higher temperatures than any other nucleator they tested. It was discovered that the efficient nucleator was associated with the bacterium *pseudomonas syringae*, (Maki et al., 1974;Lindow et al., 1989) a plant pathogen. It is generally thought that the efficient ice nucleation of *pseudomonas syringae* allows it to ingest nutrients from plants at temperature just below the melting point of water where the plants would usually avoid frost damage by supercooling. Since the discovery of the ice nucleation activity of *pseudomonas syringae* many other bacteria have been shown to nucleate ice at high temperatures (Lee Jr et al., 1995).

Other biological ice nucleators include fungi (Pouleur et al., 1992;O'Sullivan et al., 2014;Fröhlich-Nowoisky et al., 2014), pollen (Pummer et al., 2015;Pummer et al., 2012) and plankton (Schnell, 1975;Knopf et al., 2011;Alpert et al., 2011). Recently it has become increasingly clear that pollen and fungi emit separable macromolecular INP of far smaller size than the pollen and fungi themselves (Pummer et al., 2015;Pummer et al., 2012;O'Sullivan et al., 2016;O′Sullivan et al., 2015). It has recently been shown that small ice nucleating entities, most probably of biological origin, are present in the sea-surface microlayer and may be emitted to the atmosphere (Wilson et al., 2015).

Anthropogenic burning of fossil fuels and biomass contribute significantly to global aerosol (Bond et al., 2013). Various studies of ice nucleation by soots have been conducted (Diehl and Mitra, 1998;Demott, 1990;Gorbunov et al., 2001) as well as studies of ice nucleation by various biomass products (Petters et al., 2009).

AgI and related compounds were identified as good nucleators in the early days of ice nucleation research (Passarelli et al., 1973;Vonnegut and Chessin, 1971;Vonnegut, 1947)

and have been used for cloud seeding ever since. They are known to nucleate ice very efficiently (DeMott, 1995).

Various studies have also been conducted on substances that are not atmospherically relevant with the aim of learning something about ice nucleation. Experimental studies have looked at superhydrophobic coatings (Heydari et al., 2013), barium fluoride (Conrad et al., 2005), long chain alcohols (Cantrell and Robinson, 2006;Ochshorn and Cantrell, 2006;Zobrist et al., 2007;Gavish et al., 1990) and amino acids (Gavish et al., 1992). All these materials were shown to nucleate ice to some extent although comparison of efficiencies with other nucleators is difficult as values suitable for comparison were not calculated.

This is further complicated by the fact that different instruments, even those of the same type, do not always give the same answer when (Hiranuma et al., 2015). However, it is possible to say something about the general effectiveness of the different classes of nucleators. Murray et al. (2012) calculated n_s values for a wide range of immersion mode measurements. As discussed in section 1.3.2.6 n_s values are probably the best metric for comparing different nucleators. Figure 1.4 is a reproduction of the comparison figure from Murray et al. (2012). They are not perfect as calculating surface areas for species with varying natures is not straightforward.

A further problem is that many nucleators have only been tested using very small cloud sized droplets with correspondingly small amounts of nucleator surface area. As a result, there is little data at warmer temperatures for many nucleators. Conversely, biological nucleators have mostly only been tested in larger droplets, although dilution has allowed extension of the range of n_s values tested. (e.g (Wex et al., 2015)). The only examples of non-biological ice nucleators tested at n_s values below 10^3 cm^{-2} in Figure 1.4 are the volcanic ash tested by Fornea et al. (2009) and BCS 376 microcline, which was measured using the instrument described in *Chapter 2* of this work.

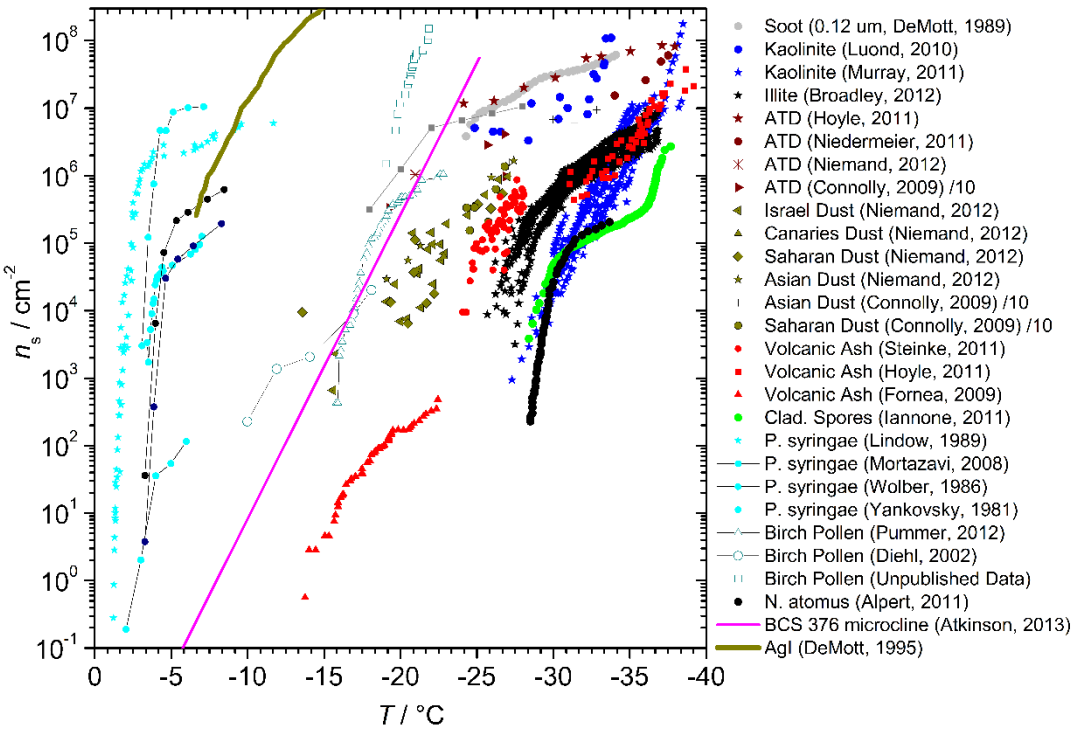

Figure 1.4: An adapted version of figure 18 from Murray et al (2012) with some additional data from subsequent studies. The figure shows ice nucleation efficiencies for a range of different nucleators. It can be seen that bacterial ice nucleators are much more effective than non-biological ice nucleators. BCS 376 microcline from Atkinson et al. (2013) nucleates ice more efficiently than other non-biological nucleators, except for AgI (DeMott, 1995).

What can be seen is that pseudomonas syringae nucleates ice far more efficiently than any other nucleator for which n_s has been calculated, with similar site concentrations to other nucleators at much warmer temperatures. BCS 376 microcline, an alkali feldspar, was tested by Atkinson et al. (2013) and shown to nucleate ice more efficiently than the atmospherically relevant minerals they tested. BCS 376 microcline also has a higher active site density at all temperatures than all other non-biological nucleators. Other feldspar minerals have also been tested (Zolles et al., 2015, Niedermeier et al., 2015, Augustin-Bauditz et al., 2014) and are of broadly similar, or somewhat lesser activity than BCS 376 microcline. Illite, kaolinite, Arizona Test Dust (ATD) and natural dusts all appear to be rather less effective nucleators than BCS 376 microcline. It seems quite likely that nucleation by ATD and natural dusts is dominated by their feldspar content (Augustin-Bauditz et al., 2014, Atkinson et al., 2013).

AgI is a highly efficient nucleator (DeMott, 1995) and is better at nucleating ice than any other non-biological nucleator that has been tested, including feldspars. Birch pollen nucleates with similar efficiency to BCS 376 microcline and the plankton N. atomus is rather less active.

Overall, biological nucleators such as *pseudomas syringae* and fungal proteins nucleate ice more efficiently than any other species. AgI and related compounds are probably the next most efficient nucleators. Alkali feldspar is more efficient than other minerals, volcanic ashes and combustion products.

While interesting and useful this information does not offer insight into why these species are effective INPs. What is it about *Pseudomonas Syringae* or a AgI crystal that makes them so good at nucleating ice? Currently, it is impossible to look at the physical properties of a substance and decide whether it will nucleate ice well. Experimental testing needs to be conducted. However, progress is being made in this direction. The next section discusses what is known about physical properties that aid ice nucleation.

1.4.2. Properties of good heterogeneous ice nucleators

The difficulty of understanding what makes a good INP stems from the small size of the ice critical nucleus (see Figure 1.2) and the small spatial extent of the nucleation event. According to CNT critical nuclei range in size from a 1 nm radius at -38°C to 10 nm at -4°C. These critical nuclei are spatially rare. Whatever volume of droplet is frozen there will usually only be a single critical nucleus present. Droplets are typically at least picometres across. No current technique is capable of locating and usefully measuring the physical properties of an event this rare. As a result, properties of ice nucleation have usually been inferred from experimental data.

1.4.2.1. The traditional view of heterogeneous ice nucleation

Historically, five properties were thought to be important for heterogeneous ice nucleation. These were listed and discussed by Pruppacher and Klett (1997). While these have never been regarded as hard and fast rules discussion of the reasons for them and where they fall down are instructive. They are:

1) The insolubility requirement: nucleators must provide an interface with water. Dissolved substances do not provide an interface and so do not nucleate ice.

2) The size requirement: observations in the atmosphere indicate that INPs tend to be ‘large’. This requirement is somewhat vague, although it stems from the observation that larger particles in the atmosphere tend to be the ones that nucleate ice. It is also assumed that an INP must be larger than a critical nucleus.
3) The chemical bond requirement: A nucleator must be able to bind to water in order to cause nucleation. Stronger bonding is likely to improve nucleation efficiency.
4) The crystallographic requirement: the classic lattice matching idea first put forward by Vonnegut (1947). Substances with a similar lattice structure and spacing to ice will provide a template for a critical nucleus.
5) The active site requirement: which was based on a combination of the observation that site specific descriptions often give the best account of ice nucleation and the fact that deposition mode ice nucleation tends to occur repeatedly on specific locations on crystals. It seems likely that this is more related to vapour condensation than ice nucleation (Marcolli, 2014).

The next sections looks at how these requirements have been challenged and revised in recent years and what is known about the mechanism of heterogeneous ice nucleation from experimental studies. Computational studies of ice nucleation are then examined and the outcomes of the two approaches discussed.

1.4.2.2. Size and solubility of heterogeneous INPs

While INPs have traditionally been regarded as ‘large’ and insoluble (Pruppacher and Klett, 1997) a number of counter examples are known. In recent times biological macromolecules associated with pollen that have been claimed as soluble have been shown to nucleate ice efficiently (Pummer et al., 2015;Pummer et al., 2012). These molecules weigh from 100- 860 KDa which equates to a radius of less than 10 nm. This is only slightly larger than the critical nuclei they nucleate. they are perhaps 10 times smaller than the particles that Pruppacher and Klett (1997) envisaged as too small to efficiently nucleate ice on the basis of older work. Similarly, Ogawa et al. (2009) showed that solutions of poly-vinyl alcohol could nucleate ice, although only at a few degrees above homogenous nucleation temperatures

1.4.2.3. Lattice matching

The best known example of inference of ice nucleation properties is the lattice matching concept of Vonnegut (1947). The idea is that substances that have a similar crystal structure to ice, with similar lattice constants will pattern the first layer of ice. The amount of lattice mismatch, or lattice disregistry (Pruppacher and Klett, 1997;Turnbull and Vonnegut, 1952) can be readily calculated from knowledge of the crystal structure. On this basis Vonnegut (Vonnegut, 1947) identified AgI as a potentially excellent nucleator and all subsequent experimentation has shown that he was correct.

The role of lattice matching in ice nucleation by AgI has been questioned for some time. Zettlemoyer et al. (1961) argued that water likely adhered to specific sites on the surface of AgI, which may have been oxidised, rather than forming a layer over the crystal on the basis of the difference in adsorption of water and nitrogen. More recently, Finnegan and Chai (2003) postulated an alternative mechanism for ice nucleation by AgI where clustering of surface charge controls ice nucleation. There is no universal agreement on the mechanism of ice nucleation by AgI from experimentalists. Experimental studies on $BaF_{2,}$ which also has a good lattice match to ice did not support the lattice matching argument (Conrad et al., 2005).

1.4.2.4. Bonding of water to INPs

Intuitively, it seems obvious that water must be able to bind to a nucleator to induce ice nucleation and that hydrophilic surfaces will nucleate ice more efficiently than hydrophobic surfaces. There is little relevant experimental work as studies where surfaces of differing but well understood hydrophilicity have been tested in the same system have not been conducted. It is also generally difficult to choose nucleators and systems such that all other possible variables are constrained.

Li et al (2012) compared the ice nucleating ability of hydrophobic and hydrophilic surfaces and obtained the somewhat surprising result that the hydrophobic surface nucleated ice more efficiently. While their technique, coating of a silicon wafer with a fluoroalkylsilane, may introduce other variables this is evidence that hydrophilic surfaces do not necessarily nucleate ice more efficiently than hydrophobic surfaces. It has been reported in the past that hydrophilic soots nucleate ice more efficiently than hydrophobic soots, although the method used leaves doubt as to the mode of ice nucleation observed (Gorbunov et al., 2001).

1.4.2.5. Active sites and topographical effects

As discussed in section 1.3.2 it has been argued that the surfaces of most immersion mode nucleators must have active sites on the basis of interpretations of droplet freezing experiments and repeated freezing droplets (Vali, 2014, 2008), although there are exceptions (Herbert et al., 2014). These experiments do not constitute direct observation of the nucleation sites. It has been known for some time that apparently depositional ice nucleation tends to occur on specific sites on both organic substances (Fukuta and Mason, 1963) and inorganic substances (Bryant et al., 1960). More recently it has been shown that nucleation from vapour of organic molecules probably follows a two-step process where small amounts of liquid condense prior to freezing (Campbell et al., 2013) and proposed that ice nucleation from vapour probably follows a similar route in many situations (Marcolli, 2014).

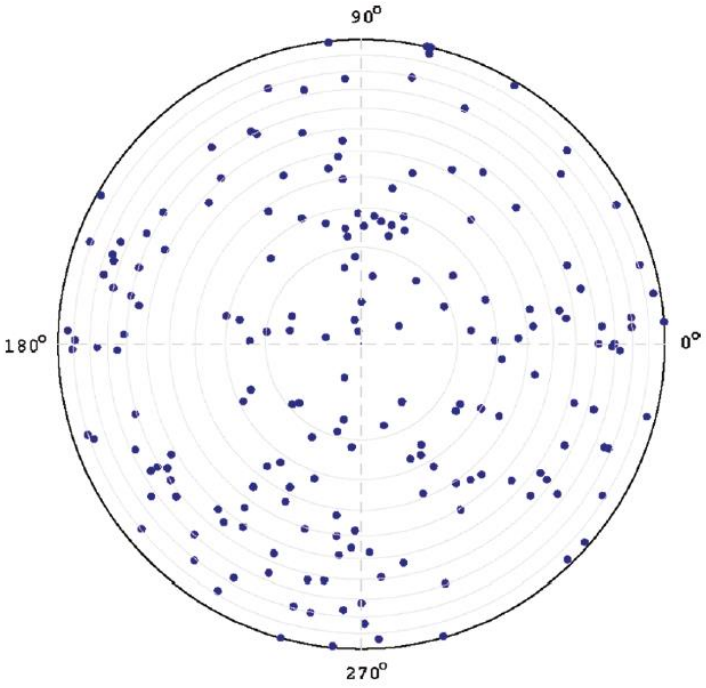

Figure 1.5: Spatial locations of nucleation events on a silicon surface covered by a 10 µl water droplet from Gurganus et al. (2011). The distribution of freezing events is random, not occurring repeatedly on any one location on the substrate. Figure taken from Gurganus et al. (2011).

It is far easier to locate a depositional nucleation site than an immersed nucleation site as crystals grow out from point of depositional nucleation relatively slowly, whereas they grow very quickly through liquid water droplets. That said, it is possible to locate nucleation points in surfaces covered by water using a high speed camera (Gurganus et

al., 2014;Gurganus et al., 2013, 2011). Gurganus et al. (2011) conducted freezing experiments of droplets on silicon wafers and saw no tendency for nucleation to occur repeatedly on the same site (figure Figure 1.5), suggesting that no specific sites on their substrate nucleated ice more efficiently than any others. Their study was aimed at determining whether nucleation tended to take place at the air-water-substrate interface (contact mode, see section 1.1.1) or elsewhere and showed no preference for nucleation at the interface. More recent work from Gurganus et al. (2014) has shown that a 'nano-textured' silicon strand (features on a scale smaller than 100 nm) nucleates ice much more effectively than a 'micro-textured' (etched features in silicon with depths from 300 nm to 900 nm) silicon substrate or a smooth silicon substrate. The difference was particularly pronounced at the point of contact between the silicon strand and the droplet surface. This interesting result shows that topographical differences between chemically very similar surfaces can cause differences in ice nucleation behaviour. The nature of topographical features implies that nucleation processes involving them must be to some extent 'site specific'.

Campbell et al. (2015) attempted to change the ice nucleating properties of silicon, glass, and mica substrates by scratching them with diamond powders ranging from 10 nm to 40-60 µm. They found that the scratching process made no significant difference to the ice nucleating efficiency of the surfaces. It might be expected that the 10 nm diamond powder would produce features on a similar scale those that Gurganus et al. (2014) observed enhancing the ice nucleating efficiency of silicon. This was not the case. There are many other differences between the two systems so it is difficult to suggest reasons for this. Other studies have also reported no impact on ice nucleation efficiency from topography on a micrometer scale (Heydari et al., 2013).

1.4.3. Computational studies of heterogeneous ice nucleation

At present, it is impossible to observe ice nucleation events directly on a scale that is useful for understanding the underlying mechanisms. An approach to defining the scale problem is to use classical nucleation theory and assume that it gives a reasonable estimate for the size of a critical nucleus required for heterogeneous nucleation at temperatures above which homogenous nucleation can be observed .

The role of lattice matching in heterogeneous ice nucleation has been studies computationally. Recent molecular dynamics (MD) results have suggested that a lattice

match is not the sole explanation for the efficiency of AgI and that a mechanism involving an ordering of water above the AgI surface, which then causes ice nucleation is more likely (Zielke et al., 2015;Reinhardt and Doye, 2014). Similarly, kaolinite had been thought of as good ice nucleator, and this efficiency had been attributed to a good lattice match of –OH groups on the basal face of kaolinite to hexagonal ice (Pruppacher and Klett, 1997). It is now seems likely that the apparent ice nucleation activity of kaolinite observed in older studies was largely due to contamination by feldspar minerals (Atkinson et al., 2013). Density Functional Theory (DFT) calculations previously questioned the validity of the lattice matching mechanism for kaolinite, instead attributing the activity to the amphoterism of the –OH groups on the surface of kaolinite which allows them to both accept and donate hydrogen bonds, favouring the formation of an overlayer of water molecules (Hu and Michaelides, 2007). Indeed, there is now a significant body of computational evidence suggesting that a simplistic lattice matching view of ice nucleation may be misleading (e.g (Cox et al., 2013;Cox et al., 2012;Fitzner et al., 2015))

Another variable that has been examined computationally is surface hydrophilicity. Lupi and Molinero (2014) found that simulated graphite surfaces nucleated ice less well when decorated with –OH groups to increase hydrophilicity. Recently, Fitzner et al. (2015) conducted a comprehensive, systematic MD study of the impact of crystallographic match and hydrophilicity on ice nucleation. By testing four different idealised crystal surfaces with varied lattice parameters and water interaction strengths they found three different mechanism by which heterogeneous ice nucleation could be promoted. They name these ‘In-Plane Template of the First Overlayer’ ‘Buckling of the First Overlayer’ ‘High Adsorption-Energy Nucleation on Compact Surfaces’. It is interesting that even in this simplified system they found complex dependency on lattice parameters and interaction strength. Bi et al (2016) also found complex dependencies of nucleation rate on the interaction between hydrophilicity and crystallinity. Computational studies have found that surface roughness on a fine scale (from several angstroms to several nanometers), with roughness of some specific periodicities found to promote nucleation better than others (Zhang et al., 2014;Fitzner et al., 2015).

1.4.4. What phase of ice nucleates?

It might be thought that the phase of ice which nucleates could provide insight into the nature of the ice nucleation mechanism. Molecular dynamics studies by Cox et al. (2013) obtained the intriguing result that the nature of nucleation mechanism may alter the phase of ice that nucleates. They found that homogeneous ice nucleation tends to produce a

stacking disordered phase while nucleation by kaolinite exclusively formed hexagonal ice.

It has typically been assumed that hexagonal ice, Ice I_h, nucleates under tropospheric conditions but experimental evidence suggests that what was previously called cubic ice typically forms (Murray and Bertram, 2006;Murray et al., 2005;Huang and Bartell, 1995). It has been shown that the ice that forms is stacking disordered hence it is now known as stacking disordered ice, Ice I_{sd} (Malkin et al., 2015;Malkin et al., 2012). Malkin et al. (2015) found that warmer nucleation temperatures tends to lead to a greater proportion of ice I_h as against Ice I_{sd}. It is probably not correct to infer anything about the nucleation mechanism from this finding as it is clear that the ice observed by powder x-ray diffraction in these types of experiments is the result of crystal growth rather than nucleation. The structure of critical nuclei is not known from experiment although several computational studies have found that homogenous nucleation of ice results in a stacking disordered critical nucleus (Molinero and Moore, 2008;Haji-Akbari and Debenedetti, 2015).

1.4.5. Summary

Overall, the picture is a complex one. It can be said with some certainty that active sites are important for ice nucleation by many nucleators. The exact properties of these active sites is much less certain. Other nucleators do not appear to have active sites. Lattice matching as a concept is well established and widely applied but increasingly questioned by both laboratory and computational studies. Hydrophilicity must play some role and simulations of ice nucleation have suggested that the relationship between hydrophilicity and lattice match can impact ice nucleation efficiency in complicated and non-intuitive ways. This may shed some light why it has proved so hard to understand ice nucleation processes in the past; relationships between physico-chemical properties and ice nucleation efficiency are not straightforward. For immersion mode ice nucleation micrometre scale topographical features have so far proved to play little role, although only limited numbers of experiments have been conducted to date. There are hints that topography on a sufficiently small scale (atomic to nanometre scale) may play a role however.

1.5. Feldspar structure

It has been shown recently that feldspar can nucleate ice more efficiently than the majority of other minerals, and that these minerals have the potential to strongly influence glaciation of mixed phase clouds (Atkinson et al., 2013). Much of this thesis is concerned with immersion mode ice nucleation by the minerals of the feldspar group. This section is a brief introduction to the structure and properties of this mineral group. The feldspars are tectosilicates (also called framework silicates) with a general formula of $XAl(Si,Al)Si_2O_8$, where X is usually K^+, Na^+ or Ca^{2+} (Megaw, 1974; Deer et al., 1992), but can also be other cations, including NH_4^+ and Ba^{2+}. Tectosilicates are made up of three dimensional frameworks of silica tetrahedra, joined at the corner by mutual bonding to O atoms. Cations occupy the cavities of the framework. Substitution of Si with Al charge balances the structure. The sodium and potassium endmembers can adopt multiple crystal structures (Megaw, 1974; Deer et al., 1992).

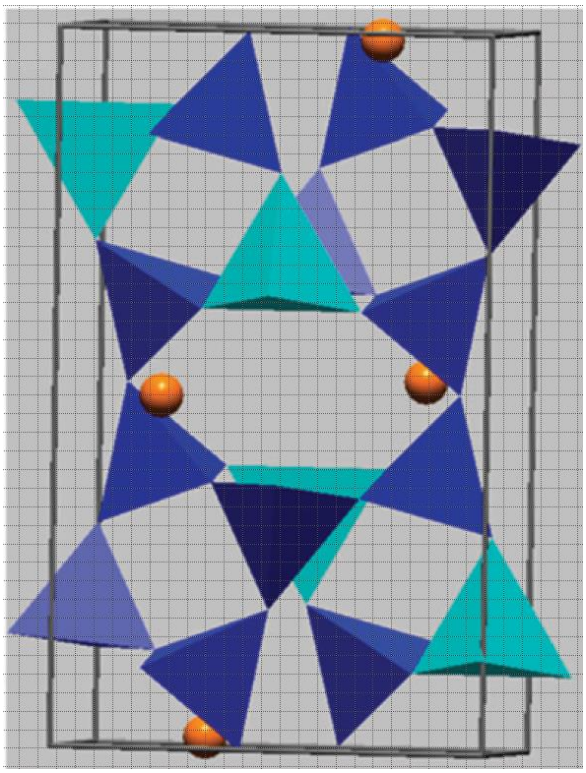

Figure 1.6: Crystal structure of the feldspar low albite. Dark blue tetrahedra represent SiO_2 and light blue tetrahedra represent AlO_4^-. The points of each tetrahedron are occupied by a single oxygen atom. Orange spheres represent Na^+. In the disordered feldspars, sanidine and high albite the locations of the Al and Si centred tetrahedra are random. Figure adapted from Murray et al. (2012).

The crystal structure obtained depends upon the temperature at which the mineral crystallises and the rate at which cooling occurs. If sodium and potassium feldspars are cooled quickly then the high temperature structures (sanidine and high albite) can persist to ambient temperatures. In ideal sanidine and high albite the Si and Al atoms are randomly distributed throughout the structure. If cooling occurs relatively slowly then there is time for ordering of the alumino-silicate network. In ideal microcline all Si and Al atoms occupy consistent positions throughout the structure (Megaw, 1974; Deer et al., 1992). The structure of the sodium rich endmember, albite, is shown Figure 1.6. The spatial relationships of the alumino-silicate tetrahedra and cations are similar in the other feldspars, although, as discussed above, the ordering of the aluminosilicate network varies, which alters the symmetry of the various feldspars. Details of the possible structures of pure minerals are given in table 1.1.

Table 1.1: Polymorph names, symmetry and space group of commons feldspars.

Chemical formulae	Polymorph	Symmetry	Space group
$KAlSi_3O_8$	Sanidine	Monoclinic	C2/*m*
	Orthoclase	Monoclinic	C2/*m*
	Microcline	Triclinic	$C\bar{1}$
$NaAlSi_3O_8$	High Albite	Triclinic	$C\bar{1}$
	Low Albite	Triclinic	$C\bar{1}$
$CaAl_2Si_2O_8$	Anorthite	Triclinic	$P\bar{1}$

Natural feldspars are very rarely pure endmembers. Effectively all natural feldspars contain mixtures of cations determined by the composition of the melt from which they form. This leads to additional complexity of structure. Feldspars containing a mixture Na^+ and Ca^{2+} cations are called plagioclase feldspars while feldspars containing a mixture of K^+ and Na^+ cations are known as alkali feldspars. Ca^{2+} and K^+ are immiscible in the feldspar structure so feldspar containing this mixture do no occur. Figure 1.7 is a phase diagram showing this and also the names assigned to various compositions of the plagioclase and alkali feldspars.

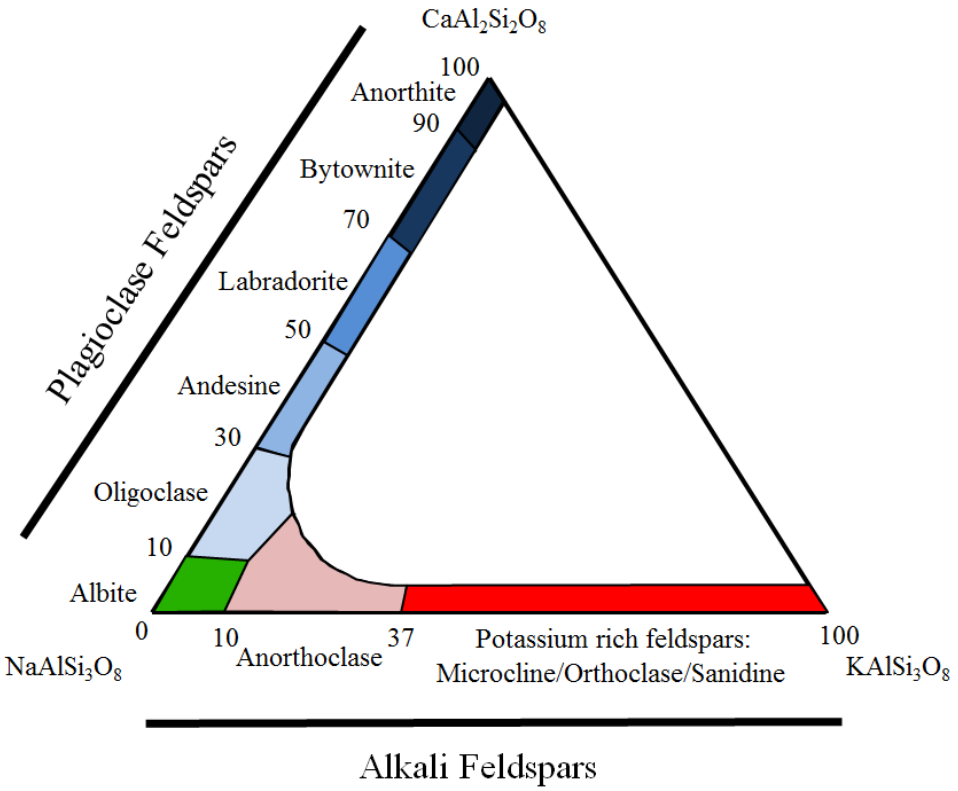

Figure 1.7: Ternary diagram of feldspar composition. The figure is based on similar figures in the literature (e.g Deer et al., 1992).

While plagioclase feldspars form a solid solution from the temperatures at which they first crystallise (>1000°C) to ambient temperatures alkali feldspars begin to exsolve at temperatures below about 600°C. Quick cooling can avoid this exsolution but the vast majority of natural alkali feldspars contain zones which are enriched in one cation and depleted in the other, along with corresponding zones of the reverse composition (Deer et al., 1992). This 'microtexture' can be on length scales from nanometers to millimetres and individual rocks containing as many as 8 distinct phases have been identified (Parsons et al., 2015). Microtextured feldspars tend to be rougher on nanometer to micrometer scales and often have a greater concentration of crystallographic dislocations and other defects than rare pristine alkali feldspars (Parsons et al. 2015). The variation of properties and the known strong ice nucleating characteristics of the feldspar group make it an ideal candidate for study of ice nucleation. By comparing the ice nucleating abilities of feldspars with subtly different characteristics (e.g differing chemical composition, crystal structure or microtextural composition) it may be possible to improve understanding of the impact of these properties on ice nucleation.

1.6. Project Objectives

The project which this thesis describes had two overarching objective. The first was to produce an instrument capable of extending the range of measurements of atmospherically relevant nucleators to warmer temperatures. It can be seen in Figure 1.4 that few measurements of n_s values have been made above about -15°C. This is largely because the atmospheric community has tended to use cloud sized droplets. While sensible this approach does not necessarily reveal all the information required for understanding how INPs are likely to affect clouds as real clouds will typically contain far larger total amounts of aerosol than can be looked at when cloud sized droplets are used. It is known that clouds regularly glaciate at relatively high temperature, warmer than -15°C (Kanitz et al., 2011;Seifert et al., 2015). As such, ice nucleation at these temperatures must be of some importance and should be studied. Ideally, the instrument should be simple, portable and flexible as well as sensitive to allow for experiments to be conducted quickly and in the field, and to allow for experimental conditions to be varied as needed. The second objective was to contribute towards understanding of the relationship between physical and chemical properties of nucleators and efficiency of heterogeneous ice nucleation. The development of the instrument described in *Chapter 2* facilitated the relatively rapid testing and comparison of ice nucleation efficiencies of multiple nucleators. From that point the strategy has been to characterise the physical and chemical properties of heterogeneous ice nucleators of similar but non-identical nature and then test their ice nucleating abilities in order that differences in ice nucleation efficiency might be related to differences in properties.

1.7. Thesis Overview

The first two chapters of this thesis are published papers while the last 3 are papers at various points of the submission process.

Chapter two consists of the paper '*A technique for quantifying heterogeneous ice nucleation in microlitre supercooled water droplets* ' (Whale et al., 2015a). In this chapter the microlitre Nucleation by Immersed Particle Instrument (µl-NIPI) instrument is described and validated.

Chapter three consists of the paper '*Ice nucleation properties of oxidized carbon nanomaterials*' (Whale et al., 2015b). In this chapter µl-NIPI is used to characterise the ice nucleation efficiency of four carbon nanomaterials. These represent a new and surprising type of heterogeneous ice nucleator as they are very small for ice nucleating

particles. Ice nucleation efficiency decreases with increasing oxidation for the four nano-materials, lending support to similar computational findings (Lupi and Molinero, 2014).

Chapter four consists of the paper '*Not all feldspar is equal: a survey of ice nucleating properties across the feldspar group of minerals*' in which µl-NIPI is used to characterise the ice nucleation efficiency of 15 plagioclase and alkali feldspars. It is demonstrated alkali feldspars nucleate ice much more efficiently than plagioclase feldspars, that some alkali feldspars are more efficient at nucleating ice than typical alkali feldspars and lose activity when exposed to water for periods of hours to days.

Chapter five consists of the upcoming paper '*The microtexture of alkali feldspars is important for its ice nucleating ability'*. It is shown that certain alkali feldspars nucleate much less efficiently than most. This difference is attributed to a lack of microtextural complexity demonstrating that the efficient ice nucleation of alkali feldspar does not depend only on bulk chemical of crystallographic properties.

Chapter six consists of the paper '*The enhancement and deactivation of immersion mode heterogeneous ice nucleation by solutes*' which demonstrates that ice nucleation by certain nucleators, notably feldspars, is enhanced by ammonium compounds and deactivated by alkali halides. Other nucleators are shown to be unaffected.

Chapter seven contains the conclusions of this thesis, synthesising the results of the proceeding four chapters and describing what progress has been made to understanding of heterogeneous ice nucleation and outlining what routes to future progress are suggested by this study.

1.8. Other Work completed during the course of my PhD

This thesis consists of 5 research papers at various stages of the publication process. I hope that these form a neat and cohesive whole that helps build understanding of the heterogeneous ice nucleation process for certain nucleators, while suggesting interesting routes for further research. During the studies that have led to this thesis I have been involved with several other papers, many of which have been cited in this introduction. In the majority of these I used the technique (µl-NIPI) described in '*A technique for quantifying heterogeneous ice nucleation in microlitre supercooled water droplets'* (Whale et al., 2015a) to measure heterogeneous ice nucleation by various nucleators. As well as providing the technical support and performing experiments I was also involved in the analysis processes and writing of the resulting papers.

Atkinson et al. (2013) showed that feldspar minerals probably account for much of the ability of mineral dusts to nucleate ice in the immersion mode and that emissions of feldspar can potentially account for INP concentrations made by field ice nucleation measurements made around the world. For this paper I conducted experiments using µl-NIPI to determine the ice nucleation efficiency at relatively high temperatures, in the range of -5°C to -15°C.

O'Sullivan et al. (2014) demonstrated that much of the activity of fertile soil samples was due to its biological content and O'Sullivan et al. (2015) showed that macromolecules associated with fungi and pollen grains can nucleate ice efficiently. I conducted experiments on mineral dusts used in both these papers with µl-NIPI.

Herbert et al. (2014) developed the FROST framework discussed in section 1.3.2.5. I conducted various experiments on mineral dusts using µl-NIPI specifically to test the framework, results which were integral to the paper.

Wilson et al. (2015) reported the discovery of a potential new source of marine biogenic INPs. I participated in one of the Arctic field campaign, making measurements of the ice nucleating ability of the sea surface microlayer using µl-NIPI. This was this instrument's first field campaign and I was integral to training the other users of the instrument and to producing a comprehensive data set.

Hiranuma et al. (2015) was a large intercomparison of many ice nucleation instruments used by the atmospheric ice nucleation community. I conducted experiments on NX-illite using µl-NIPI that constituted the University of Leeds participation in this study.

Malkin et al. (2015) was a perspective article describing the present state of knowledge on the subject of stacking disordered ice. It included some new data which I helped to produce by synthesising ice II and converting it into ice I_{sd}. I also drew together historic literature data.

Vali et al. (2015) was an effort to standardise terminology used by researchers working on ice nucleation. It involved extensive commenting by many interested parties on a draft produced by the co-authors, using the discussion section of *Atmospheric Chemistry and Physics (ACP)* as a forum. I played a supporting role to the main author, Professor Gabor Vali, by helping to write the initial draft and then to synthesise the subsequent and final version from the many comments made on the *ACP* discussion forum.

References

Alpert, P. A., Aller, J. Y., and Knopf, D. A.: Ice nucleation from aqueous nacl droplets with and without marine diatoms, Atmos. Chem. Phys., 11, 5539-5555, 10.5194/acp-11-5539-2011, 2011.

Alpert, P. A., and Knopf, D. A.: Analysis of isothermal and cooling-rate-dependent immersion freezing by a unifying stochastic ice nucleation model, Atmos. Chem. Phys., 16, 2083-2107, 10.5194/acp-16-2083-2016, 2016.

Ansmann, A., Mattis, I., Müller, D., Wandinger, U., Radlach, M., Althausen, D., and Damoah, R.: Ice formation in saharan dust over central europe observed with temperature/humidity/aerosol raman lidar, J. Geophys. Res.: Atmos., 110, D18S12, 10.1029/2004jd005000, 2005.

Ansmann, A., Tesche, M., Seifert, P., Althausen, D., Engelmann, R., Fruntke, J., Wandinger, U., Mattis, I., and Müller, D.: Evolution of the ice phase in tropical altocumulus: Samum lidar observations over cape verde, J. Geophys. Res.: Atmos, 114, D17208, 10.1029/2008jd011659, 2009.

Asghar, W., El Assal, R., Shafiee, H., Anchan, R. M., and Demirci, U.: Preserving human cells for regenerative, reproductive, and transfusion medicine, Biotech. J., 9, 895-903, 10.1002/biot.201300074, 2014.

Atkinson, J. D., Murray, B. J., Woodhouse, M. T., Whale, T. F., Baustian, K. J., Carslaw, K. S., Dobbie, S., O'Sullivan, D., and Malkin, T. L.: The importance of feldspar for ice nucleation by mineral dust in mixed-phase clouds, Nature, 498, 355-358, 10.1038/nature12278, 2013.

Barbas, J. P., and Mascarenhas, R. D.: Cryopreservation of domestic animal sperm cells, Cell Tissue Bank., 10, 49-62, 10.1007/s10561-008-9081-4, 2008.

Barlow, T. W., and Haymet, A. D. J.: Alta: An automated lag-time apparatus for studying the nucleation of supercooled liquids, Rev. Sci. Instr., 66, 2996-3007, doi:http://dx.doi.org/10.1063/1.1145586, 1995.

Bi, Y., Cabriolu, R., and Li, T.: Heterogeneous ice nucleation controlled by the coupling of surface crystallinity and surface hydrophilicity, J. Phys. Chem. C, 120, 1507-1514, 10.1021/acs.jpcc.5b09740, 2016.

Bond, T. C., Doherty, S. J., Fahey, D. W., Forster, P. M., Berntsen, T., DeAngelo, B. J., Flanner, M. G., Ghan, S., Karcher, B., Koch, D., Kinne, S., Kondo, Y., Quinn, P. K., Sarofim, M. C., Schultz, M. G., Schulz, M., Venkataraman, C., Zhang, H., Zhang, S., Bellouin, N., Guttikunda, S. K., Hopke, P. K., Jacobson, M. Z., Kaiser, J. W., Klimont, Z., Lohmann, U., Schwarz, J. P., Shindell, D., Storelvmo, T., Warren, S. G., and Zender, C. S.: Bounding the role of black carbon in the climate system: A scientific assessment, J. Geophys. Res.-Atmos., 118, 5380-5552, 10.1002/jgrd.50171, 2013.

Boucher, O., Randall, D., Artaxo, P., Bretherton, C., Feingold, G., Forster, P., Kerminen, V.-M., Kondo, Y., Liao, H., and Lohmann, U.: Clouds and aerosols, in: Climate change 2013: The physical science basis. Contribution of working group i to the fifth assessment report of the intergovernmental panel on climate change, Cambridge University Press, 571-657, 2013.

Broadley, S. L., Murray, B. J., Herbert, R. J., Atkinson, J. D., Dobbie, S., Malkin, T. L., Condliffe, E., and Neve, L.: Immersion mode heterogeneous ice nucleation by an illite rich powder representative of atmospheric mineral dust, Atmos. Chem. Phys., 12, 287-307, 10.5194/acp-12-287-2012, 2012.

Bryant, G. W., Hallett, J., and Mason, B. J.: The epitaxial growth of ice on single-crystalline substrates, J. Phys. Chem. Solids, 12, 189-IN118, http://dx.doi.org/10.1016/0022-3697(60)90036-6, 1960.

Campbell, J. M., Meldrum, F. C., and Christenson, H. K.: Characterization of preferred crystal nucleation sites on mica surfaces, Cryst. Growth Des., 13, 1915-1925, 10.1021/cg301715n, 2013.

Campbell, J. M., Meldrum, F. C., and Christenson, H. K.: Is ice nucleation from supercooled water insensitive to surface roughness?, J. Phys. Chem. C, 119, 1164-1169, 10.1021/jp5113729, 2015.

Cantrell, W., and Robinson, C.: Heterogeneous freezing of ammonium sulfate and sodium chloride solutions by long chain alcohols, Geophys. Res. Lett., 33, L07802 10.1029/2005gl024945, 2006.

Chen, J.-P., Hazra, A., and Levin, Z.: Parameterizing ice nucleation rates using contact angle and activation energy derived from laboratory data, Atmos. Chem. Phys., 8, 7431-7449, 2008.

Choi, Y.-S., Lindzen, R. S., Ho, C.-H., and Kim, J.: Space observations of cold-cloud phase change, Proc. Natl. Acad. Sci. USA, 107, 11211-11216, 10.1073/pnas.1006241107, 2010.

Connolly, P. J., Möhler, O., Field, P. R., Saathoff, H., Burgess, R., Choularton, T., and Gallagher, M.: Studies of heterogeneous freezing by three different desert dust samples, Atmos. Chem. Phys., 9, 2805-2824, 10.5194/acp-9-2805-2009, 2009.

Conrad, P., Ewing, G. E., Karlinsey, R. L., and Sadtchenko, V.: Ice nucleation on baf2 (111), J. Chem. Phys., 122, 064709-064709, 2005.

Cox, S. J., Kathmann, S. M., Purton, J. A., Gillan, M. J., and Michaelides, A.: Non-hexagonal ice at hexagonal surfaces: The role of lattice mismatch, Phys. Chem. Chem. Phys., 14, 7944-7949, 10.1039/c2cp23438f, 2012.

Cox, S. J., Raza, Z., Kathmann, S. M., Slater, B., and Michaelides, A.: The microscopic features of heterogeneous ice nucleation may affect the macroscopic morphology of atmospheric ice crystals, Faraday Discussions, 167, 389-403, 10.1039/c3fd00059a, 2013.

Cui, Z. Q., Carslaw, K. S., Yin, Y., and Davies, S.: A numerical study of aerosol effects on the dynamics and microphysics of a deep convective cloud in a continental environment, J. Geophys. Res.-Atmos., 111, 2006.

de Boer, G., Morrison, H., Shupe, M. D., and Hildner, R.: Evidence of liquid dependent ice nucleation in high-latitude stratiform clouds from surface remote sensors, Geophys. Res. Lett., 38, L01803, 10.1029/2010gl046016, 2011.

De Souza, Y. G., and Greenspan, J. S.: Biobanking past, present and future: Responsibilities and benefits, AIDS (London, England), 27, 303, 2013.

Debenedetti, P. G.: Metastable liquids: Concepts and principles, Princeton University Press, 1996.

Deer, W. A., Howie, R. A., and Zussman, J.: An introduction to the rock forming minerals, 2nd ed., Addison Wesley Longman, Harlow, UK, 1992.

DeMott, P. J.: An exploratory-study of ice nucleation by soot aerosols, J. App. Meteorol., 29, 1072-1079, 1990.

DeMott, P. J.: Quantitative descriptions of ice formation mechanisms of silver iodide-type aerosols, Atmos. Res., 38, 63-99, 10.1016/0169-8095(94)00088-U, 1995.

Denman, K. L., Brasseur, G., Chidthaisong, A., Ciais, P., Cox, P. M., Dickinson, R. E., Hauglustaine, D., Heinze, C., Holland, E., Jacob, D., Lohmann, U., Ramachandran, S., da Silva Dias, P. L., Wofsy, S. C., and Zhang, X.: Couplings between changes in the climate system and biogeochemistry. In: Climate change 2007: The physical science basis. Contribution of working group i to the fourth assessment report of the intergovernmental panel on climate change, Cambridge University Press, Cambridge, United Kingdom, 2007.

Diehl, K., and Mitra, S. K.: A laboratory study of the effects of a kerosene-burner exhaust on ice nucleation and the evaporation rate of ice crystals, Atmos. Environ., 32, 3145-3151, 1998.

Diehl, K., Matthias-Maser, S., Jaenicke, R., and Mitra, S. K.: The ice nucleating ability of pollen: Part ii. Laboratory studies in immersion and contact freezing modes, Atmos. Res., 61, 125-133, 2002.

Emersic, C., Connolly, P. J., Boult, S., Campana, M., and Li, Z.: Investigating the discrepancy between wet-suspension- and dry-dispersion-derived ice nucleation efficiency of mineral particles, Atmos. Chem. Phys., 15, 11311-11326, 10.5194/acp-15-11311-2015, 2015.

Fahy, G. M., Macfarlane, D. R., Angell, C. A., and Meryman, H. T.: Vitrification as an approach to cryopreservation, Cryobiology, 21, 407-426, 1984.

Field, C. B., Barros, V. R., Mach, K. J., Mastrandrea, M. D., Aalst, M. v., Adger, W. N., Arent, D. J., Barnett, J., Betts, R., Bilir, T. E., Birkmann, J., Carmin, J., Chadee, D. D., Challinor, A. J., Chatterjee, M., Cramer, W., Davidson, D. J., Estrada, Y. O., Gattuso, J. P., Hijioka, Y., Hoegh-Guldberg, O., Huang, H. Q., Insarov, G. E., Jones, R. N., Kovats, R. S., Lankao, P. R., Larsen, J. N., Losada, I. J., Marengo, J. A., McLean, R. F., Mearns, L. O., Mechler, R., Morton, J. F., Niang, I., Oki, T., Olwoch, J. M., Opondo, M., Poloczanska, E. S., Pörtner, H. O., Redsteer, M. H., Reisinger, A., Revi, A., Schmidt, D. N., Shaw, M. R., Solecki, W., Stone, D. A., Stone, J. M. R., Strzepek, K. M., Suarez, A. G., Tschakert, P., Valentini, R., Vicuña, S., Villamizar, A., Vincent, K. E., Warren, R., White, L. L., Wilbanks, T. J., Wong, P. P., and Yohe, G. W.: Technical summary, in: Climate change 2014: Impacts, adaptation, and vulnerability. Part a: Global and sectoral aspects. Contribution of working group ii to the fifth assessment report of the intergovernmental panel on climate change, edited by: Field, C. B., Barros, V. R., Dokken, D. J., Mach, K. J., Mastrandrea, M. D., Bilir, T. E., Chatterjee, M., Ebi, K. L., Estrada, Y. O., Genova, R. C., Girma, B., Kissel, E. S., Levy, A. N., MacCracken, S., Mastrandrea, P. R., and White, L. L., Cambridge University Press, Cambridge, United Kingdom and New York, NY, USA, 35-94, 2014.

Finnegan, W. G., and Chai, S. K.: A new hypothesis for the mechanism of ice nucleation on wetted agi and agi center dot agcl particulate aerosols, J. Atmos. Sci., 60, 1723-1731, 10.1175/1520-0469(2003)060<1723:anhftm>2.0.co;2, 2003.

Fitzner, M., Sosso, G. C., Cox, S. J., and Michaelides, A.: The many faces of heterogeneous ice nucleation: Interplay between surface morphology and hydrophobicity, J. Am. Chem. Soc., 137, 13658-13669, 10.1021/jacs.5b08748, 2015.

Fornea, A. P., Brooks, S. D., Dooley, J. B., and Saha, A.: Heterogeneous freezing of ice on atmospheric aerosols containing ash, soot, and soil, J. Geophys. Res.-Atmos., 114, D13201, 10.1029/2009jd011958, 2009.

Fröhlich-Nowoisky, J., Hill, T. C. J., Pummer, B. G., Franc, G. D., and Pöschl, U.: Ice nucleation activity in the widespread soil fungus mortierella alpina, Biogeosciences Discuss., 11, 12697-12731, 10.5194/bgd-11-12697-2014, 2014.

Fu, Q., Liu, E., Wilson, P., and Chen, Z.: Ice nucleation behaviour on sol–gel coatings with different surface energy and roughness, Phys. Chem. Chem. Phys., 17, 21492-21500, 2015.

Fukuta, N., and Mason, B. J.: Epitaxial growth of ice on organic crystals, J. Phys. Chem. Solids, 24, 715-718, http://dx.doi.org/10.1016/0022-3697(63)90217-8, 1963.

Fuller, B., and Paynter, S.: Fundamentals of cryobiology in reproductive medicine, Reprod. Biomed. Online, 9, 680-691, http://dx.doi.org/10.1016/S1472-6483(10)61780-4, 2004.

Fuller, B. J.: Cryoprotectants: The essential antifreezes to protect life in the frozen state, Cryolett., 25, 375-388, 2004.

Fuller, B. J., Lane, N., and Benson, E. E.: Life in the frozen state, CRC Press, 2004.

Garimella, S., Kristensen, T. B., Ignatius, K., Welti, A., Voigtländer, J., Kulkarni, G. R., Sagan, F., Kok, G. L., Dorsey, J., Nichman, L., Rothenberg, D., Rösch, M., Kirchgäßner, A., Ladkin, R., Wex, H., Wilson, T. W., Ladino, L. A., Abbatt, J. P. D., Stetzer, O., Lohmann, U., Stratmann, F., and Cziczo, D. J.: The spectrometer for ice nuclei (spin): An instrument to investigate ice nucleation, Atmos. Meas. Tech. Discuss., 2016, 1-37, 10.5194/amt-2015-400, 2016.

Gavish, M., Popovitz-Biro, R., Lahav, M., and Leiserowitz, L.: Ice nucleation by alcohols arranged in monolayers at the surface of water drops, Science, 250, 973-975, 10.2307/2878239, 1990.

Gavish, M., Wang, J., Eisenstein, M., Lahav, M., and Leiserowitz, L.: The role of crystal polarity in alpha-amino acid crystals for induced nucleation of ice, Science, 256, 815-818, 1992.

Gorbunov, B., Baklanov, A., Kakutkina, N., Windsor, H. L., and Toumi, R.: Ice nucleation on soot particles, J. Aerosol Sci., 32, 199-215, 10.1016/s0021-8502(00)00077-x, 2001.

Gurganus, C., Kostinski, A. B., and Shaw, R. A.: Fast imaging of freezing drops: No preference for nucleation at the contact line, J. Phys. Chem. Lett., 2, 1449-1454, 10.1021/jz2004528, 2011.

Gurganus, C., Kostinski, A. B., and Shaw, R. A.: High-speed imaging of freezing drops: Still no preference for the contact line, J. Phys. Chem., 117, 6195-6200, 10.1021/jp311832d, 2013.

Gurganus, C. W., Charnawskas, J. C., Kostinski, A. B., and Shaw, R. A.: Nucleation at the contact line observed on nanotextured surfaces, Phys. Rev. Lett., 113, 235701, 2014.

Haji-Akbari, A., and Debenedetti, P. G.: Direct calculation of ice homogeneous nucleation rate for a molecular model of water, Proc. Nat. Acad. Sci., 112, 10582-10588, 10.1073/pnas.1509267112, 2015.

Hallett, J., and Mossop, S. C.: Production of secondary ice particles during the riming process, Nature, 249, 26-28, 10.1038/249026a0, 1974.

Hansen, L. J. J., Daoussi, R., Vervaet, C., Remon, J. P., and De Beer, T. R. M.: Freeze-drying of live virus vaccines: A review, Vaccine, 33, 5507-5519, http://dx.doi.org/10.1016/j.vaccine.2015.08.085, 2015.

Hartmann, D. L., Ockert-Bell, M. E., and Michelsen, M. L.: The effect of cloud type on earth's energy balance: Global analysis, J. Clim., 5, 1281-1304, 10.1175/1520-0442(1992)005<1281:teocto>2.0.co;2, 1992.

Herbert, R. J., Murray, B. J., Whale, T. F., Dobbie, S. J., and Atkinson, J. D.: Representing time-dependent freezing behaviour in immersion mode ice nucleation, Atmos. Chem. Phys., 14, 8501-8520, 10.5194/acp-14-8501-2014, 2014.

Herbert, R. J., Murray, B. J., Dobbie, S. J., and Koop, T.: Sensitivity of liquid clouds to homogenous freezing parameterizations, Geophys. Res. Lett., 42, 1599-1605, 10.1002/2014gl062729, 2015.

Heydari, G., Thormann, E., Järn, M., Tyrode, E., and Claesson, P. M.: Hydrophobic surfaces: Topography effects on wetting by supercooled water and freezing delay, J. Phys. Chem. C, 117, 21752-21762, 10.1021/jp404396m, 2013.

Hill, T. C., Moffett, B. F., DeMott, P. J., Georgakopoulos, D. G., Stump, W. L., and Franc, G. D.: Measurement of ice nucleation-active bacteria on plants and in precipitation by quantitative pcr, Appl. Environ. Microb., 80, 1256-1267, 2014.

Hiranuma, N., Augustin-Bauditz, S., Bingemer, H., Budke, C., Curtius, J., Danielczok, A., Diehl, K., Dreischmeier, K., Ebert, M., Frank, F., Hoffmann, N., Kandler, K., Kiselev, A., Koop, T., Leisner, T., Möhler, O., Nillius, B., Peckhaus, A., Rose, D., Weinbruch, S., Wex, H., Boose, Y., DeMott, P. J., Hader, J. D., Hill, T. C. J., Kanji, Z. A., Kulkarni, G., Levin, E. J. T., McCluskey, C. S., Murakami, M., Murray, B. J., Niedermeier, D., Petters, M. D., O'Sullivan, D., Saito, A., Schill, G. P., Tajiri, T., Tolbert, M. A., Welti, A., Whale, T. F., Wright, T. P., and Yamashita, K.: A comprehensive laboratory study on the immersion freezing behavior of illite nx particles: A comparison of 17 ice nucleation measurement techniques, Atmos. Chem. Phys., 15, 2489-2518, 10.5194/acp-15-2489-2015, 2015.

Hoose, C., and Möhler, O.: Heterogeneous ice nucleation on atmospheric aerosols: A review of results from laboratory experiments, Atmos. Chem. Phys., 12, 9817-9854, 10.5194/acp-12-9817-2012, 2012.

Hu, X. L., and Michaelides, A.: Ice formation on kaolinite: Lattice match or amphoterism?, Surf. Sci., 601, 5378-5381, 10.1016/j.susc.2007.09.012, 2007.

Huang, J., and Bartell, L. S.: Kinetics of homogeneous nucleation in the freezing of large water clusters, J. Phys. Chem., 99, 3924-3931, 10.1021/j100012a010, 1995.

Kanitz, T., Seifert, P., Ansmann, A., Engelmann, R., Althausen, D., Casiccia, C., and Rohwer, E. G.: Contrasting the impact of aerosols at northern and southern midlatitudes on heterogeneous ice formation, Geophys. Res. Lett., 38, L17802, 10.1029/2011gl048532, 2011.

Kasper, J. C., and Friess, W.: The freezing step in lyophilization: Physico-chemical fundamentals, freezing methods and consequences on process performance and quality attributes of biopharmaceuticals, Eur. J. Pharm. Biopharm., 78, 248-263, 2011.

Knopf, D. A., Alpert, P. A., Wang, B., and Aller, J. Y.: Stimulation of ice nucleation by marine diatoms, Nature Geosci., 4, 88-90, 2011.

Kovács, T., Meldrum, F. C., and Christenson, H. K.: Crystal nucleation without supersaturation, J. Phys. Chem. Lett., 3, 1602-1606, 10.1021/jz300450g, 2012.

Krämer, B., Hübner, O., Vortisch, H., Wöste, L., Leisner, T., Schwell, M., Rühl, E., and Baumgärtel, H.: Homogeneous nucleation rates of supercooled water measured in single levitated microdroplets, J. Chem. Phys., 111, 6521-6527, 10.1063/1.479946, 1999.

Kuleshova, L. L.: 17. Ten years of success in vitrification of human oocytes, Cryobiology, 59, 374-375, http://dx.doi.org/10.1016/j.cryobiol.2009.10.031, 2009.

Kumai, M.: Snow crystals and the identification of the nuclei in the northern united states of america, J. Meteorol., 18, 139-150, 10.1175/1520-0469(1961)018<0139:scatio>2.0.co;2, 1961.

Langham, E. J., and Mason, B. J.: The heterogeneous and homogeneous nucleation of supercooled water, Proc. R. Soc. Lon. Ser-A, 247, 493-&, DOI 10.1098/rspa.1958.0207, 1958.

Lee Jr, R., Warren, G. J., and Gusta, L. V.: Biological ice nucleation and its applications, American Phytopathological Society, 1995.

Levine, J.: Statistical explanation of spontaneous freezing of water droplets, NACA Tech. Note, p. 2234, 1950.

Li, K., Xu, S., Shi, W., He, M., Li, H., Li, S., Zhou, X., Wang, J., and Song, Y.: Investigating the effects of solid surfaces on ice nucleation, Langmuir, 28, 10749-10754, 2012.

Lindow, S. E., Arny, D. C., and Upper, C. D.: Bacterial ice nucleation: A factor in frost injury to plants, Plant Physiol., 70, 1084-1089, 1982.

Lindow, S. E., Lahue, E., Govindarajan, A. G., Panopoulos, N. J., and Gies, D.: Localization of ice nucleation activity and the icec gene product in pseudomonas syringae and escherichia coli, Mol. Plant-Microbe Interact., 2, 262-272, 10.1094/MPMI-2-262, 1989.

Lohmann, U., and Feichter, J.: Global indirect aerosol effects: A review, Atmos. Chem. Phys., 5, 715-737, 10.5194/acp-5-715-2005, 2005.

Lovelock, J.: The haemolysis of human red blood-cells by freezing and thawing, Biochim. Biophys. Acta, 10, 414-426, 1953.

Lüönd, F., Stetzer, O., Welti, A., and Lohmann, U.: Experimental study on the ice nucleation ability of size-selected kaolinite particles in the immersion mode, J. Geophys. Res., 115, D14201, 10.1029/2009jd012959, 2010.

Lupi, L., and Molinero, V.: Does hydrophilicity of carbon particles improve their ice nucleation ability?, J. Phys. Chem. A, 118, 7330-7337, 10.1021/jp4118375, 2014.

Maki, L. R., Galyan, E. L., Chang-Chien, M.-M., and Caldwell, D. R.: Ice nucleation induced by pseudomonas syringae, Appl. Microbiol., 28, 456-459, 1974.

Malkin, T. L., Murray, B. J., Brukhno, A. V., Anwar, J., and Salzmann, C. G.: Structure of ice crystallized from supercooled water, Proc. Natl. Acad. Sci. U.S.A, 109, 1041-1045, 10.1073/pnas.1113059109, 2012.

Malkin, T. L., Murray, B. J., Salzmann, C. G., Molinero, V., Pickering, S. J., and Whale, T. F.: Stacking disorder in ice i, Phys. Chem. Chem. Phys., 17, 60-76, 2015.

Marcolli, C., Gedamke, S., Peter, T., and Zobrist, B.: Efficiency of immersion mode ice nucleation on surrogates of mineral dust, Atmos. Chem. Phys., 7, 5081-5091, 10.5194/acp-7-5081-2007, 2007.

Marcolli, C.: Deposition nucleation viewed as homogeneous or immersion freezing in pores and cavities, Atmos. Chem. Phys., 14, 2071-2104, 10.5194/acp-14-2071-2014, 2014.

Mazur, P., Leibo, S. P., and Chu, E. H. Y.: A two-factor hypothesis of freezing injury, Exp. Cell Res., 71, 345-355, http://dx.doi.org/10.1016/0014-4827(72)90303-5, 1972.

Mazur, P., Seki, S., Pinn, I. L., Kleinhans, F. W., and Edashige, K.: Extra- and intracellular ice formation in mouse oocytes, Cryobiology, 51, 29-53, http://dx.doi.org/10.1016/j.cryobiol.2005.04.008, 2005.

Megaw, H.: The architecture of the feldspars, The Feldspars, 2-24, 1974

Michelmore, R. W., and Franks, F.: Nucleation rates of ice in undercooled water and aqueous solutions of polyethylene glycol, Cryobiology, 19, 163-171, 1982.

Molinero, V., and Moore, E. B.: Water modeled as an intermediate element between carbon and silicon†, The Journal of Physical Chemistry B, 113, 4008-4016, 10.1021/jp805227c, 2008.

Morris, G. J., and Acton, E.: Controlled ice nucleation in cryopreservation - a review, Cryobiology, 66, 85-92, 10.1016/j.cryobiol.2012.11.007, 2013.

Mullin, J. W.: Crystallization, Elsevier, Oxford, UK, 2001.

Murphy, D. M., and Koop, T.: Review of the vapour pressures of ice and supercooled water for atmospheric applications, Q. J. R. Meteorol. Soc., 131, 1539-1565, 10.1256/qj.04.94, 2005.

Murray, B. J., Knopf, D. A., and Bertram, A. K.: The formation of cubic ice under conditions relevant to earth's atmosphere, Nature, 434, 202-205, 2005.

Murray, B. J., and Bertram, A. K.: Formation and stability of cubic ice in water droplets, Phys. Chem. Chem. Phys., 8, 186-192, 2006.

Murray, B. J., Broadley, S. L., Wilson, T. W., Bull, S. J., Wills, R. H., Christenson, H. K., and Murray, E. J.: Kinetics of the homogeneous freezing of water, Phys. Chem. Chem. Phys., 12, 10380-10387, 10.1039/c003297b, 2010.

Murray, B. J., Broadley, S. L., Wilson, T. W., Atkinson, J. D., and Wills, R. H.: Heterogeneous freezing of water droplets containing kaolinite particles, Atmos. Chem. Phys., 11, 4191-4207, 10.5194/acp-11-4191-2011, 2011.

Murray, B. J., O'Sullivan, D., Atkinson, J. D., and Webb, M. E.: Ice nucleation by particles immersed in supercooled cloud droplets, Chem. Soc. Rev., 41, 6519-6554, 10.1039/C2CS35200A, 2012.

Niedermeier, D., Shaw, R., Hartmann, S., Wex, H., Clauss, T., Voigtländer, J., and Stratmann, F.: Heterogeneous ice nucleation: Exploring the transition from stochastic to singular freezing behavior, Atmos. Chem. Phys., 11, 8767-8775, 2011.

Niedermeier, D., Ervens, B., Clauss, T., Voigtländer, J., Wex, H., Hartmann, S., and Stratmann, F.: A computationally efficient description of heterogeneous freezing: A simplified version of the soccer ball model, Geophys. Res. Lett., 41, 736-741, 10.1002/2013gl058684, 2014.

Niemand, M., Möhler, O., Vogel, B., Vogel, H., Hoose, C., Connolly, P., Klein, H., Bingemer, H., DeMott, P. J., Skrotzki, J., and Leisner, T.: A particle-surface-area-based parameterization of immersion freezing on desert dust particles, J. Atmos. Sci., 69, 10.1175/jas-d-11-0249.1, 2012.

O'Sullivan, D., Murray, B. J., Malkin, T. L., Whale, T. F., Umo, N. S., Atkinson, J. D., Price, H. C., Baustian, K. J., Browse, J., and Webb, M. E.: Ice nucleation by fertile soil dusts: Relative importance of mineral and biogenic components, Atmos. Chem. Phys., 14, 1853-1867, 10.5194/acp-14-1853-2014, 2014.

O'Sullivan, D., Murray, B. J., Ross, J., and Webb, M. E.: The adsorption of fungal ice-nucleating proteins on mineral dusts: A terrestrial reservoir of atmospheric ice-nucleating particles, Atmos. Chem. Phys. Discuss., 2016, 1-22, 10.5194/acp-2015-1018, 2016.

O′Sullivan, D., Murray, B. J., Ross, J. F., Whale, T. F., Price, H. C., Atkinson, J. D., Umo, N. S., and Webb, M. E.: The relevance of nanoscale biological fragments for ice nucleation in clouds, Sci. Rep., 5, 10.1038/srep08082, 2015.

Ochshorn, E., and Cantrell, W.: Towards understanding ice nucleation by long chain alcohols, J. Chem. Phys., 124, 054714, doi:http://dx.doi.org/10.1063/1.2166368, 2006.

Ogawa, S., Koga, M., and Osanai, S.: Anomalous ice nucleation behavior in aqueous polyvinyl alcohol solutions, Chem. Phys. Let., 480, 86-89, http://dx.doi.org/10.1016/j.cplett.2009.08.046, 2009.

Parsons, I., Fitz Gerald, J. D., and Lee, M. R.: Routine characterization and interpretation of complex alkali feldspar intergrowths, Am. Mineral., 100, 1277-1303, 10.2138/am-2015-5094, 2015

Passarelli, R. E., Chessin, H., and Vonnegut, B.: Ice nucleation by solid solutions of silver-copper iodide, Science, 181, 549-551, 1973.

Petters, M. D., Parsons, M. T., Prenni, A. J., DeMott, P. J., Kreidenweis, S. M., Carrico, C. M., Sullivan, A. P., McMeeking, G. R., Levin, E., Wold, C. E., Collett, J. L., and Moosmüller, H.: Ice nuclei emissions from biomass burning, Journal of Geophysical Research: Atmospheres, 114, 10.1029/2008jd011532, 2009.

Phillips, V., Choularton, T., Illingworth, A., Hogan, R., and Field, P.: Simulations of the glaciation of a frontal mixed-phase cloud with the explicit microphysics model, Q. J. R. Meteorol. Soc., 129, 1351-1371, 2003.

Pinti, V., Marcolli, C., Zobrist, B., Hoyle, C. R., and Peter, T.: Ice nucleation efficiency of clay minerals in the immersion mode, Atmos. Chem. Phys. Discuss., 12, 3213-3261, 10.5194/acpd-12-3213-2012, 2012.

Pitter, R. L., and Pruppacher, H. R.: Wind-tunnel investigation of freezing of small water drops falling at terminal velocity in air, Q. J. R. Meteorol. Soc., 99, 540-550, 10.1002/qj.49709942111, 1973.

Pouleur, S., Richard, C., Martin, J.-G., and Antoun, H.: Ice nucleation activity in fusarium acuminatum and fusarium avenaceum, Appl. Environ. Microb., 58, 2960-2964, 1992.

Pratt, K. A., DeMott, P. J., French, J. R., Wang, Z., Westphal, D. L., Heymsfield, A. J., Twohy, C. H., Prenni, A. J., and Prather, K. A.: In situ detection of biological particles in cloud ice-crystals, Nature Geosci, 2, 398-401, 10.1038/ngeo521, 2009.

Prospero, J. M., Ginoux, P., Torres, O., Nicholson, S. E., and Gill, T. E.: Environmental characterization of global sources of atmospheric soil dust identified with the nimbus 7 total ozone mapping spectrometer (TOMS) absorbing aerosol product, Rev. Geophys., 40, 1002, 10.1029/2000rg000095, 2002.

Pruppacher, H. R., and Klett, J. D.: Microphysics of clouds and precipitation, 2nd ed., Kluwer Academic Publishers, 1997.

Pummer, B. G., Bauer, H., Bernardi, J., Bleicher, S., and Grothe, H.: Suspendable macromolecules are responsible for ice nucleation activity of birch and conifer pollen, Atmos. Chem. Phys., 12, 2541-2550, 10.5194/acp-12-2541-2012, 2012.

Pummer, B. G., Budke, C., Augustin-Bauditz, S., Niedermeier, D., Felgitsch, L., Kampf, C. J., Huber, R. G., Liedl, K. R., Loerting, T., Moschen, T., Schauperl, M., Tollinger, M., Morris, C. E., Wex, H., Grothe, H., Pöschl, U., Koop, T., and Fröhlich-Nowoisky, J.: Ice nucleation by water-soluble macromolecules, Atmos. Chem. Phys., 15, 4077-4091, 10.5194/acp-15-4077-2015, 2015.

Rall, W. F., and Fahy, G. M.: Ice-free cryopreservation of mouse embryos at -196 [deg]c by vitrification, Nature, 313, 573-575, 1985.

Reinhardt, A., and Doye, J. P. K.: Effects of surface interactions on heterogeneous ice nucleation for a monatomic water model, J. Chem. Phys., 141, 10.1063/1.4892804, 2014.

Riechers, B., Wittbracht, F., Hütten, A., and Koop, T.: The homogeneous ice nucleation rate of water droplets produced in a microfluidic device and the role of temperature uncertainty, Phys. Chem. Chem. Phys., 15, 5873-5887, 10.1039/C3CP42437E, 2013.

Rogers, D. C.: Development of a continuous flow thermal gradient diffusion chamber for ice nucleation studies, Atmos. Res., 22, 149-181, 1988.

Sassen, K., and Dodd, G. C.: Homogeneous nucleation rate for highly supercooled cirrus cloud droplets, J. Atmos. Sci., 45, 1357-1369, 1988.

Schnell, R. C., and Vali, G.: Atmospheric ice nuclei from decomposing vegetation, Nature, 236, 163-165, 1972.

Schnell, R. C.: Ice nuclei produced by laboratory cultured marine phytoplankton, Geophys. Res. Lett., 2, 500-502, 10.1029/GL002i011p00500, 1975.

Sear, R. P.: The non-classical nucleation of crystals: Microscopic mechanisms and applications to molecular crystals, ice and calcium carbonate, International Materials Reviews, 57, 328-356, 2012.

Sear, R. P.: Quantitative studies of crystal nucleation at constant supersaturation: Experimental data and models, CrystEngComm, 16, 6506-6522, 10.1039/c4ce00344f, 2014.

Searles, J. A., Carpenter, J. F., and Randolph, T. W.: The ice nucleation temperature determines the primary drying rate of lyophilization for samples frozen on a temperature-controlled shelf, J. Pharm. Sci., 90, 860-871, 10.1002/jps.1039, 2001.

Seifert, P., Kunz, C., Baars, H., Ansmann, A., Bühl, J., Senf, F., Engelmann, R., Althausen, D., and Artaxo, P.: Seasonal variability of heterogeneous ice formation in stratiform clouds over the amazon basin, Geophys. Res. Lett., 42, 5587-5593, 10.1002/2015gl064068, 2015.

Slater, B., Michaelides, A., Salzmann, C. G., and Lohmann, U.: A blue-sky approach to understanding cloud formation, B. Am. Meteorol. Soc., 10.1175/bams-d-15-00131.1, 2015.

Stan, C. A., Schneider, G. F., Shevkoplyas, S. S., Hashimoto, M., Ibanescu, M., Wiley, B. J., and Whitesides, G. M.: A microfluidic apparatus for the study of ice nucleation in supercooled water drops, Lab Chip, 9, 2293-2305, 10.1039/b906198c, 2009.

Stetzer, O., Baschek, B., Lüönd, F., and Lohmann, U.: The zurich ice nucleation chamber (zinc)-a new instrument to investigate atmospheric ice formation, Aerosol Sci. Technol., 42, 64-74, 2008.

Tang, X. C., and Pikal, M. J.: Design of freeze-drying processes for pharmaceuticals: Practical advice, Pharm. Res., 21, 191-200, 2004.

Towey, J. J., and Dougan, L.: Structural examination of the impact of glycerol on water structure, J. Phys. Chem. B, 116, 1633-1641, 10.1021/jp2093862, 2012.

Turnbull, D., and Vonnegut, B.: Nucleation catalysis, Ind. Eng. Chem. Res., 44, 1292-1298, 10.1021/ie50510a031, 1952.

Vali, G., and Stansbury, E. J.: Time-dependent characteristics of heterogeneous nucleation of ice, Can. J. Phys 44, 477-&, 10.1139/p66-044, 1966.

Vali, G.: Nucleation terminology, J. Aerosol Sci., 16, 575-576, 10.1016/0021-8502(85)90009-6, 1985.

Vali, G.: Freezing rate due to heterogeneous nucleation, J. Atmos. Sci., 51, 1843-1856, doi:10.1175/1520-0469(1994)051<1843:FRDTHN>2.0.CO;2, 1994.

Vali, G.: Principles of ice nucleation, in: Biological ice nucleation and its applications, edited by: Lee Jr, R., Warren, G. J., and Gusta, L. V., American Phytopathological Society, St. Paul, Mn, USA, 1-28, 1995.

Vali, G.: Repeatability and randomness in heterogeneous freezing nucleation, Atmos. Chem. Phys., 8, 5017-5031, 10.5194/acp-8-5017-2008, 2008.

Vali, G.: Interpretation of freezing nucleation experiments: Singular and stochastic; sites and surfaces, Atmos. Chem. Phys., 14, 5271-5294, 10.5194/acp-14-5271-2014, 2014.

Vali, G., DeMott, P. J., Möhler, O., and Whale, T. F.: Technical note: A proposal for ice nucleation terminology, Atmos. Chem. Phys., 15, 10263-10270, 10.5194/acp-15-10263-2015, 2015.

Vonnegut, B.: The nucleation of ice formation by silver iodide, J. Appl. Phys., 18, 593-595, 10.1063/1.1697813, 1947.

Vonnegut, B., and Chessin, H.: Ice nucleation by coprecipitated silver iodide and silver bromide, Science, 174, 945-946, 1971.

Wex, H., Augustin-Bauditz, S., Boose, Y., Budke, C., Curtius, J., Diehl, K., Dreyer, A., Frank, F., Hartmann, S., Hiranuma, N., Jantsch, E., Kanji, Z. A., Kiselev, A., Koop, T., Möhler, O., Niedermeier, D., Nillius, B., Rösch, M., Rose, D., Schmidt, C., Steinke, I., and Stratmann, F.: Intercomparing different devices for the investigation of ice nucleating particles using snomax® as test substance, Atmos. Chem. Phys., 15, 1463-1485, 10.5194/acp-15-1463-2015, 2015.

Whale, T. F., Murray, B. J., O'Sullivan, D., Wilson, T. W., Umo, N. S., Baustian, K. J., Atkinson, J. D., Workneh, D. A., and Morris, G. J.: A technique for quantifying heterogeneous ice nucleation in microlitre supercooled water droplets, Atmos. Meas. Tech., 8, 2437-2447, 10.5194/amt-8-2437-2015, 2015a.

Whale, T. F., Rosillo-Lopez, M., Murray, B. J., and Salzmann, C. G.: Ice nucleation properties of oxidized carbon nanomaterials, J. Phys. Chem. Lett., 3012-3016, 10.1021/acs.jpclett.5b01096, 2015b.

Wilson, T. W., Ladino, L. A., Alpert, P. A., Breckels, M. N., Brooks, I. M., Browse, J., Burrows, S. M., Carslaw, K. S., Huffman, J. A., Judd, C., Kilthau, W. P., Mason, R. H., McFiggans, G., Miller, L. A., Najera, J. J., Polishchuk, E., Rae, S., Schiller, C. L., Si, M., Temprado, J. V., Whale, T. F., Wong, J. P. S., Wurl, O., Yakobi-Hancock, J. D., Abbatt, J. P. D., Aller, J. Y., Bertram, A. K., Knopf, D. A., and Murray, B. J.: A marine biogenic source of atmospheric ice-nucleating particles, Nature, 525, 234-238, 10.1038/nature14986, 2015.

Yano, J.-I., and Phillips, V. T. J.: Ice–ice collisions: An ice multiplication process in atmospheric clouds, J. Atmos. Sci., 68, 322-333, doi:10.1175/2010JAS3607.1, 2011.

Zettlemoyer, A. C., Tcheurekdjian, N., and Chessick, J. J.: Surface properties of silver iodide, Nature, 192, 653-653, 1961.

Zhang, X.-X., Chen, M., and Fu, M.: Impact of surface nanostructure on ice nucleation, J. Chem. Phys., 141, 124709, doi:http://dx.doi.org/10.1063/1.4896149, 2014.

Zielke, S. A., Bertram, A. K., and Patey, G. N.: A molecular mechanism of ice nucleation on model agi surfaces, J. Phys. Chem. B, 119, 9049-9055, 10.1021/jp508601s, 2015.

Zobrist, B., Koop, T., Luo, B. P., Marcolli, C., and Peter, T.: Heterogeneous ice nucleation rate coefficient of water droplets coated by a nonadecanol monolayer, J. Phys. Chem., 111, 2149-2155, 10.1021/jp066080w, 2007.

Zolles, T., Burkart, J., Häusler, T., Pummer, B., Hitzenberger, R., and Grothe, H.: Identification of ice nucleation active sites on feldspar dust particles, J. Phys. Chem. A, 119, 2692-2700, 10.1021/jp509839x, 2015.

2. A technique for quantifying heterogeneous ice nucleation in microlitre supercooled water droplets

This chapter has been published in *Atmospheric Measurement Techniques* as:

Whale, T. F., Murray, B. J., O'Sullivan, D., Wilson, T. W., Umo, N. S., Baustian, K. J., Atkinson, J. D., Workneh, D. A., and Morris, G. J. 'A technique for quantifying heterogeneous ice nucleation in microlitre supercooled water droplets', AMT (2015).

Abstract

In many clouds, the formation of ice requires the presence of particles capable of nucleating ice. Ice nucleating particles (INPs) are rare in comparison to cloud condensation nuclei. However, the fact that only a small fraction of aerosol particles can nucleate ice means that detection and quantification of INPs is challenging. This is particularly true at temperatures above about -20°C since the population of particles capable of serving as INPs decreases dramatically with increasing temperature. In this paper, we describe an experimental technique in which droplets of microlitre volume containing ice nucleating material are cooled down at a controlled rate and their freezing temperatures recorded. The advantage of using large droplet volumes is that the surface area per droplet is vastly larger than in experiments focused on single aerosol particles or cloud-sized droplets. This increases the probability of observing the effect of less common, but important, high temperature INPs and therefore allows the quantification of their ice nucleation efficiency. The potential artefacts which could influence data from this experiment, and other similar experiments, are mitigated and discussed. Experimentally determined heterogeneous ice nucleation efficiencies for K-feldspar (microcline), kaolinite, chlorite, NX-illite, Snomax®, and silver iodide are presented.

2.1. Introduction

Cloud droplets can supercool to temperatures below -37°C (Rosenfeld and Woodley, 2000), but can freeze at much warmer temperatures in the presence of ice nucleating particles (INPs). In fact, mixed-phase stratus clouds are observed to glaciate at temperatures warmer than -15°C, but only in certain locations (Kanitz et al., 2011). In addition, ice formation in the ice multiplication regime around -3 to -8°C is critically important in the formation of precipitation from convective clouds (Crawford et al., 2012;Pruppacher and Klett, 1997). However, recent assessments of laboratory ice

nucleation data for a range of atmospherically relevant materials concluded that it is unclear which aerosol species trigger freezing above -15°C (Murray et al., 2012;Hoose and Möhler, 2012). Part of the problem is that many quantitative experimental techniques for determining ice nucleation efficiency are not sufficiently sensitive to quantify the efficiency of many nucleants at temperatures warmer than -15°C.

There are a number of instrument types that have been used for research into immersion mode ice nucleation and reviews on the subject are available (Hoose and Möhler, 2012;Murray et al., 2012). These instruments include cloud chambers e.g. (Jiang et al., 2014;Niemand et al., 2012;Cotton et al., 2007), continuous flow diffusion chambers (CFDCs) e.g. (Salam et al., 2006;Rogers et al., 2001) and a wide variety of droplet freezing experiments e.g. (Knopf and Alpert, 2013;Vali, 2008;Murray et al., 2011;Budke and Koop, 2015). Cloud chambers and CFDCs quantify the ice nucleation ability of a dispersion of aerosol particles as a function of relative humidity and temperature. In contrast, droplet freezing experiments tend to have multiple particles suspended in individual water droplets.

A common way of quantifying the ice nucleation efficiency of a material is using the ice active surface site density, n_s ,which is the cumulative number of nucleation sites per unit surface area of nucleant that become active on cooling from 0ºC to a temperature T (Connolly et al., 2009).

$$\frac{n(T)}{N} = 1 - \exp(-n_s(T)A) \quad (1)$$

Where $n(T)$ is the number of droplets frozen at temperature (T), N is the total number of droplets in the experiment and A is the surface area of nucleant per droplet. In using this approximation it is assumed that the time dependence of nucleation arising from the stochastic nature of ice nucleation is negligible.

In general, instrumentation employing single aerosol particles suspended in gas and droplet experiments working with cloud sized droplets (10's of micrometers) report values of n_s down to about 10^3 cm^{-2} (e.g. see Fig. 18 of Murray et al., 2012 for a compilation). These measurements are clearly valuable and applicable to the atmosphere, but even smaller n_s values are also relevant (Murray et al., 2012). For example, if we consider a dust influenced atmosphere with 5 dust particles per cubic centimetre with a mean radius of 500 nm, then in order to generate 10 ice crystals per cubic metre an n_s of only 60 cm^{-2} would be required. Hence, it is important that we have the capacity to measure n_s smaller than 10^3 cm^{-2} in addition to the capacity to measure larger values.

Our experimental approach builds on techniques employing aliquots of water much larger than the dimensions of typical cloud droplets which have been used since the very early days of ice nucleation studies (Vali, 1995;Vali, 1971) and continue to be used in the present day (Stopelli et al., 2014;Conen et al., 2011;Knopf and Forrester, 2011;Garcia et al., 2012;Budke and Koop, 2015). The advantage of this approach is that the surface area of nucleant per droplet scales with the volume of the droplet (for a constant mass fraction of nucleant in water). Hence, increasing the size of droplet from cloud droplet sizes (~10 µm; picolitre) to 1 mm (microlitre) increases the surface area per droplet by six orders of magnitude. This allows the quantification of n_s to much smaller values than is possible using cloud sized droplets.

The basic concept of a droplet freezing experiment (or droplet freezing assay) is to take an aqueous suspension and subdivide it into multiple aliquots of ideally identical volume; although polydisperse droplet distributions can also be used (Vali, 1971;Murray et al., 2011). The multiple droplets are then cooled identically. Experiments can be conducted using either a constant cooling rate, isothermally or with a stepped temperature profile, and have differed widely in terms of droplet volume, droplet production and cooling method (Vali, 1995). The fraction of droplets frozen at a given temperature or after a certain time interval can hence be determined. There are various methods of analysing the resultant data (Vali, 2014). These include deterministic models (such as equation 1) that link droplet fraction frozen directly to temperature e.g. (Vali, 1971) and time dependent models of varying complexity (e.g. (Marcolli et al., 2007;Herbert et al., 2014;Broadley et al., 2012).

In this paper we present a method of conducting a droplet freezing experiment using microlitre scale droplets. While the principle of the technique is not new, the specific application of the technique is and the aim of this paper is to document the equipment, methods and analysis associated with the technique. Our instrument, the microlitre Nucleation by Immersed Particle Instrument (µl-NIPI), is based around a Stirling cryocooler which cools a hydrophobic surface that supports microlitre volume droplets. The freezing of the droplets is monitored using a digital camera. We present new data for the nucleation efficiency of K-feldspar (microcline), kaolinite, chlorite, NX-illite, Snomax® and silver iodide. This data is used to illustrate several potential freezing artefacts and how to avoid them.

2.2. Description of the µl-Nucleation by Immersed Particle Instrument (µl-NIPI)

The µl-NIPI forms part of a suite of instruments which are designed to make measurements of n_s over 10 orders of magnitude, thus covering the range relevant for the atmosphere. We have previously described a droplet freezing technique using picolitre volume droplets which has been used to study mineral dusts (Atkinson et al., 2013;Broadley et al., 2012;Murray et al., 2011), soil particles (O'Sullivan et al., 2014) and homogeneous nucleation (Murray et al., 2010), and a technique using nanolitre droplets with soil (O'Sullivan et al., 2014) and combustion ash particles (Umo et al., 2014). The microlitre technique described in detail here has been used to study ice nucleation by mineral dusts (Atkinson et al., 2013), soil (O'Sullivan et al., 2014), nanoscale INPs (O′Sullivan et al., 2015), combustion ash (Umo et al., 2014) and time dependence of nucleation by kaolinite and K-feldspar (Herbert et al., 2014). This instrument was also included in an intercomparison between 17 instruments (Hiranuma et al., 2015). The resulting n_s values for nx-illite were within one order of magnitude of other immersion mode instruments, whereas the cloud chamber and FRIDGE instruments report larger n_s values in the same temperature range. The causes for this discrepancy are not clear, but are discussed by Hiranuma et al (2015).

The µl-NIPI also offers a number of advantages over some other instruments: Experiments can be performed relatively quickly; freezing events are easy to detect and the continuous monitoring of freezing during a controlled temperature ramp allows the generation of a nucleation spectrum; and in addition, as it has no need for cooling fluids and the equipment is portable allowing it to be readily deployed in field settings.

The general layout of the µl-NIPI is shown in Figure 2.1.The µl-NIPI consists of a cold stage, a hydrophobic surface which supports the droplets, an enclosure in which the humidity experienced by the droplets can be controlled, and a digital camera to monitor the state of the droplets. To provide cooling and temperature monitoring, a Grant-Asymptote EF600 cold stage was employed. The EF600 was developed for the purpose of cooling samples for biological cryopreservation and can control the temperature of a sample between 20 °C and -100 °C. For cryopreservation, a top plate capable of holding multiple cryovials is typically employed. However, a flat aluminium top plate is also available and was used for this experimental setup. To conduct a droplet freezing experiment, a 22 mm diameter hydrophobic silanised glass slide of 0.22 mm thickness (Hampton Research HR3-231) was placed onto this flat top plate. Prior to the

experiments, the slide was cleaned using water, methanol, and chloroform. Around 40 droplets of 1 µl volume were pipetted onto the slide using a Picus Biohit electronic pipette while the slide was at room temperature. To ensure that individual droplets contained the same amount of material the suspensions were stirred during the pipetting process. The uncertainty in volume quoted by the manufacturer is ± 0.025 µl. The droplets and slide were then covered within a Perspex chamber with ports for a camera (Microsoft Lifecam HD) and stainless steel pipes for delivering a gas flow to the cell. A recessed rubber O-ring was used to seal the chamber to the EF600 cold stage and an O-ring is also used to seal the camera opening. Both O-rings were coated with vacuum grease. A flow of dry zero grade nitrogen (0.2 l/min) was passed through the cell in order to prevent frost growth (see discussion in section 3.1).

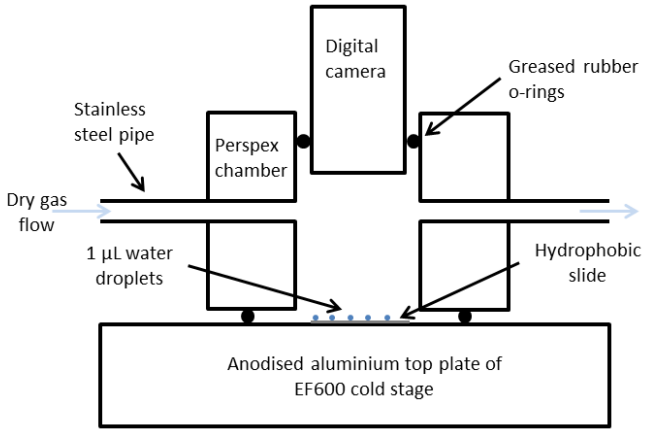

Figure 2.1: Diagram illustrating the key components of the µL-NIPI.

The EF600 was internally controlled by a Eurotherm 2416 PID controller, run via Eurotherm's iTools control software. For all work presented here, this software was used to program and commence a 1 °C min^{-1} temperature ramp from 1 °C to -35 °C. Once the ramp was commenced data logger software associated with the EF600 was started and used to produce a log of temperature against time. A LabView program was used to record an image series from the digital camera, typically at a rate of 1 frame per second, and to produce a timestamp for each frame. Hence, the temperature of the cold stage during each frame was known. Videos were reviewed frame by frame and the temperature of freezing of each droplet recorded. Stills from the digital camera at several stages in the freezing experiment are shown in Figure 2.2. The first change in droplet structure leading to droplet freezing was taken to be the nucleation event and this information was used to establish the fraction of droplets frozen as a function of temperature.

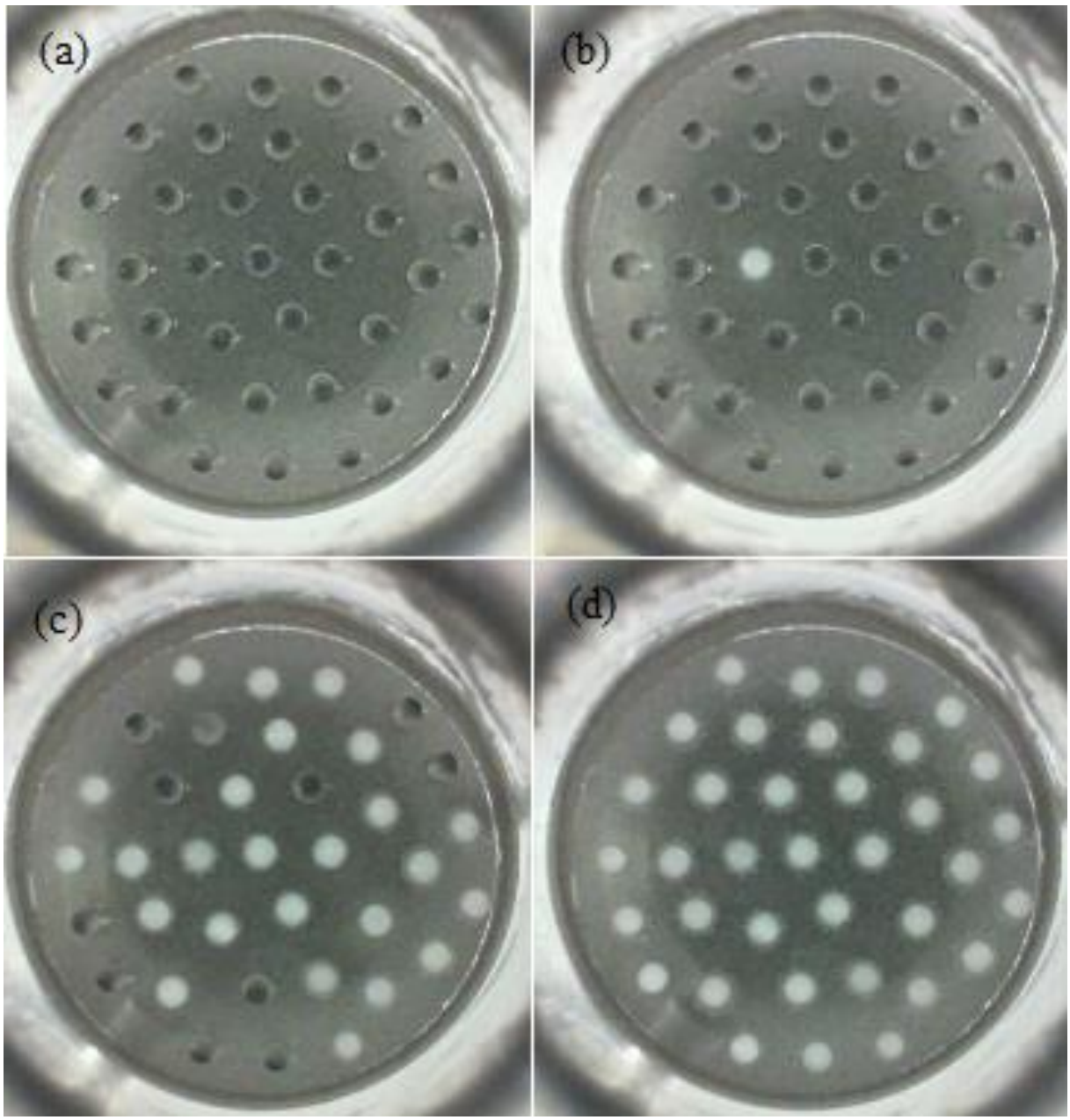

Figure 2.2: The progression of a µl-NIPI freezing experiment. The experiment shown used a dispersion containing 0.01 wt% K-feldspar. Frame (a) was taken at around -10 °C, shortly before the onset of freezing, frame (b) immediately after the first droplet had frozen, frame (c) at -14 °C and frame (d) at -20 °C, after the completion of freezing. The top left of frame (c) shows a droplet in the process of freezing. Droplets of this size typically take 2 - 4 seconds to freeze completely, proceeding much faster at lower temperatures. The initial change in the droplet leading to freezing is taken as the occurrence of ice nucleation.

The EF600 has a quoted temperature uncertainty of ±0.15 °C at -7 °C. To check the reliability of temperature measurement across a range of temperatures, a variety of compounds with known melting points were frozen and then melted by heating at 0.1 °C min^{-1}. The melting temperature range was determined visually. Results from this process

are presented in Table 2.1. It is necessary to calibrate using melting points, rather than freezing points, crystallisation observed during cooling is always subject to nucleation making them unsuitable for calibration of temperature unless the nucleation temperatures are very well defined (Riechers et al., 2013). By propagating the temperature error of the EF600 and the melting point range seen for water a maximum temperature error of ±0.4 °C has been estimated.

Table 2.1: Melting points of solvents used to calibrate temperature of the µl-NIPI. Recorded melting points are the average of 5 measurements. Literature melting points were taken from the 2007 CRC hand book.

Chemical	Literature melting temperature (°C)	Recorded melting temperature (°C)	Standard deviation of melting point	Start (°C)	Finish (°C)	Range (°C)
Dodecane	-9.57	-9.5	0.09	-9.7	-9.3	0.4
Octanol	-14.8	-14.9	0.08	-15.1	-14.8	0.4
Undecane	-25.5	-25.4	0.10	-25.7	-25.3	0.4
Water	0.00	0.27	0.13	-0.1	0.6	0.7

2.2.1. Suspension preparation

As in previous studies suspensions of solid material in Milli-Q purified water (18.2 MΩ·cm) are made up gravimetrically and are then mixed using a magnetic stirrer plate overnight (Atkinson et al., 2013;O'Sullivan et al., 2014). In this study we used four mineral dusts (K-feldspar, kaolinite, chlorite and NX illite), Snomax® (a commercial ice nucleant derived from *Pseudomonas syringae* bacteria), and silver iodide (details in Table 2). Mineralogies and other details are given in Table 2.2. The specific surface area of K-feldspar sample used was measured using the Brunauer–Emmett–Teller (BET) N_2 adsorption method using a Micromeritics TriStar 3000. The data presented in Section 4 using these nucleants is to illustrate the utility of the µl-NIPI and also illustrate potential artefacts the user should be aware of and how to avoid them. Uncertainty in surface area

per droplet has been estimated at around ±15% by propagating uncertainties in weighing of samples, the BET surface area and the volume error of the pipette.

Table 2.2: Characteristics of the materials used in this study. For silver iodide and Snomax® BET surface areas are not reported.

Nucleant	N_2 BET surface area (m^2 g^{-1})	Purity	Impurities	Supplier	Reference
K-feldspar (microcline)	1.86	78.1%	3.9% quartz, 16.0% Na/Ca feldspar	Bureau of Analysed Samples, UK	(Atkinson et al., 2013)
KGa-1b kaolinite	11.2	96%	Crandallite, mica, illite. anatase	Clay Mineral Society	(Chipera and Bish, 2001;Murray et al., 2011)
NX illite	104.2	Mixed dust	-	Arginotec	(Hiranuma et al., 2015;Broadley et al., 2012)
Chlorite	25.0	99.6%	unknown	School of Earth and Environment Specimen Collection	(Atkinson et al., 2013)
Silver iodide	-	99.9999%	-	Alfa-Aesar premion	-
Snomax®	-	-	-	York Snow Inc.	-

2.2.2. Control experiments

Droplets on the microlitre scale are notoriously difficult to produce free of any heterogeneous INPs. For example, Langham and Mason (1958) recorded a median freezing temperature of around -28°C for droplets of a volume on the order of a few microlitres and only occasionally saw drops reaching what is thought to be homogeneous nucleation temperatures (~ -33 °C; Murray et al., 2010) in a system that suspended water droplets between two liquids of different densities. This was despite the use of a complex distillation system to obtain high purity water. To the best of our knowledge, only Fornea et al. (2009) have reported being able to reach the freezing temperatures predicted by CNT for microlitre volume droplets repeatably, reporting an average freezing temperature of -33.1 ± 0.6 °C for 2.0 µl droplets of high-performance liquid chromatography water. Given the difficulty in producing microlitre droplets free of suspended INPs and surfaces free of ice active sites or contaminants it is necessary to establish the temperature limit below which freezing cannot be assumed to have been induced by a heterogeneous nucleant.

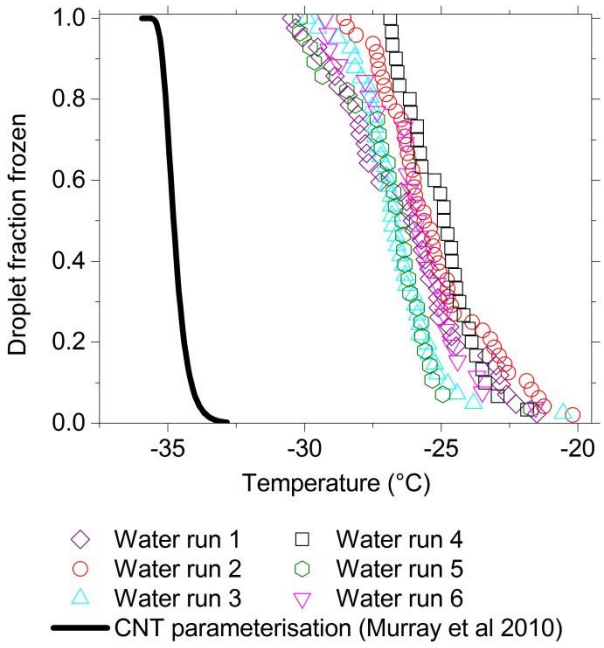

Figure 2.3: Temperature against fraction frozen for 6 different experiments using Milli-Q water. Also included is a line indicating the temperature of freezing expected for 1 µl pure water droplets from Classical Nucleation Theory (CNT) according to the parameterisation by Murray et al (2010).

Freezing temperatures for Milli-Q water droplets are shown in Figure 2.3. These droplets froze mostly between -20 and -30°C, substantially above the temperatures expected for

homogeneous nucleation. Additionally, there is a 2-3 degree spread in the freezing temperatures of separate experiments, which is larger than would be expected if the freezing pathway was homogeneous. We conclude that there are variable quantities of heterogeneous ice nucleating sites present that are active below about -20°C, but it is not clear if nucleation is occurring on the slide or on impurities in the water. Milli-Q water is filtered through a 0.22 µm filter and is specified to have less than 1 particle per millilitre larger than this size. However, no specification is provided for smaller particles. Impurities could also be introduced at points during the experimental procedure or from airborne particles in the laboratory. In light of these control experiments, -20°C has been taken as the lower limit for most of the heterogenous ice nucleation experiments in this study.

2.3. Discussion of potential artefacts and uses of droplet freezing experiments

Droplet freezing experiments can suffer from a range of practical difficulties. This section addresses these problems and the solutions employed. As discussed by Stopelli et al. (2014), certain problems are encountered when using open droplet systems, where droplets are arranged on a hydrophobic surface, compared to closed droplet experiments, where each droplet is held in a separate container, or under inert oil. In an open droplet system there is potential for droplets to evaporate over time, for contamination of droplets from airborne particles or for the freezing of droplets to influence neighbouring droplets by frost growth or splintering. As the µl-NIPI is an open droplet system these issues must be overcome. Closed droplet systems avoid some of these problems, but monitoring of freezing becomes more challenging as the droplets are not easily visible (Stopelli et al., 2014).

2.3.1. Frost Growth

Early experiments on the apparatus were conducted without a flow of dry N_2 over the droplets. This can cause significant issues when freezing of a droplet induces freezing in nearby droplets. Images of experiments with and without a dry flow of gas are shown in Figure 2.4. In these experiments 10 droplets were seeded with silver iodide while the remainder were composed of pure water. When there was no flow of dry gas (panel b) there is extensive frost on the surface which triggers freezing in neighbouring droplets; this artificially enhances the number of frozen droplets by 80% at -12°C in this case. Panel a shows an experiment conducted with a dry flow in which the seeded droplets froze at

around -5°C, as expected, while the pure water droplets remained liquid down to below -20°C, indicating that with a dry flow there is no enhancement of freezing temperatures due to frost growth.

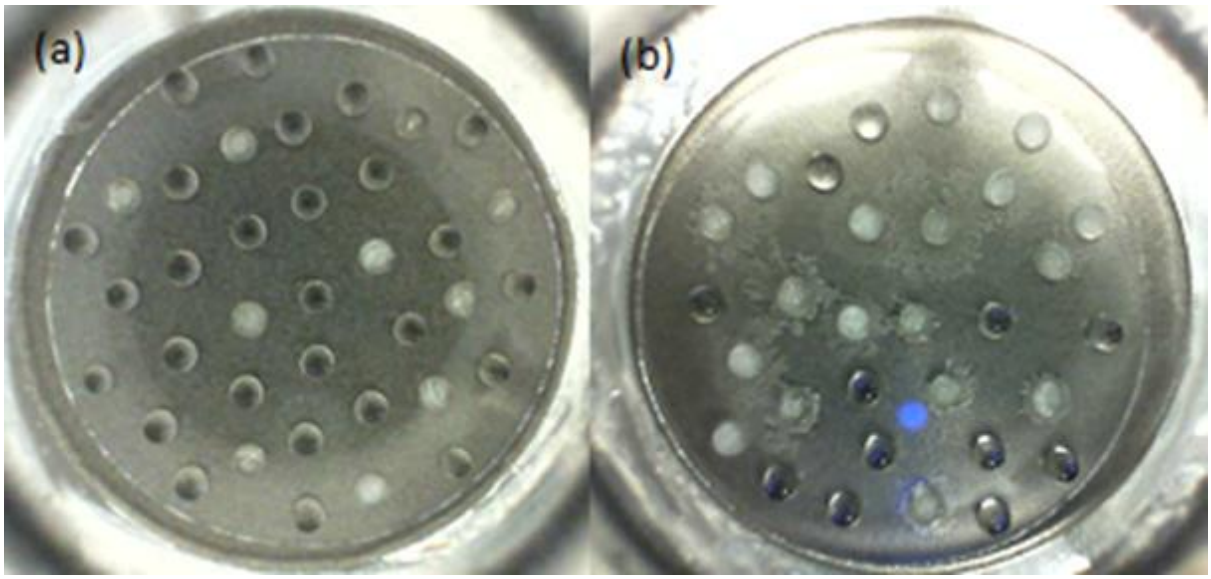

Figure 2.4: Examples of experiments conducted (a) with and (b) without a flow of dry nitrogen gas. a) shows a single frame from an experiment where 10 droplets containing silver iodide were spread among droplets of pure water. A dry flow was employed to ensure ice growth did not take place. b) Shows a similar experiment where the dry flow was not employed and the resultant growth of ice across the slide which triggered freezing in pure water droplets. Both frames were taken at -12 °C.

There are two distinct origins of the frost on the surface. Firstly, Jung et al. (2012) describe the formation of liquid condensation haloes, formed by the sudden increase in vapour pressure of water associated with the latent heat release of droplet freezing. They show that this halo can freeze if it persists. After freezing, subsequent frost growth directly from the vapour phase could come into contact with neighbouring droplets and trigger freezing in those droplets. Both of these effects have the potential to artificially increase the fraction frozen and the problem will be most acute if the droplets freeze over a wide range of temperatures (our test with silver iodide containing droplets next to pure water droplets represents an extreme case). Our example illustrates that the use of a 0.2 l min^{-1} flow of dry gas eliminates the problems of frost haloes and frost growth. The condensation halo, consisting of very small droplets, evaporates rapidly in low humidity conditions and frost growth is reduced to the extent that it does not impact neighbouring droplets. Some small amount of frost growth is still observed in the immediate vicinity of

a frozen droplet, taking the form of a very narrow ring around the droplet, but it does not extend far enough to interfere with neighbouring droplets. The flow of zero grade nitrogen has the additional benefit that it flushes the chamber reducing the chance of contact with aerosol particles from external sources.

2.3.2. Droplet Evaporation

Using a dry flow as described in section 3.1 has the potential to introduce additional issues. Droplets will evaporate to some extent through the course of the experiment (the extent will depend on the length of the experiment). This will increase the concentration of the contents of the droplets. Current descriptions of heterogeneous ice nucleation assume that the freezing temperature is dependent on the surface area of nucleant in a droplet, which will be constant despite evaporation. Therefore, it is assumed that changes in droplet volume will not affect experimental results. If solution droplets are being analysed, concentration changes due to droplet shrinkage will need to be accounted for as colligative effects will change the nucleation temperatures (Zobrist et al., 2008).

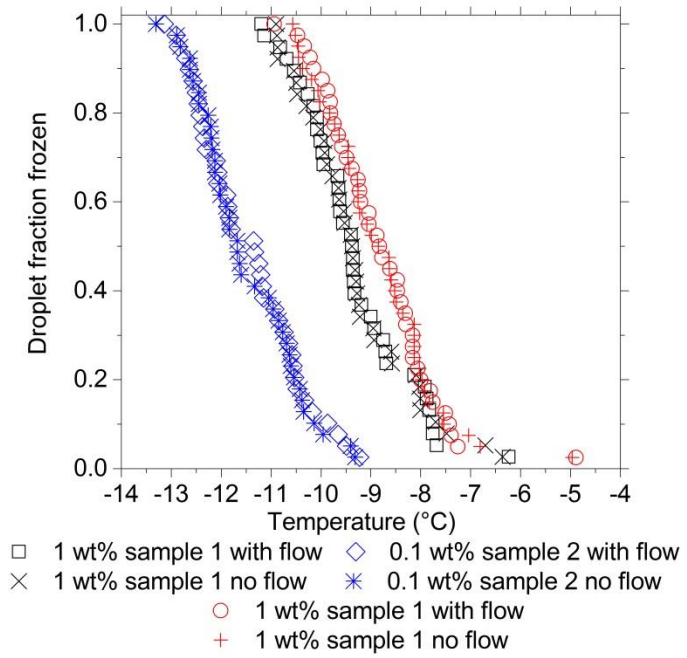

Figure 2.5: Temperature against droplet fraction frozen with and without dry gas flowing over them. Four different sets of droplets containing K-feldspar were used. It can be seen that switching the dry flow on or off made no systematic difference to freezing temperatures.

A second potential problem is that evaporation of water from droplets will cause cooling and may lead to the droplets being colder than the cold stage temperature. In order to test for this evaporative cooling effect a series of experiments was conducted both with and

without the dry flow. Droplets containing 0.1 wt% and 1 wt% K-feldspar were tested with the dry flow switched on. They were then thawed and refrozen with the dry flow switched off. Figure 2.5 shows the results of this experiment. Freezing by K-feldspar is described well by a singular model (Herbert et al., 2014), suggesting that each droplet freezes with a repeatable characteristic temperature (Vali, 2014, 2008;Wright and Petters, 2013). Freezing temperatures did not shift, showing that the cooling effect of the dry flow is smaller than the temperature measurement uncertainty (± 0.4°C). The small freezing temperature range of these experiments (~4 °C) meant that frost growth from frozen droplets did not spread to neighbouring droplets even with the dry flow switched off.

2.4. Test experiments and analysis

Several example datasets are presented here to demonstrate the efficacy of the µl-NIPI. The freezing temperatures for droplets containing K-feldspar (microcline), kaolinite, chlorite, Snomax®, and silver iodide are shown in Figure 2.6. The concentration of K-feldspar was varied between 0.01 and 1 wt%, and as expected the droplets containing more K-feldspar froze at a higher temperature. Droplets containing 1 % chlorite and kaolinite froze at lower temperatures than droplets containing K-feldspar which is consistent with Atkinson et al. (2013) who presented a case suggesting that K-feldspar is the most important mineral component of atmospheric mineral dusts.

Silver iodide is known to be capable of nucleating ice at high temperatures (DeMott, 1995;Vonnegut, 1947), and even with a mass concentration 100 times less than that of 1 wt% K-feldspar it still nucleated ice at higher temperature. Interestingly, when a 0.1 wt% suspension was left on a windowsill for several days in a glass vial the freezing temperature increased by around 2 °C. There is a precedent for light exposure improving of the ice nucleating ability of silver iodide in the literature, albeit in deposition mode, rather than immersion mode (Rowland et al., 1964). There is also evidence from older work showing that light exposure can reduce the effectiveness of silver iodide as an ice nucleus (Fletcher, 1959;Smith et al., 1955). Further work is necessary to understand and quantify these effects.

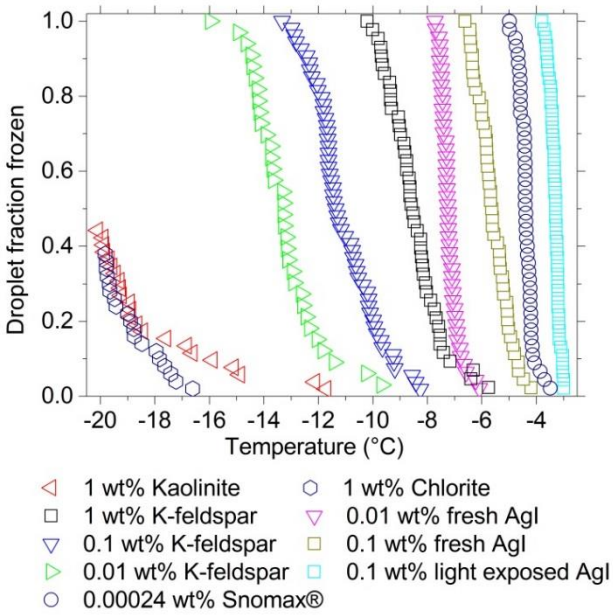

Figure 2.6 Temperature against fraction frozen for a variety of nucleants with a range of concentrations. The freezing temperature of droplets containing K-feldspar can be seen to steadily increase with increasing K-feldspar contamination.

Snomax® is a commercial preparation which contains fragments of a cultivated strain of *Pseudomonas Syringae* and is used in the production of artificial snow at ski resorts (Cochet and Widehem, 2000). Droplets containing Snomax® nucleated ice around -4ºC in this set of test experiments. Again, Snomax® is likely to exhibit variability in its ice nucleation activity between batches and individual samples depending on storage history, hence quantitative comparison with previous data is difficult. Nevertheless, Möhler et al. (2008) also report freezing by Snomax® containing droplets at very high temperatures with about 1% of particles freezing at -5.6ºC. Hartmann et al. (2013) observed freezing in Snowmax containing droplets at temperatures up to -6ºC. Similarly, Wood et al. (2002) report freezing up to -6ºC in free falling micron-scaled droplets containing Snomax®. One feature reported in these previous studies is that the probability of freezing increases very steeply with decreasing temperature, which is again qualitatively consistent with our present measurements where the fraction frozen curve is extremely steep (Figure 2.6). Recently, Wex et al. (2015) have published an extensive intercomparison of instruments using Snomax® as the test sample. The most similar instrument to µL-NIPI intercompared, BINARY (Budke and Koop, 2015) gave qualitatively very similar results to those generated here at the most similar weight fraction tested. Our experiment (2.4×10^{-4} wt%) and those from from Wex et al. (2015) (2.9×10^{-4} wt%) both gave very steep fraction frozen curves at -4°C.

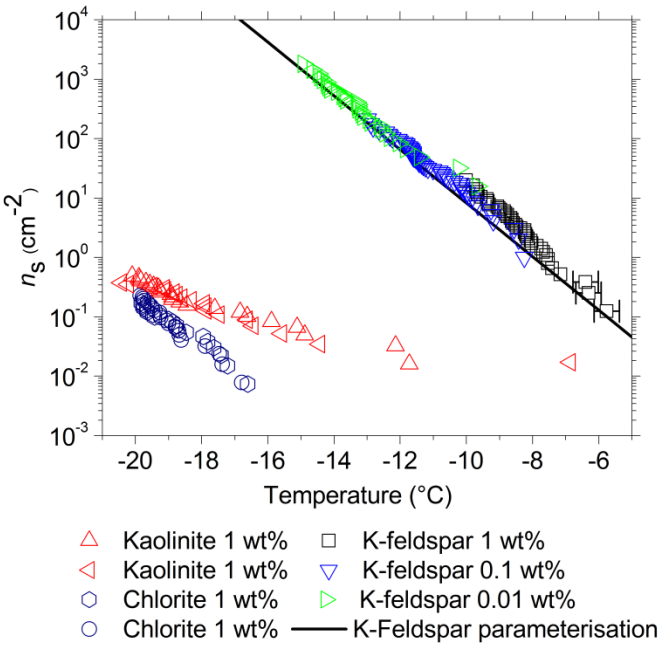

Figure 2.7: n_s values for K-feldspar, kaolinite and chlorite. Example temperature error bars are shown on the first three points of the 1 wt% K-feldspar experiment. Estimated uncertainty in n_s due to uncertainty in the surface area of material per droplet is estimated at ±15 % and is too small to be shown on the chart. The K-feldspar parameterisation is from Atkinson et al. (2013).

While droplet freezing temperatures and fraction frozen data is useful for comparing ice nucleation abilities of different materials within the context of a single experimental setup, it is necessary to normalise the data to some measure of the amount of material per droplet, typically surface area (Murray et al., 2012). The resulting values of n_s are shown in Figure 2.7, and we start this discussion with the data for K-feldspar. Over the three experiments the mineral surface area per droplet was varied by two orders of magnitude and the n_s values fall on a single line and the data is in good agreement with our previous study by Atkinson et al. (2013). Atkinson et al. (2013) produced this parameterisation for K-feldspar through a combination of experiments with the µL-NIPI and pL-NIPI. The K-feldspar used in the present study is from the same stock sample used by Atkinson et al. (2013) but was ground separately and has a different specific surface area; 1.86 $m^2 g^{-1}$ rather than 3.15 $m^2 g^{-1}$ for the powder used by Atkinson et al. (2013). The chlorite and kaolinite n_s values are much lower than the K-feldspar values, as expected and are consistent with the conclusions of Atkinson et al. (2013). The data in Figure 2.7 also illustrate the reproducibility of the derived n_s values with this technique, with repeat runs for kaolinite and chlorite being identical within uncertainty.

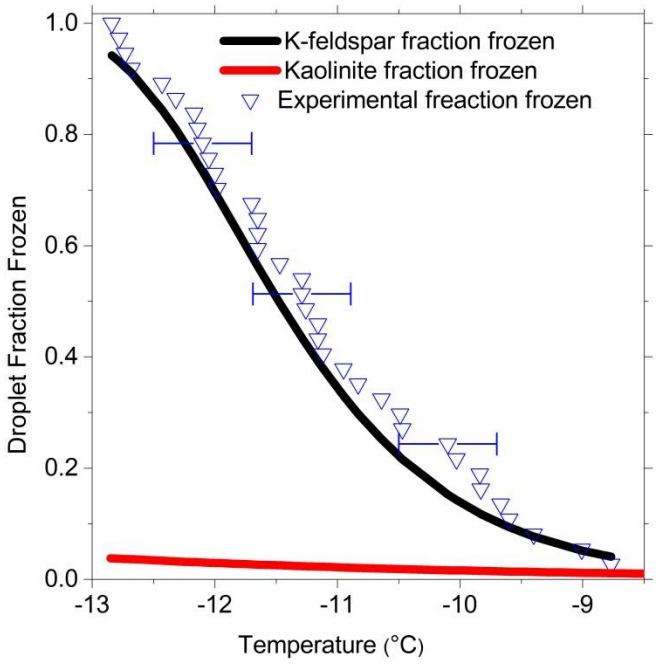

Figure 2.8: Fraction frozen for water droplets contaminated with 0.1 wt% K-feldspar and 1 wt% kaolinite. For comparison the expected fractions calculated from parameterisations for n_s for relevant amounts of each material are included. In each droplet there is approximately 60 times more surface area of kaolinite than K-feldspar. Nevertheless, the experimental fraction frozen clearly tracks the fraction frozen calculated based upon the K-feldspar component. This demonstrates why it is important to quantify the precise composition of mineral dusts for ice nucleation measurements.

By using relatively large droplets containing large surface areas of heterogeneous nucleants, higher freezing temperatures can be accessed using the µL-NIPI than are possible in smaller scale droplet freezing experiments or techniques employing particles dispersed in gas. A consequence of this is very small amounts of a relatively efficient nucleant can dominate the ice nucleating ability of a given sample. For instance, if an impurity in a material is 1000 times more active than the bulk material, i.e. its n_s is 1000 times higher than that of the bulk material, then the probability of freezing due to a 1 wt% contamination would be 10 times higher than of the bulk material and the impurity would dominate observed ice nucleation. This effect is illustrated in Figure 2.8, where a sample containing a 60 times larger surface area of kaolinite than K-feldspar is shown to nucleate ice at essentially the same temperatures that the K-feldspar component of the mixture would be expected to do so. In this example it would easy to attribute the ice nucleation activity observed to kaolinite, when in fact it all comes from the feldspar 'contaminant'. If the aim of a study is to further fundamental understanding of ice nucleation by a particular material it is important to recognise the potential impact of small impurities

when working with larger droplets. While it is true that such an issue might also be observed with systems investigating smaller droplets, the smaller the amount of material in a droplet the less chance there is of a contaminating particle being present. Hence, there is a trade-off between measuring smaller n_s values and increasing the risk of contamination by minor components.

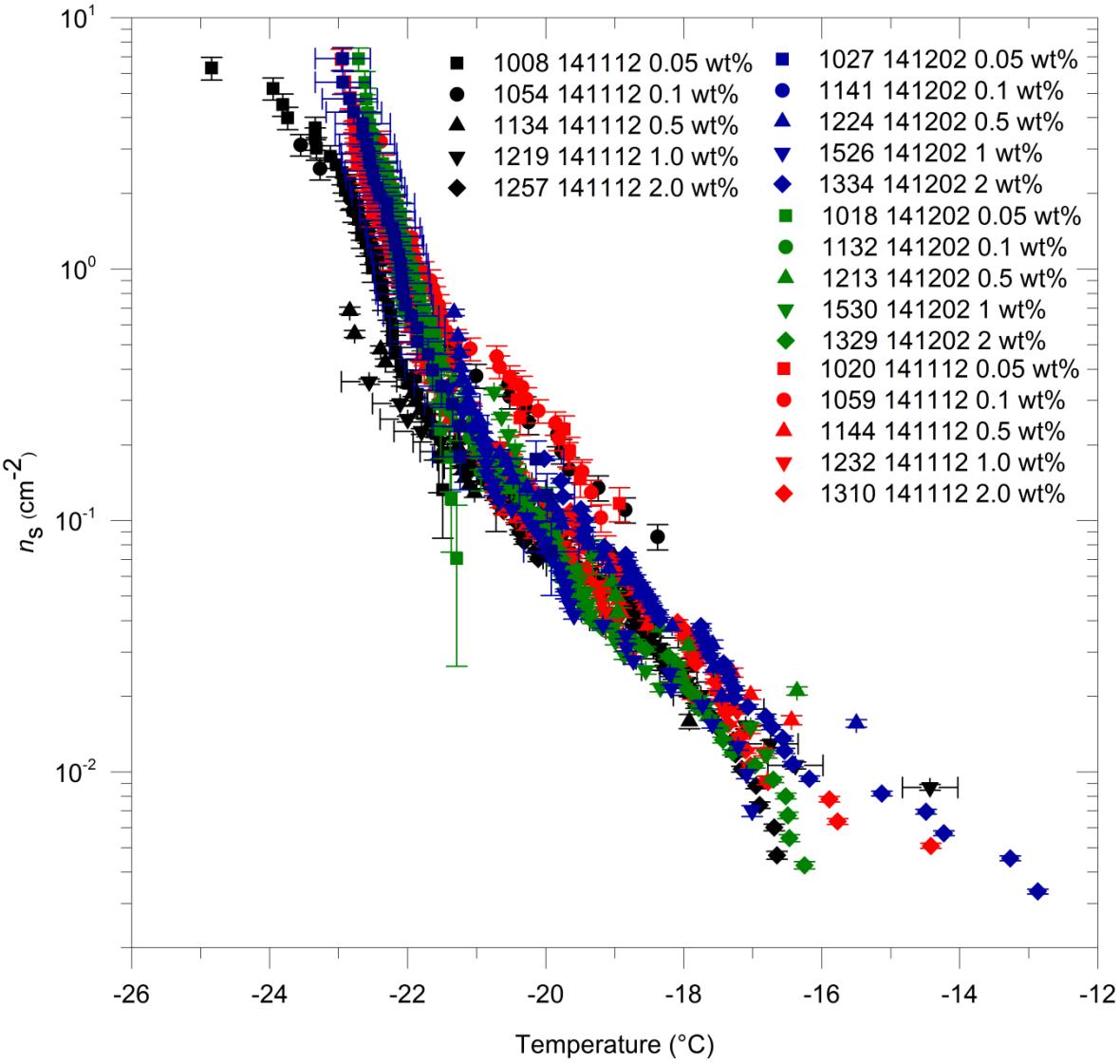

Figure 2.9: n_s values for NX-illite determined from experiments with suspensions of a range of concentrations. Y-Error bars have been calculated using the background subtraction method described in O'Sullivan et al (2015) which includes the error propagation described in section 2.1. X-Error bars have included on certain datasets to facilitate comparison.

Some materials such as mineral dusts are known to aggregate when in aqueous suspension and it has been hypothesised that this could lead to a reduced surface area and therefore underestimate in n_s (Hiranuma, 2015; Emersic, 2015). It is known that that aggregation

of mineral dusts is concentration dependent (Emersic et al. 2015), hence reducing the dust concentration should reduce the impact on n_s. In order to test if aggregation is affecting our measured n_s we have performed a sequence of experiments with NX-illite suspensions of concentrations ranging from 0.05 to 2 wt% (see Figure 2.9). It can be seen that the resulting n_s values are self-consistent, indicating that occlusion of surface are by aggregation is not significant. Aggregates that do form are sufficiently porous that water can still reach all relevant surfaces of the dust. In addition, n_s for droplets containing 0.01 to 1 wt% K-feldspar also falls on a single line (Figure 2.7), suggesting that aggregation does not lead to the occlusion of surface area in K-feldspar either. Although aggregation does not affect n_s in these mineral dusts, it is worth bearing in mind that aggregation could conceivably reduce surface area in some nucleants and it is therefore well worth testing for this by varying nucleant concentration and checking for consistency.

2.5. Summary

A new design of droplet freezing experiment for ice nucleation experiments has been constructed and tested. The µl-NIPI uses a Stirling engine based cryocooler to cool microlitre volume droplets at a controlled rate in order to determine the efficiency with which immersed particles nucleate ice. Many modern atmospheric ice nucleation measurement techniques measure the nucleation by aerosolised particles or particles suspended in cloud sized droplets. The advantage of working with droplets much larger than cloud droplets is that they contain a far larger surface area of nucleant. This allows the determination of nucleation efficiencies over a wider range of temperatures than is possible using only smaller droplets and complement the flowing aerosol and cloud-sized droplet techniques in widespread use.

In most ice nucleation experiments, efficient minor components in samples can dominate observed results, meaning that great care is needed in interpretation of results. While this is particularly true for experiments using such relatively large amounts of sample as the technique presented here, the ability to detect the activity of relatively rare, high temperature ice nucleation events is valuable. The µl-NIPI may be particularly useful in a field setting, where its low detection limit and simplicity of operation offer advantages over, and complementarity to, more complex instruments.

References

Atkinson, J. D., Murray, B. J., Woodhouse, M. T., Whale, T. F., Baustian, K. J., Carslaw, K. S., Dobbie, S., O'Sullivan, D., and Malkin, T. L.: The importance of feldspar for ice nucleation by mineral dust in mixed-phase clouds, Nature, 498, 355-358, 10.1038/nature12278, 2013.

Broadley, S. L., Murray, B. J., Herbert, R. J., Atkinson, J. D., Dobbie, S., Malkin, T. L., Condliffe, E., and Neve, L.: Immersion mode heterogeneous ice nucleation by an illite rich powder representative of atmospheric mineral dust, Atmos. Chem. Phys., 12, 287-307, 10.5194/acp-12-287-2012, 2012.

Budke, C., and Koop, T.: Binary: An optical freezing array for assessing temperature and time dependence of heterogeneous ice nucleation, Atmos. Meas. Tech., 8, 689-703, 10.5194/amt-8-689-2015, 2015.

Chipera, S. J., and Bish, D. L.: Baseline studies of the clay minerals society source clays: Powder x-ray diffraction analyses, Clays Clay Miner., 49, 398-409, 10.1346/ccmn.2001.0490507, 2001.

Cochet, N., and Widehem, P.: Ice crystallization by pseudomonas syringae, Appl. Microbiol. Biotechnol., 54, 153-161, 10.1007/s002530000377, 2000.

Conen, F., Morris, C. E., Leifeld, J., Yakutin, M. V., and Alewell, C.: Biological residues define the ice nucleation properties of soil dust, Atmos. Chem. Phys., 11, 9643-9648, 10.5194/acp-11-9643-2011, 2011.

Connolly, P. J., Möhler, O., Field, P. R., Saathoff, H., Burgess, R., Choularton, T., and Gallagher, M.: Studies of heterogeneous freezing by three different desert dust samples, Atmos. Chem. Phys., 9, 2805-2824, 10.5194/acp-9-2805-2009, 2009.

Cotton, R. J., Benz, S., Field, P. R., Mohler, O., and Schnaiter, M.: Technical note: A numerical test-bed for detailed ice nucleation studies in the aida cloud simulation chamber, Atmos. Chem. Phys., 7, 243-256, 10.5194/acp-7-243-2007, 2007.

Crawford, I., Bower, K. N., Choularton, T. W., Dearden, C., Crosier, J., Westbrook, C., Capes, G., Coe, H., Connolly, P. J., Dorsey, J. R., Gallagher, M. W., Williams, P., Trembath, J., Cui, Z., and Blyth, A.: Ice formation and development in aged, wintertime cumulus over the uk: Observations and modelling, Atmos. Chem. Phys., 12, 4963-4985, 10.5194/acp-12-4963-2012, 2012.

DeMott, P. J.: Quantitative descriptions of ice formation mechanisms of silver iodide-type aerosols, Atmos. Res., 38, 63-99, 10.1016/0169-8095(94)00088-U, 1995.

Fletcher, N. H.: A descriptive theory of the photo de-activation of silver iodide as an ice-crystal nucleus, J. Meteorol., 16, 249-255, Doi 10.1175/1520-0469(1959)016<0249:Adtotp>2.0.Co;2, 1959.

Fornea, A. P., Brooks, S. D., Dooley, J. B., and Saha, A.: Heterogeneous freezing of ice on atmospheric aerosols containing ash, soot, and soil, J. Geophys. Res.-Atmos., 114, D13201, 10.1029/2009jd011958, 2009.

Garcia, E., Hill, T. C. J., Prenni, A. J., DeMott, P. J., Franc, G. D., and Kreidenweis, S. M.: Biogenic ice nuclei in boundary layer air over two u.S. High plains agricultural regions, J. Geophys. Res.-Atmos., 117, Artn D18209 Doi 10.1029/2012jd018343, 2012.

Hartmann, S., Augustin, S., Clauss, T., Wex, H., Šantl-Temkiv, T., Voigtländer, J., Niedermeier, D., and Stratmann, F.: Immersion freezing of ice nucleation active protein complexes, Atmos. Chem. Phys., 13, 5751-5766, 10.5194/acp-13-5751-2013, 2013.

Herbert, R. J., Murray, B. J., Whale, T. F., Dobbie, S. J., and Atkinson, J. D.: Representing time-dependent freezing behaviour in immersion mode ice nucleation, Atmos. Chem. Phys. Discuss., 14, 1399-1442, 10.5194/acpd-14-1399-2014, 2014.

Hiranuma, N., Augustin-Bauditz, S., Bingemer, H., Budke, C., Curtius, J., Danielczok, A., Diehl, K., Dreischmeier, K., Ebert, M., Frank, F., Hoffmann, N., Kandler, K., Kiselev, A., Koop, T., Leisner, T., Möhler, O., Nillius, B., Peckhaus, A., Rose, D., Weinbruch, S., Wex, H., Boose, Y., DeMott, P. J., Hader, J. D., Hill, T. C. J., Kanji, Z. A., Kulkarni, G., Levin, E. J. T., McCluskey, C. S., Murakami, M., Murray, B. J., Niedermeier, D., Petters, M. D., O'Sullivan, D., Saito, A., Schill, G. P., Tajiri, T., Tolbert, M. A., Welti, A., Whale, T. F., Wright, T. P., and Yamashita, K.: A comprehensive laboratory study on the immersion freezing behavior of illite nx particles: A comparison of 17 ice nucleation measurement techniques, Atmos. Chem. Phys., 15, 2489-2518, 10.5194/acp-15-2489-2015, 2015.

Hoose, C., and Möhler, O.: Heterogeneous ice nucleation on atmospheric aerosols: A review of results from laboratory experiments, Atmos. Chem. Phys., 12, 9817-9854, 10.5194/acp-12-9817-2012, 2012.

Jiang, H., Yin, Y., Yang, L., Yang, S., Su, H., and Chen, K.: The characteristics of atmospheric ice nuclei measured at different altitudes in the huangshan mountains in southeast china, Adv. Atmos. Sci., 31, 396-406, 10.1007/s00376-013-3048-5, 2014.

Jung, S., Tiwari, M. K., and Poulikakos, D.: Frost halos from supercooled water droplets, Proc. Natl. Acad. Sci. U.S.A., 109, 16073-16078, 10.1073/pnas.1206121109, 2012.

Kanitz, T., Seifert, P., Ansmann, A., Engelmann, R., Althausen, D., Casiccia, C., and Rohwer, E. G.: Contrasting the impact of aerosols at northern and southern midlatitudes on heterogeneous ice formation, Geophys. Res. Lett., 38, L17802, 10.1029/2011gl048532, 2011.

Knopf, D. A., and Forrester, S. M.: Freezing of water and aqueous nacl droplets coated by organic monolayers as a function of surfactant properties and water activity, J. Phys. Chem. A, 115, 5579-5591, 10.1021/jp2014644, 2011.

Knopf, D. A., and Alpert, P. A.: A water activity based model of heterogeneous ice nucleation kinetics for freezing of water and aqueous solution droplets, Faraday Discuss, 165, 513-534, 10.1039/c3fd00035d, 2013.

Langham, E. J., and Mason, B. J.: The heterogeneous and homogeneous nucleation of supercooled water, Proc R Soc Lon Ser-A, 247, 493-&, DOI 10.1098/rspa.1958.0207, 1958.

Marcolli, C., Gedamke, S., Peter, T., and Zobrist, B.: Efficiency of immersion mode ice nucleation on surrogates of mineral dust, Atmos. Chem. Phys., 7, 5081-5091, 10.5194/acp-7-5081-2007, 2007.

Mohler, O., Georgakopoulos, D. G., Morris, C. E., Benz, S., Ebert, V., Hunsmann, S., Saathoff, H., Schnaiter, M., and Wagner, R.: Heterogeneous ice nucleation activity of bacteria: New laboratory experiments at simulated cloud conditions, Biogeosciences, 5, 1425-1435, 2008.

Murray, B. J., Broadley, S. L., Wilson, T. W., Bull, S. J., Wills, R. H., Christenson, H. K., and Murray, E. J.: Kinetics of the homogeneous freezing of water, Phy.s Chem. Chem. Phys., 12, 10380-10387, 10.1039/c003297b, 2010.

Murray, B. J., Broadley, S. L., Wilson, T. W., Atkinson, J. D., and Wills, R. H.: Heterogeneous freezing of water droplets containing kaolinite particles, Atmos. Chem. Phys., 11, 4191-4207, 10.5194/acp-11-4191-2011, 2011.

Murray, B. J., O'Sullivan, D., Atkinson, J. D., and Webb, M. E.: Ice nucleation by particles immersed in supercooled cloud droplets, Chem. Soc. Rev., 41, 6519-6554, 10.1039/C2CS35200A, 2012.

Niemand, M., Möhler, O., Vogel, B., Vogel, H., Hoose, C., Connolly, P., Klein, H., Bingemer, H., DeMott, P. J., Skrotzki, J., and Leisner, T.: A particle-surface-area-based parameterization of immersion freezing on desert dust particles, J. Atmos. Sci., 69, 10.1175/jas-d-11-0249.1, 2012.

O'Sullivan, D., Murray, B. J., Malkin, T. L., Whale, T. F., Umo, N. S., Atkinson, J. D., Price, H. C., Baustian, K. J., Browse, J., and Webb, M. E.: Ice nucleation by fertile soil dusts: Relative importance of mineral and biogenic components, Atmos. Chem. Phys., 14, 1853-1867, 10.5194/acp-14-1853-2014, 2014.

O′Sullivan, D., Murray, B. J., Ross, J. F., Whale, T. F., Price, H. C., Atkinson, J. D., Umo, N. S., and Webb, M. E.: The relevance of nanoscale biological fragments for ice nucleation in clouds, Sci. Rep., 5, 10.1038/srep08082, 2015.

Pruppacher, H. R., and Klett, J. D.: Microphysics of clouds and precipitation, 2nd ed., Kluwer Academic Publishers, 1997.

Riechers, B., Wittbracht, F., Hütten, A., and Koop, T.: The homogeneous ice nucleation rate of water droplets produced in a microfluidic device and the role of temperature uncertainty, Phys. Chem. Chem. Phys., 15, 5873-5887, 10.1039/C3CP42437E, 2013.

Rogers, D. C., DeMott, P. J., Kreidenweis, S. M., and Chen, Y. L.: A continuous-flow diffusion chamber for airborne measurements of ice nuclei, J. Atmos. Ocean. Tech., 18, 725-741, Doi 10.1175/1520-0426(2001)018<0725:Acfdcf>2.0.Co;2, 2001.

Rosenfeld, D., and Woodley, W. L.: Deep convective clouds with sustained supercooled liquid water down to -37.5 °c, Nature, 405, 440-442, 10.1038/35013030, 2000.

Rowland, S. C., Layton, R. G., and Smith, D. R.: Photolytic activation of silver iodide in the nucleation of ice, J. Atmos. Sci., 21, 698-700, 10.1175/1520-0469(1964)021<0698:paosii>2.0.co;2, 1964.

Salam, A., Lohmann, U., Crenna, B., Lesins, G., Klages, P., Rogers, D., Irani, R., MacGillivray, A., and Coffin, M.: Ice nucleation studies of mineral dust particles with a new continuous flow diffusion chamber, Aerosol. Sci. Tech., 40, 134-143, Doi 10.1080/02786820500444853, 2006.

Smith, E. J., Heffernan, K. J., and Seely, B. K.: The decay of ice-nucleating properties of silver iodide in the atmosphere, J. Meteorol., 12, 379-385, Doi 10.1175/1520-0469(1955)012<0379:Tdoinp>2.0.Co;2, 1955.

Stopelli, E., Conen, F., Zimmermann, L., Alewell, C., and Morris, C. E.: Freezing nucleation apparatus puts new slant on study of biological ice nucleators in precipitation, Atmos. Meas. Tech., 7, 129-134, 10.5194/amt-7-129-2014, 2014.

Umo, N. S., Murray, B. J., Baeza-Romero, M. T., Jones, J. M., Lea-Langton, A. R., Malkin, T. L., O'Sullivan, D., Plane, J. M. C., and Williams, A.: Ice nucleation by combustion ash particles at conditions relevant to mixed-phase clouds, Atmos. Chem. Phys. Discuss., 14, 28845-28883, 10.5194/acpd-14-28845-2014, 2014.

Vali, G.: Quantitative evaluation of experimental results an the heterogeneous freezing nucleation of supercooled liquids, J. Atmos. Sci., 28, 402-409, 10.1175/1520-0469(1971)028<0402:qeoera>2.0.co;2, 1971.

Vali, G.: Principles of ice nucleation, Biological ice nucleation and its applications, edited by: Lee, R. E., Jr., Warren, G. J., and Gusta, L. V., American Phytopathological Society (APS) Press {a}, 3340 Pilot Knob Road, St. Paul, Minnesota 55121, USA, 1-28 pp., 1995.

Vali, G.: Repeatability and randomness in heterogeneous freezing nucleation, Atmos. Chem. Phys., 8, 5017-5031, 10.5194/acp-8-5017-2008, 2008.

Vali, G.: Interpretation of freezing nucleation experiments: Singular and stochastic; sites and surfaces, Atmos. Chem. Phys., 14, 5271-5294, 10.5194/acp-14-5271-2014, 2014.

Vonnegut, B.: The nucleation of ice formation by silver iodide, J. Appl. Phys., 18, 593-595, 10.1063/1.1697813, 1947.

Wex, H., Augustin-Bauditz, S., Boose, Y., Budke, C., Curtius, J., Diehl, K., Dreyer, A., Frank, F., Hartmann, S., Hiranuma, N., Jantsch, E., Kanji, Z. A., Kiselev, A., Koop, T., Möhler, O., Niedermeier, D., Nillius, B., Rösch, M., Rose, D., Schmidt, C., Steinke, I., and Stratmann, F.: Intercomparing different devices for the investigation of ice nucleating particles using snomax® as test substance, Atmos. Chem. Phys., 15, 1463-1485, 10.5194/acp-15-1463-2015, 2015.

Wood, S. E., Baker, M. B., and Swanson, B. D.: Instrument for studies of homogeneous and heterogeneous ice nucleation in free-falling supercooled water droplets, Review of Scientific Instruments, 73, 3988-3996, 10.1063/1.1511796 2002.

Wright, T. P., and Petters, M. D.: The role of time in heterogeneous freezing nucleation, J. Geophys. Res.-Atmos., 118, 3731-3743, 10.1002/jgrd.50365, 2013.

Zobrist, B., Marcolli, C., Peter, T., and Koop, T.: Heterogeneous ice nucleation in aqueous solutions: The role of water activity, The Journal of Physical Chemistry A, 112, 3965-3975, 10.1021/jp7112208, 2008.

3. Ice Nucleation Properties of Oxidized Carbon Nanomaterials

This chapter has been published The Journal of Physical Chemistry Letters as:

Whale, T. F., Rosillo-Lopez, M., Murray, B. J., and Salzmann, C. G. 'Ice nucleation properties of oxidized carbon nanomaterials', published in J. Phys. Chem. Lett. (2015).

The published article has a supplement, which is included after the main text.

ABSTRACT

Heterogeneous ice nucleation is an important process in many fields, particularly atmospheric science, but is still poorly understood. All known inorganic ice nucleating particles are relatively large in size and tend to be hydrophilic. Hence it is not obvious that carbon nanomaterials should nucleate ice. However, in this paper we show that four different readily water-dispersible carbon nanomaterials are capable of nucleating ice. The tested materials were carboxylated graphene nanoflakes, graphene oxide, oxidized single walled carbon nanotubes and oxidized multiwalled carbon nanotubes. The carboxylated graphene nanoflakes have a diameter of ~30 nm and are among the smallest entities observed so far to nucleate ice. Overall, carbon nanotubes were found to nucleate ice more efficiently than flat graphene species, and less oxidized materials nucleated ice more efficiently than more oxidized species. These well-defined carbon nanomaterials may pave the way to bridging the gap between experimental and computational studies of ice nucleation.

Freezing of liquid water to ice I must be initiated by an ice nucleation event. In many situations this event is induced by a heterogeneous ice nucleating particle (INP). Ice nucleation is an important process for understanding of atmospheric processes (Murray et al., 2012;Hoose and Möhler, 2012;Pruppacher and Klett, 1997) and also has relevance in other fields such as the cryopreservation of biological samples (Morris and Acton, 2013), freeze drying of pharmaceuticals (Searles et al., 2001) and other substances (Aksan et al., 2014) and freezing of foodstuffs (Kiani and Sun, 2011). Much effort has been devoted to the quantification of the efficiencies of heterogeneous ice nucleants of potential atmospheric relevance. As such the ice nucleating efficiencies of various mineral dusts, biological entities, volcanic ashes and carbonaceous combustion aerosols (Diehl and Mitra, 1998;Demott, 1990) have been measured using a wide range of techniques (Murray et al., 2012;Hoose and Möhler, 2012).

It is often assumed that INPs tend to be relatively 'large' in size (Pruppacher and Klett, 1997). Indeed, the concentration of atmospheric INP is correlated with the concentration of particles larger than 0.5 μm in diameter (DeMott et al., 2010). However, it has been found that nanoscale, readily dispersible biological particles that are shed from both pollen particles and fungi in water can also nucleate ice efficiently (Pummer et al., 2012;Fröhlich-Nowoisky et al., 2014;O′Sullivan et al., 2015) and that small particles of polyvinyl alcohol can nucleate ice (Ogawa et al., 2009). Of late, there has been a great deal of interest in the synthesis and characterization of carbon nanomaterials. The ice nucleation activity of these species has not been examined to date.

Here, we have synthesized 4 different carbon nanomaterials and determined their ice nucleating efficiencies. These are carboxylated graphene nanoflakes (*cx*-GNFs) and graphene oxide (GO) as well as oxidized multiwall (o-MWCNTS) and single wall carbon nanotubes (o-SWCNTs). Representative structures for these species are shown in Figure 3.1. The oxygen / carbon ratios for these materials were determined by X-ray photoelectron spectroscopy (XPS). The *cx*-GNFs are small graphene sheets with an average lateral diameter of ~30 nm (Salzmann et al., 2010). The edges of the flakes are decorated with carboxylic acid groups. They contain 66.3% carbon and 33.7% oxygen. GO consists of much larger sheets of carbon, average diameter 1 μm. The structure has a wider range of functional groups than that of the *cx*-GNFs with alcohol and epoxide groups present as well as carboxylic acids (He et al., 1996). The face of the GO sheets is oxidized as well as the edges. The GO sample contains 72.0% carbon and 28.0% oxygen.

MWCNTS are needle-like tubes of carbon and consist of multiple single layers of carbon wrapped concentrically. Our oxidized material contains 82.2% carbon and 17.8% oxygen. SWCNTS are structurally similar but consist of a single layer of carbon only. After chemical oxidation of the SWCNTs we find 86.2% carbon and 13.8% oxygen according to XPS. We also present freezing data for a solution of mellitic acid, a molecular species structurally analogous to *cx*-GNFs, consisting of a single benzene ring with six carboxylic acid groups.

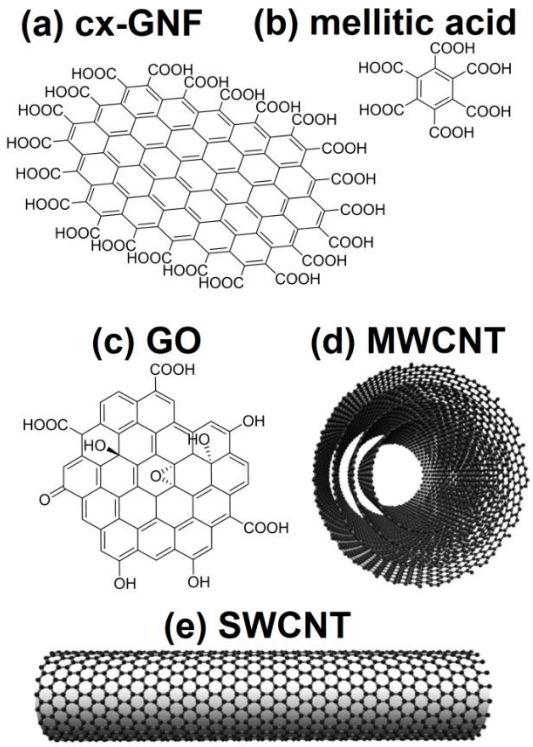

Figure 3.1: Chemical structures of the various of carbon nanomaterials tested for their ice nucleation activity. (a) Small carboxylated graphene nanoflake (cx-GNF), (b) mellitic acid, (c) graphene oxide (GO), (d) multiwalled carbon nanotube (MWCNT) and (e) single walled carbon nanotube (SWCNT). GO sheets have an average lateral diameter of 1 µm while the GNFs have an average lateral diameter of 30 nm (Salzmann et al., 2010).

These materials were chosen for this study because their oxidized nature allows them to readily disperse in water. Attempts to conduct experiments with carbonized *cx*-GNFs, for example, proved impossible as they did not disperse in water. The oxidized carbon nanomaterials, apart from the o-SWCNTs, all disperse readily in water with stirring. No more than 0.07 wt% of the o-SWCNTs could be dispersed. The 1 wt% and 0.1 wt% dispersions of *cx*-GNFs are very stable and were not observed to settle even after several months. Suspensions of GO, o-MWCNTs and o-SWCNTs were less stable, and settle

over the course of hours. Dispersions of carbon nanomaterials were tested for the ice nucleating activity immediately after preparation.

Ice nucleation experiments were conducted using the µl-Nucleation by Immersed Particles Instrument (µl-NIPI) (Whale et al., 2015). This instrument allows determination of the freezing temperatures of around 50 microlitre droplets of water under constant cooling. Here, a cooling rate of 1°C min^{-1} has been used. The freezing curve for pure water in
Figure 3.2 (a) consists of 737 separate freezing events from 17 experiments and has been reported previously by Umo et al. (2015). The freezing observed in the pure water is unlikely to be induced by homogenous nucleation, which is predicted by classical nucleation theory to occur at temperatures colder than -30°C in 1 µl droplets (Riechers et al., 2013;Murray et al., 2010). Instead it is likely that the freezing observed is caused by a combination of impurities in the water used and on the silanized glass slide used to support the droplets.

Droplets containing *cx*-GNFs, GO, o-MWCNTs and o-SWCNTs all nucleate ice at temperatures warmer than the pure water droplets, as shown in
Figure 3.2 (a). This constitutes the first observations of ice nucleation by these types of materials. In contrast, it can be seen in
Figure 3.2 (a) that mellitic acid does not nucleate ice within the sensitivity of the experimental setup used, with recorded freezing temperatures indistinguishable to those of pure water. This is entirely expected as mellitic acid is a dissolved molecular species so there is no reason to suppose it would interact with water in a way that would encourage ice formation. It is interesting to note that the structurally analogous *cx*-GNFs do nucleate ice well, showing that the increase in size allows interactions with water suitable for encouraging ice nucleation to occur.

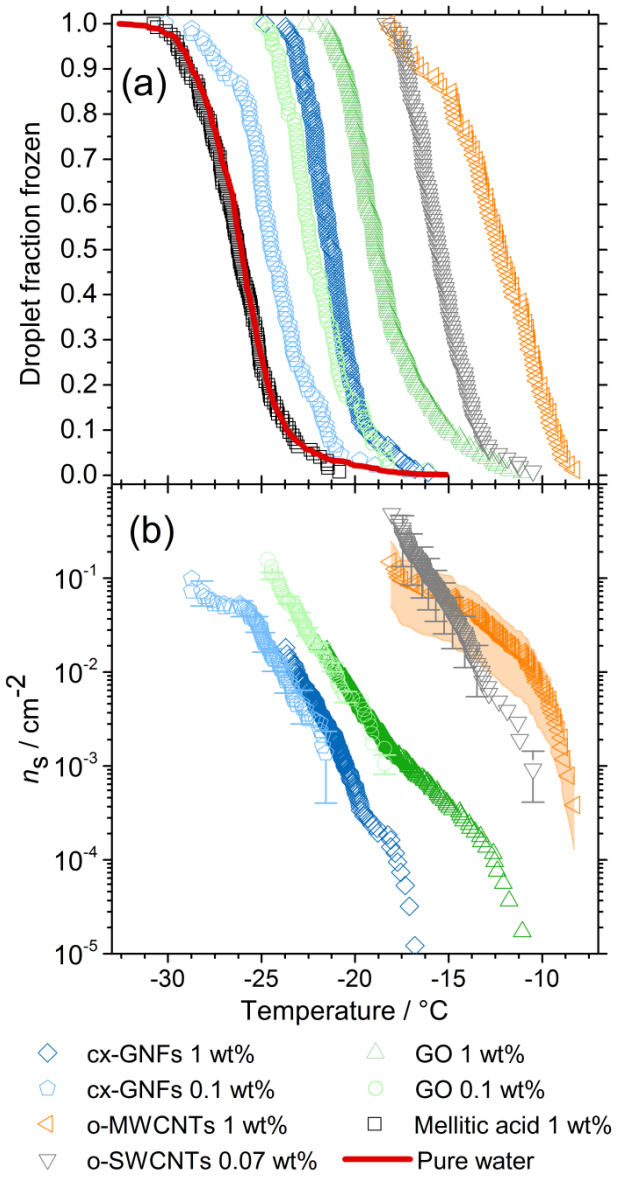

Figure 3.2 (a) Droplet fraction frozen against temperature for 1 and 0.1 wt% dispersions of GO and cx-GNFs, a 1 wt% dispersion of o-MWCNTs, a 0.07 wt% dispersion of o-SWCNTs, a 1 wt% solution of mellitic acid and pure water. (b) ns values for all tested carbon nanomaterials. The ns values reported for the o-MWCNTs assume that they have 9 layers, the average number for the starting material for their synthesis. The shaded area shows the area encompassed by calculating ns for the minimum and maximum wall numbers of the starting material. Experimental uncertainty in ns was calculated by propagation of uncertainty from weighing, droplet size and background subtraction. In many cases uncertainties are too small to show on the plot. Temperature uncertainty is ±0.4°C in (a) and (b).

To allow comparison between the carbon nanomaterial nucleants these values have been normalized to surface area according to a time independent description of ice nucleation (Vali, 2014;Herbert et al., 2014). To calculate theoretical n_s values for the graphene species presented in

Figure 3.2 (b) the total surface area of the *cx*-GNFs and GO was calculated by assuming that all graphene sheets were completely dissociated from each other and using:

$$\frac{n(T)}{N} = 1 - exp(-n_s(T)\sigma) \qquad 3.1$$

where n_s is the cumulative number of surface sites per unit surface area of nucleant that become active on cooling from 273.15 K to a temperature *T*, σ is the surface of nucleant per droplet and $\frac{n(T)}{N}$ is the cumulative fraction of droplets frozen.

It can be seen in

Figure 3.2 (a) that GO nucleates ice more efficiently than the *cx*-GNFs per mass of material, and that the o-MWCNTs and o-SWCNTs nucleate ice more efficiently than the flat species. The carbon nanotubes (CNTs) are similar to each other. The shapes of the n_s curves for the two CNT species are different however. The curve for the o-MWCNTs flattens at lower temperature, meaning that the number of effective INPs increases less quickly with increasing supersaturation than for the o-SWCNTs. There has been interest in the ordering of water in CNT cavities (Koga et al., 2001). It is intriguing to suggest that the interior cavities of the CNTs interact with water in a way that promotes ice nucleation and that this is responsible for the strong nucleation we have observed. Both kinds of CNTs are rather less oxidized than the graphene species. The overall trend is therefore that the less oxidized species nucleate ice more efficiently. The 1 wt% dispersion of *cx*-GNFs has a median nucleation temperature of -21.3°C and an oxygen content of 33.7% while the 1 wt% dispersion o-MWCNTs has a median nucleation temperature of -12.2°C and an oxygen content of 17.8%. We note in this context that XPS is a surface-sensitive technique and the determined atom percentages may therefore not necessarily reflect the bulk composition of the samples but more the composition of the sample at the interface with water.

The *cx*-GNFs in particular are light compared to most other INPs. Their average mass is approximately 325 kDa. In their recent paper Pummer et al. (2015) reviewed a range of small INPs. The *cx*-GNFs are comparable in mass to Birch pollen derived ice nucleating macromolecules discovered by Pummer et al. (2012) and fungal proteins sized by

O'Sullivan et al. (2015) and somewhat larger than certain polyvinyl alcohols discovered by Ogawa et al. (2009), which were shown to nucleate ice at molecular weights as low as 1.7 kDa. All other known INPs are heavier than the *cx*-GNFs.

The approach we have used to calculate n_s assumes that all possible surface area is in contact with water. It is hard to evaluate how realistic this is for the carbon nanomaterials, hence, the n_s values reported are most likely lower limits in the case of these nanomaterials. This also means that comparison with existing measurements of other carbon materials such as soots (Diehl and Mitra, 1998;Demott, 1990) is difficult. It can be seen in
Figure 3.2 (b) that n_s derived from lower concentrations dispersions of GO and *cx*-GNF fall on the same line as higher concentrations suggesting that similar surface areas of material are available per mass of material in both concentrations. This indicates that the materials are not aggregated in dispersion since aggregation is concentration dependent. Calculating n_s for the o-MWCNTs was less straightforward as the precise number of layers in the MWCNTs from which the o-MWCNTs were synthesized is unknown. Manufacturer specifications for the starting material includes maximum and minimum numbers of walls, n_s values have been calculated using these to provide upper and lower limits as seen in
Figure 3.2 (b). We have assumed that the exterior surface area of the o-MWCNTs is solely responsible for nucleation observed and calculated surface area exposed to water on this basis. The interior surfaces may well play a role, even a dominant one, in the nucleation observed but the assumptions made seem reasonable for comparative purposes.

While it is difficult to infer details about the specific mechanism of ice nucleation from droplet freezing experiments some insight into the nature of ice nucleation observed can be derived from its time dependence. The *Framework for Reconciling Observable Stochastic Time-dependence* (FROST) condenses the key information about time dependence of ice nucleation into a single parameter, λ, which is a nucleant specific parameter that describes the time dependence of the ice nucleation properties (further details are given in the SI) (Herbert et al., 2014). FROST facilitates comparison of different materials through calculation of λ using:

$$T' = T - \frac{1}{\lambda}(\ln \frac{1}{r}) \qquad 3.2$$

Where, for a given experiment, T' is the modified temperature, the freezing temperature that would be expected if an experiment were conducted at a standard rate of 1°C min^{-1}, T is the measured freezing temperature and r is the cooling rate in °C min^{-1}. To calculate λ from multiple fraction frozen curves the difference between calculated T' values is minimized by varying λ iteratively.

We have cooled *cx*-GNFs at rates from 0.2°C min^{-1} to 5°C min^{-1}, the results of which are shown in Figure 3.4 (a), and analyzed the resulting data using FROST (Herbert et al., 2014). A λ value of 3.3°C^{-1} has been determined and Figure 3.4 (b) shows the normalized data. This λ value is higher than those of the majority of nucleants evaluated by Herbert et al. (2014) and might be regarded as a 'large' λ value, indicating that ice nucleation by *cx*-GNFs is relatively insensitive to changes in cooling rate.

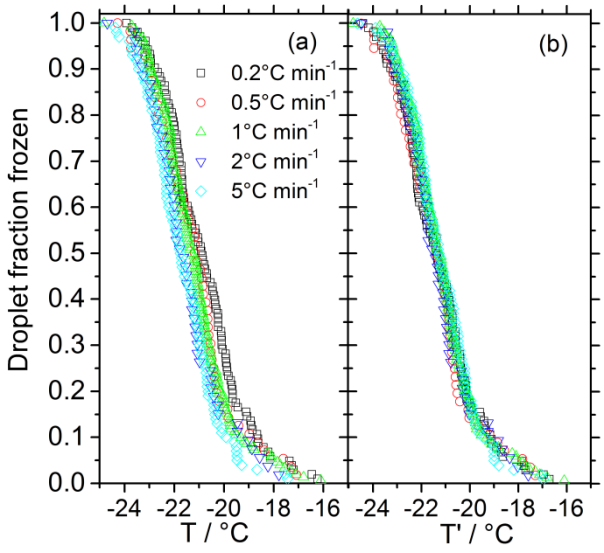

Figure 3.3: (a) Droplet fraction frozen against temperature for 1 wt% cx-GNFs at 5 different cooling rates. (b) Droplet fraction frozen against modified temperature as defined in eq. 2 for the same experiments. Temperature uncertainty is ±0.4°C in (a) and (b).

The FROST analysis also reveals if there is a strong particle-to-particle variability in ice nucleating ability. If the value $d\ln(n_s)/dT$, termed ω, is equal to λ then all surfaces of the nucleant has the same potential to nucleate ice. In contrast, if $\omega < \lambda$ then some parts of the surface have a greater potential to nucleate ice. For *cx*-GNFs cooled at 1°C min^{-1} we have determined ω to be 0.83°C^{-1} which is clearly much smaller than λ. This suggests that the nucleation observed may be site specific, meaning that there may be specific sites on the cx-GNFs that are responsible for the ice nucleation (Herbert et al.,

2014;Vali, 2014). The precise nature of these sites and the reason for their apparent nucleating activity is unclear. It is known that small monomers such as the water molecule can interact with carboxylic acid groups such as those present on *cx*-GNFs (Cheng et al., 2010;Guzmán et al., 2006b;Guzmán et al., 2006a). It may be that such site-specific interactions are related to the observed ice nucleation.

At present there is no case where the mechanism of heterogeneous ice nucleation is well understood. Even the longstanding and elegant lattice matching hypothesis to which the ice nucleating activity of silver iodide is attributed has been questioned (Finnegan and Chai, 2003;Massey et al., 2014). Various molecular dynamics simulations have been conducted by a few different groups in order to address this issue (Hu and Michaelides, 2007;Fraux and Doye, 2014;Reinhardt and Doye, 2014;Cox et al., 2013;Cox et al., 2012;Cox et al., 2015a). This includes several studies looking specifically at carbon species.(Cox et al., 2015b;Cabriolu and Li, 2015;Lupi and Molinero, 2014;Lupi et al., 2014a;Lupi et al., 2014b) Currently, there is a gap between experimental and computational work into ice nucleation that has proved very difficult to bridge, due to the vast differences in spatial scale and time scale of the systems that can be examined experimentally and computationally.

Recent work by Lupi et al. (Lupi and Molinero, 2014;Lupi et al., 2014a) using molecular dynamics simulations to study ice nucleation on carbon surfaces has provided certain qualitative predictions that might be experimentally accessible. Specifically, they found that flat carbon surfaces without any oxidation or roughness nucleated ice most efficiently. Any oxidation (Lupi and Molinero, 2014) roughness or curvature (Lupi et al., 2014a) was found to decrease the nucleation temperatures observed in the simulations. The result that oxidized carbon surfaces nucleate ice less well than pristine ones is somewhat counterintuitive and in contrast to the commonly stated ‘chemical bonding’ requirement for ice nucleation (Pruppacher and Klett, 1997) as it might be expected that oxidation will offer greater opportunity for water to bond to a surface and so promote water structuring and ice nucleation. Our work here is consistent with the alternative hypothesis that reduced oxidation leads to enhanced ice nucleation efficiency although more species would need to be investigated to establish a statistically significant trend. Also, there are differences in structure and size between the nanomaterials investigated here, as well as extent of oxidation. These differences would need to be closely controlled to generate a firm experimental conclusion as to the effect of oxidation of carbon

nanomaterials on ice nucleation efficiency. By thoroughly characterizing relatively simple ice nucleating species it might be possible to conduct practical experiments that can be meaningfully related to computational studies. In general, by investigating closely related nucleants and observing differences in their ice nucleating efficiency it may be possible to infer information about the causes of ice nucleating activity in these samples. Work here might be regarded as a first step in this direction and, now that their capacity to nucleate ice is known, carbon nanomaterials may prove to be a good candidate for further work on building a fundamental understanding of ice nucleation.

References

Aksan, A., Ragoonanan, V., and Hirschmugl, C.: Freezing- and drying-induced micro- and nano-heterogeneity in biological solutions, in: Biophysical methods for biotherapeutics, John Wiley & Sons, Inc., 269-284, 2014.

Cabriolu, R., and Li, T.: Ice nucleation on carbon surface supports the classical theory for heterogeneous nucleation, Physical Review E, 91, 052402, 2015.

Cheng, J., Soetjipto, C., Hoffmann, M. R., and Colussi, A. J.: Confocal fluorescence microscopy of the morphology and composition of interstitial fluids in freezing electrolyte solutions, The Journal of Physical Chemistry Letters, 1, 374-378, 10.1021/jz9000888, 2010.

Cox, S. J., Kathmann, S. M., Purton, J. A., Gillan, M. J., and Michaelides, A.: Non-hexagonal ice at hexagonal surfaces: The role of lattice mismatch, Phys. Chem. Chem. Phys., 14, 7944-7949, 10.1039/c2cp23438f, 2012.

Cox, S. J., Raza, Z., Kathmann, S. M., Slater, B., and Michaelides, A.: The microscopic features of heterogeneous ice nucleation may affect the macroscopic morphology of atmospheric ice crystals, Faraday Discussions, 167, 389-403, 10.1039/c3fd00059a, 2013.

Cox, S. J., Kathmann, S. M., Slater, B., and Michaelides, A.: Molecular simulations of heterogeneous ice nucleation. I. Controlling ice nucleation through surface hydrophilicity, The Journal of Chemical Physics, 142, 184704, doi:http://dx.doi.org/10.1063/1.4919714, 2015a.

Cox, S. J., Kathmann, S. M., Slater, B., and Michaelides, A.: Molecular simulations of heterogeneous ice nucleation. Ii. Peeling back the layers, The Journal of Chemical Physics, 142, 184705, doi:http://dx.doi.org/10.1063/1.4919715, 2015b.

Demott, P. J.: An exploratory-study of ice nucleation by soot aerosols, J. App. Meteorol., 29, 1072-1079, 1990.

DeMott, P. J., Prenni, A. J., Liu, X., Kreidenweis, S. M., Petters, M. D., Twohy, C. H., Richardson, M. S., Eidhammer, T., and Rogers, D. C.: Predicting global atmospheric ice nuclei distributions and their impacts on climate, Proc. Natl. Acad. Sci. USA, 107, 11217-11222, 10.1073/pnas.0910818107, 2010.

Diehl, K., and Mitra, S. K.: A laboratory study of the effects of a kerosene-burner exhaust on ice nucleation and the evaporation rate of ice crystals, Atmos. Environ., 32, 3145-3151, 1998.

Finnegan, W. G., and Chai, S. K.: A new hypothesis for the mechanism of ice nucleation on wetted agi and agi center dot agcl particulate aerosols, J. Atmos. Sci., 60, 1723-1731, 10.1175/1520-0469(2003)060<1723:anhftm>2.0.co;2, 2003.

Fraux, G., and Doye, J. P. K.: Note: Heterogeneous ice nucleation on silver-iodide-like surfaces, Journal of Chemical Physics, 141, 10.1063/1.4902382, 2014.

Fröhlich-Nowoisky, J., Hill, T. C. J., Pummer, B. G., Franc, G. D., and Pöschl, U.: Ice nucleation activity in the widespread soil fungus mortierella alpina, Biogeosciences Discuss., 11, 12697-12731, 10.5194/bgd-11-12697-2014, 2014.

Guzmán, M. I., Colussi, A. J., and Hoffmann, M. R.: Photogeneration of distant radical pairs in aqueous pyruvic acid glasses, The Journal of Physical Chemistry A, 110, 931-935, 10.1021/jp053449t, 2006a.

Guzmán, M. I., Hildebrandt, L., Colussi, A. J., and Hoffmann, M. R.: Cooperative hydration of pyruvic acid in ice, J. Am. Chem. Soc., 128, 10621-10624, 10.1021/ja062039v, 2006b.

He, H., Riedl, T., Lerf, A., and Klinowski, J.: Solid-state nmr studies of the structure of graphite oxide, The Journal of Physical Chemistry, 100, 19954-19958, 10.1021/jp961563t, 1996.

Herbert, R. J., Murray, B. J., Whale, T. F., Dobbie, S. J., and Atkinson, J. D.: Representing time-dependent freezing behaviour in immersion mode ice nucleation, Atmos. Chem. Phys., 14, 8501-8520, 10.5194/acp-14-8501-2014, 2014.

Hoose, C., and Möhler, O.: Heterogeneous ice nucleation on atmospheric aerosols: A review of results from laboratory experiments, Atmos. Chem. Phys., 12, 9817-9854, 10.5194/acp-12-9817-2012, 2012.

Hu, X. L., and Michaelides, A.: Ice formation on kaolinite: Lattice match or amphoterism?, Surface Science, 601, 5378-5381, 10.1016/j.susc.2007.09.012, 2007.

Kiani, H., and Sun, D. W.: Water crystallization and its importance to freezing of foods: A review, Trends Food Sci. Technol., 22, 407-426, 10.1016/j.tifs.2011.04.011, 2011.

Koga, K., Gao, G. T., Tanaka, H., and Zeng, X. C.: Formation of ordered ice nanotubes inside carbon nanotubes, Nature, 412, 802-805, 10.1038/35090532, 2001.

Lupi, L., Hudait, A., and Molinero, V.: Heterogeneous nucleation of ice on carbon surfaces, J. Am. Chem. Soc., 136, 3156-3164, 10.1021/ja411507a, 2014a.

Lupi, L., Kastelowitz, N., and Molinero, V.: Vapor deposition of water on graphitic surfaces: Formation of amorphous ice, bilayer ice, ice i, and liquid water, Journal of Chemical Physics, 141, 10.1063/1.4895543, 2014b.

Lupi, L., and Molinero, V.: Does hydrophilicity of carbon particles improve their ice nucleation ability?, J. Phys. Chem. A, 118, 7330-7337, 10.1021/jp4118375, 2014.

Massey, A., McBride, F., Darling, G. R., Nakamura, M., and Hodgson, A.: The role of lattice parameter in water adsorption and wetting of a solid surface, Phys. Chem. Chem. Phys., 16, 24018-24025, 10.1039/c4cp03164d, 2014.

Morris, G. J., and Acton, E.: Controlled ice nucleation in cryopreservation - a review, Cryobiology, 66, 85-92, 10.1016/j.cryobiol.2012.11.007, 2013.

Murray, B. J., Broadley, S. L., Wilson, T. W., Bull, S. J., Wills, R. H., Christenson, H. K., and Murray, E. J.: Kinetics of the homogeneous freezing of water, Phys. Chem. Chem. Phys., 12, 10380-10387, 10.1039/c003297b, 2010.

Murray, B. J., O'Sullivan, D., Atkinson, J. D., and Webb, M. E.: Ice nucleation by particles immersed in supercooled cloud droplets, Chem. Soc. Rev., 41, 6519-6554, 10.1039/C2CS35200A, 2012.

O′Sullivan, D., Murray, B. J., Ross, J. F., Whale, T. F., Price, H. C., Atkinson, J. D., Umo, N. S., and Webb, M. E.: The relevance of nanoscale biological fragments for ice nucleation in clouds, Sci. Rep., 5, 10.1038/srep08082, 2015.

Ogawa, S., Koga, M., and Osanai, S.: Anomalous ice nucleation behavior in aqueous polyvinyl alcohol solutions, Chemical Physics Letters, 480, 86-89, http://dx.doi.org/10.1016/j.cplett.2009.08.046, 2009.

Pruppacher, H. R., and Klett, J. D.: Microphysics of clouds and precipitation, 2nd ed., Kluwer Academic Publishers, 1997.

Pummer, B. G., Bauer, H., Bernardi, J., Bleicher, S., and Grothe, H.: Suspendable macromolecules are responsible for ice nucleation activity of birch and conifer pollen, Atmos. Chem. Phys., 12, 2541-2550, 10.5194/acp-12-2541-2012, 2012.

Pummer, B. G., Budke, C., Augustin-Bauditz, S., Niedermeier, D., Felgitsch, L., Kampf, C. J., Huber, R. G., Liedl, K. R., Loerting, T., Moschen, T., Schauperl, M., Tollinger, M., Morris, C. E., Wex, H., Grothe, H., Pöschl, U., Koop, T., and Fröhlich-Nowoisky, J.: Ice nucleation by water-soluble macromolecules, Atmos. Chem. Phys., 15, 4077-4091, 10.5194/acp-15-4077-2015, 2015.

Reinhardt, A., and Doye, J. P. K.: Effects of surface interactions on heterogeneous ice nucleation for a monatomic water model, Journal of Chemical Physics, 141, 10.1063/1.4892804, 2014.

Riechers, B., Wittbracht, F., Hütten, A., and Koop, T.: The homogeneous ice nucleation rate of water droplets produced in a microfluidic device and the role of temperature uncertainty, Phys. Chem. Chem. Phys., 15, 5873-5887, 10.1039/C3CP42437E, 2013.

Salzmann, C. G., Nicolosi, V., and Green, M. L.: Edge-carboxylated graphene nanoflakes from nitric acid oxidised arc-discharge material, Journal of Materials Chemistry, 20, 314-319, 2010.

Searles, J. A., Carpenter, J. F., and Randolph, T. W.: The ice nucleation temperature determines the primary drying rate of lyophilization for samples frozen on a temperature-controlled shelf, J. Pharm. Sci., 90, 860-871, 10.1002/jps.1039, 2001.

Umo, N. S., Murray, B. J., Baeza-Romero, M. T., Jones, J. M., Lea-Langton, A. R., Malkin, T. L., O'Sullivan, D., Neve, L., Plane, J. M. C., and Williams, A.: Ice nucleation by combustion ash particles at conditions relevant to mixed-phase clouds, Atmos. Chem. Phys., 15, 5195-5210, 10.5194/acp-15-5195-2015, 2015.

Vali, G.: Interpretation of freezing nucleation experiments: Singular and stochastic; sites and surfaces, Atmos. Chem. Phys., 14, 5271-5294, 10.5194/acp-14-5271-2014, 2014.

Whale, T. F., Murray, B. J., O'Sullivan, D., Wilson, T. W., Umo, N. S., Baustian, K. J., Atkinson, J. D., Workneh, D. A., and Morris, G. J.: A technique for quantifying heterogeneous ice nucleation in microlitre supercooled water droplets, Atmos. Meas. Tech., 8, 2437-2447, 10.5194/amt-8-2437-2015, 2015.

3.1. Supplementary information to Chapter 3

3.1.1. Preparation of Materials

The preparation of the carboxylated graphene nanoflakes (*cx*-GNFs) was achieved using an optimized procedure using MWCNTs from Bayer (C150 P) as the starting material (Salzmann et al., 2010). Oxidized MWCNTs (o-MWCNTs) and SWCNTs (o-SWCNTs) were prepared by treatment of MWCNTs and SWCNTs respectively in a 3:1 mixture of conc. sulphuric / conc. nitric acid (Morales-Torres et al., 2014). Graphene oxide (GO) was prepared using an improved version of the Hummer's method (Chen et al., 2013). Mellitic acid was purchased from Sigma-Aldrich and used as received.

3.1.2. XPS Measurements

XPS measurements for elemental analysis were carried out on a Thermo Scientific K-Alpha XPS machine with a monochromated Al K_α source (E=1486.6 eV). A dual beam flood gun (electrons and argon ions) was used to compensate for charge accumulation on the measured surfaces. All survey scans, shown in Figure 3.4, were scanned three times with a resolution of 1 eV, 400 µm spot size and 50 ms dwell time.

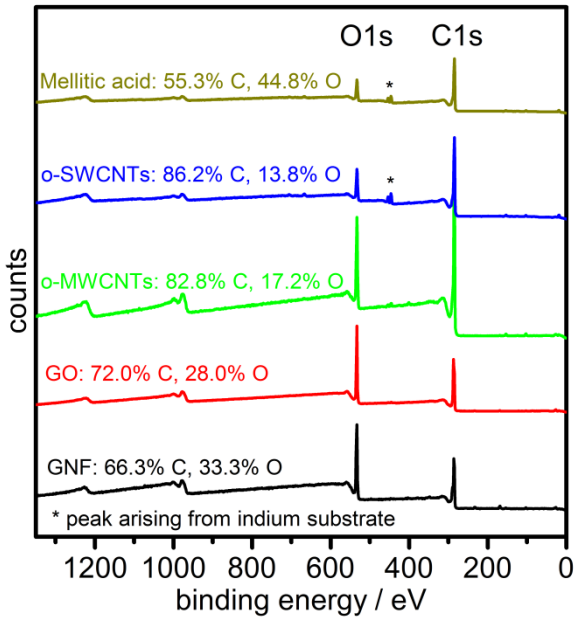

Figure 3.4: Survey XPS scan of mellitic acid and the carbon nanomaterials tested for ice nucleation activity.

Figure 3.5 shows high-resolution spectra of the C1s region indicating the presence of C/O functional groups. The spectra were each scanned 10 times with a dwell time of 50 ms and a spot size of 400 microns.

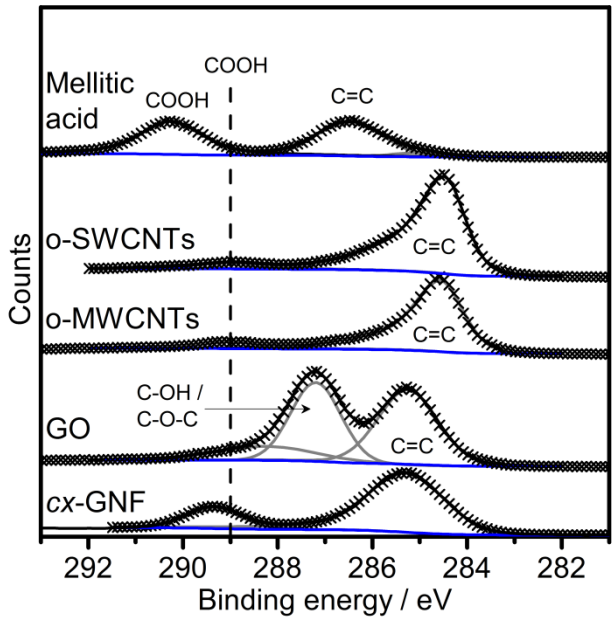

Figure 3.5: High-resolution XPS spectra in the C1s region. Blue lines are the fitted background and the gray lines are fitted peaks.

3.1.3. Ice Nucleation Measurements

The µl-NIPI is described in detail by Whale et al. (2015). Briefly, 45-55 1 µl droplets are placed on a 0.22 mm thick silanised slide (Hampton Research HR3-231) supported by a Grant-Asymptote EF600 stirling cryocooler using a Picus Biohit electronic micropipette. Suspensions are made up using 18.2 MΩ Milli-Q water and carefully weighed quantities of the nucleant under test. The suspension of O-SWCNTs, which did not disperse completely, was filtered through glass wool prior to use to remove undispersed material. The weight percent of the resulting dispersion was determined by evaporating water from a sample and weighing the remaining mass of material.

The EF600 is used to cool down the droplets at a controlled rate and monitor temperature. In this study a cooling rate of 1°C/min has been used unless otherwise stated. The slide and droplets are covered by a Perspex chamber with a port for a camera and a gas inlet and outlet. Dry nitrogen is gently flown over the droplets to prevent condensation of water and ice. A camera is used to monitor droplet freezing. Figure 3.6 shows the layout of the apparatus. µl-NIPI is used to determine the fraction of droplets frozen at a given temperature. All datasets reported here consist of multiple (2-5) individual experiments. Here we have determined surface site active densities (n_s) values using Equation 1 and also used FROST of Herbert et al.(2014) to determine the time dependence of ice nucleation by the *cx*-GNFs.

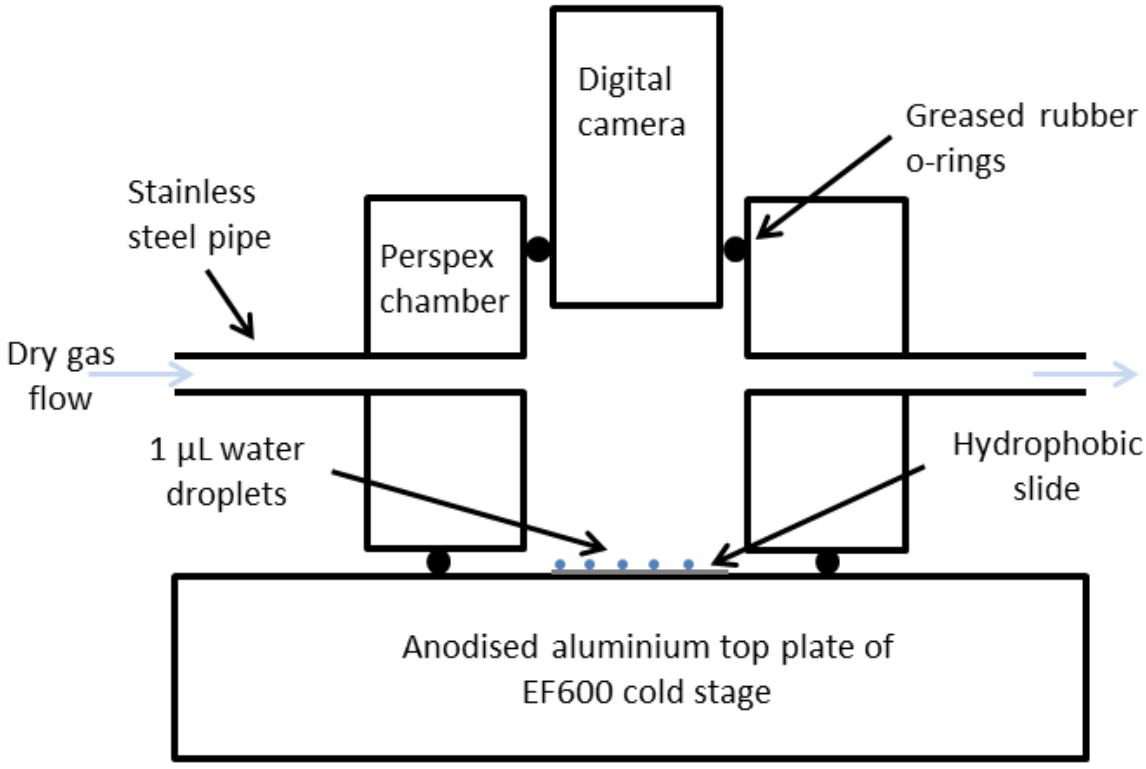

Figure 3.6: Layout of the µl-NI used PI instrument used in this study. Figure is reproduced from Whale et al. (2015) under Creative Commons 3.0.

3.1.4. Analysis of Time Dependence in Ice Nucleation Data

The *Framework for Reconciling Observable Stochastic Time-dependence* (FROST) (Herbert et al., 2014) describes the cooling rate dependence in droplet freezing experiments which is summarised by the following expression:

$$\Delta T_f = \frac{1}{\lambda} \ln\left(\frac{r_1}{r_2}\right) \qquad 3.2$$

Where ΔT_f is the change in temperature at a given fraction frozen observed in a droplet freezing experiment upon a change in cooling rate from r_1 to r_2. The systematic shift in cumulative fraction frozen for a change in cooling rate is dependent only on λ, which is an intrinsic property of the nucleant in question. A similar result had been observed experimentally by Vali and Stansbury (Vali and Stansbury, 1966). The same λ value can also describe the change in the number of droplets expected to freeze in isothermal experiments of varying durations.

Equation 2 can be derived from Equation S1 by choosing a standard cooling rate of 1°C min^{-1}. Modified temperatures can then be calculated for experiments conducted at other ramp rates. As can been seen in Herbert et al. (2014) multiple experiments conducted at different ramp rates fall onto the same line when normalized using λ demonstrating that this single parameter describes the cooling rate dependence of ice nucleation.

Herbert et al. (2014) showed that when a single temperature dependent nucleation rate, $J(T)$, can adequately describe the result of a droplet freezing experiment then ω, the slope of the natural logarithm of freezing rate (or n_s) against temperature will equal λ. In this case, known as single component stochastic nucleation, nucleation by the particles in each droplet can be described by the same $J(T)$. In contrast, when $\omega < \lambda$ there is particle to particle variability with some particles having a larger $J(T)$. This is termed multiple-component stochastic nucleation and the observed nucleation events will be spread out over a larger temperature range than in the case where each droplet has the same nucleation rate. Hence, observation of ω lower than λ for the same data can be interpreted as evidence for the existence of discrete nucleating sites on the nucleant, as opposed to a single nucleation rate across the whole surface area of the nucleant (Herbert et al., 2014;Vali, 2014). For many nucleating materials it is important to describe the particle-to-particle variability, hence the pragmatic singular description (in the form of n_s) is used which describes the density of active sites, but neglects the time dependence of nucleation.

References

Chen, J., Yao, B. W., Li, C., and Shi, G. Q.: An improved hummers method for eco-friendly synthesis of graphene oxide, Carbon, 64, 225-229, 10.1016/j.carbon.2013.07.055, 2013.

Herbert, R. J., Murray, B. J., Whale, T. F., Dobbie, S. J., and Atkinson, J. D.: Representing time-dependent freezing behaviour in immersion mode ice nucleation, Atmos. Chem. Phys., 14, 8501-8520, 10.5194/acp-14-8501-2014, 2014.

Morales-Torres, S., Silva, T. L., Pastrana-Martínez, L. M., Brandão, A. T., Figueiredo, J. L., and Silva, A. M.: Modification of the surface chemistry of single-and multi-walled carbon nanotubes by hno 3 and h 2 so 4 hydrothermal oxidation for application in direct contact membrane distillation, Phys. Chem. Chem. Phys., 16, 12237-12250, 2014.

Salzmann, C. G., Nicolosi, V., and Green, M. L. H.: Edge-carboxylated graphene nanoflakes from nitric acid oxidised arc-discharge material, Journal of Materials Chemistry, 20, 314-319, 10.1039/b914288f, 2010.

Vali, G., and Stansbury, E. J.: Time-dependent characteristics of heterogeneous nucleation of ice, Canadian Journal of Physics, 44, 477-&, 10.1139/p66-044, 1966.

Vali, G.: Interpretation of freezing nucleation experiments: Singular and stochastic; sites and surfaces, Atmos. Chem. Phys., 14, 5271-5294, 10.5194/acp-14-5271-2014, 2014.

Whale, T. F., Murray, B. J., O'Sullivan, D., Wilson, T. W., Umo, N. S., Baustian, K. J., Atkinson, J. D., Workneh, D. A., and Morris, G. J.: A technique for quantifying heterogeneous ice nucleation in microlitre supercooled water droplets, Atmos. Meas. Tech., 8, 2437-2447, 10.5194/amt-8-2437-2015, 2015.

4. Not all feldspar is equal: a survey of ice nucleating properties across the feldspar group of minerals

This chapter is under review for Atmospheric Physics and Chemistry and is publically available on *Atmospheric Physics and Chemistry Discussions* as:

Harrison, A. D., Whale, T. F., Carpenter, M. A., Holden, M. A., Neve, L., O'Sullivan, D., Vergara Temprado, J., and Murray, B. J. 'Not all feldspar is equal: A survey of ice nucleating properties across the feldspar group of minerals' submitted for review in Atmospheric Chemistry and Physics Discussions (2016)

Abstract

Mineral dust particles from wind-blown soils are known to act as effective ice nucleating particles in the atmosphere and are thought to play an important role in the glaciation of mixed phase clouds. Recent work suggests that feldspars are the most efficient nucleators of the minerals commonly present in atmospheric mineral dust. However, the feldspar group of minerals is complex, encompassing a range of chemical compositions and crystal structures. To further investigate the ice-nucleating properties of the feldspar group we measured the ice nucleation activities of 15 characterised feldspar samples. We show that alkali feldspars, in particular the potassium feldspars, generally nucleate ice more efficiently than feldspars containing significant amounts of calcium in the plagioclase series. We also find that there is variability in ice nucleating ability within these groups. While five out of six potassium-rich feldspars have a similar ice nucleating ability, one potassium rich feldspar sample and one sodium-rich feldspar sample were significantly more active. The hyper-active Na-feldspar was found to lose activity with time suspended in water with a decrease in mean freezing temperature of about 16°C over 16 months; the mean freezing temperature of the hyper-active K-feldspar decreased by 2°C over 16 months, whereas the 'standard' K-feldspar did not change activity within the uncertainty of the experiment. These results, in combination with a review of the available literature data, are consistent with the previous findings that potassium feldspars are important components of soil dusts for ice nucleation. However, we also show that there is the possibility that some alkali feldspars can have enhanced ice nucleating abilities, which could have implications for prediction of ice nucleating particle concentrations in the atmosphere.

4.1. Introduction

Clouds containing supercooled liquid water play an important role in our planet's climate and hydrological cycle, but the formation of ice in these clouds remains poorly understood (Hoose and Möhler, 2012). Cloud droplets can supercool to below -35°C in the absence of particles capable of nucleating ice (Riechers et al., 2013; Herbert et al., 2015), hence clouds are sensitive to the presence of ice nucleating particles (INPs). A variety of aerosol types have been identified as INPs (Murray et al., 2012; Hoose and Möhler, 2012) , but mineral dusts from deserts are thought to be important INPs over much of the globe and in a variety of cloud types (Atkinson et al., 2013; DeMott et al., 2003; Hoose et al., 2010; Hoose et al., 2008; Niemand et al., 2012).

Atmospheric mineral dusts are composed of weathered mineral particles from rocks and soils, and are predominantly emitted to the atmosphere in arid regions such as the Sahara (Ginoux et al., 2012). The composition and relative concentrations of dust varies spatially and temporally but it is generally made up of only a handful of dominant minerals. The most common components of dust reflect the composition of the continental crust and soil cover, with clay minerals, feldspars and quartz being major constituents. Until recently, major emphasis for research has been placed on the most common minerals in transported atmospheric dusts, the clays. It has now been shown that, when immersed in water, the feldspar component nucleates ice much more efficiently than the other main minerals that make up typical desert dust (Augustin-Bauditz et al., 2014; O'Sullivan et al., 2014; Atkinson et al., 2013; Niedermeier et al., 2015; Zolles et al., 2015). While all available evidence indicates that feldspars are very effective INPs, it must also be recognised that feldspars are a group of minerals with differing compositions and crystal structures. Therefore, in this study we examine ice nucleation by a range of feldspar samples under conditions pertinent to mixed phase clouds.

An additional motivation is that determining the nature of nucleation sites is of significant fundamental mechanistic interest and is likely to help with further understanding of ice nucleation in the atmosphere (Vali, 2014; Freedman, 2015; Slater et al., 2015). By characterising a range of feldspars and associating them with differences in ice nucleation activity it might be possible to build understanding of the ice nucleation sites on feldspars. Some work has been conducted in this area already. Augustin-Bauditz et al. (2014) concluded that microcline nucleates ice more efficiently than orthoclase on the basis of ice nucleation results looking at a microcline feldspar and several mixed dusts. Zolles et al. (2015) recently found that a plagioclase and an albite feldspar nucleated ice less well

than a potassium feldspar and suggested that the difference in the ice nucleation activity of these feldspars is related to the difference in ionic radii of the cations and the local chemical configuration at the surface. They suggested that only potassium feldspar will nucleate ice efficiently because the K^+ is kosmotropic (structure making) in the water hydration shell while Ca^{2+} and Na^+ are chaotropic (structure breaking).

There has been much interest in the study of ice nucleation using molecular dynamics simulations e.g. (Cox et al., 2015a, b; Cox et al., 2012; Hu and Michaelides, 2007; Fitzner et al., 2015; Reinhardt and Doye, 2014; Lupi and Molinero, 2014; Lupi et al., 2014; Zielke et al., 2015). To date there has been little overlap between work of this nature and laboratory experiment. This has been due to difficulties conducting experiments on similar timescales and spatial extents in both real-world and computational systems. While these obstacles are likely to remain in place for some time, the feldspar system may offer the opportunity to address this deficit by providing qualitative corroboration between computational and laboratory results. For instance, it may be possible to study ice nucleation on different types of feldspar computationally. If differences in nucleation rate observed also occur in the laboratory greater weight may be placed on mechanisms determined by such studies and so a mechanistic understanding of ice nucleation may be built up.

In this paper we have surveyed 15 feldspar samples with varying composition for their ice nucleating ability. It will be shown that feldspars rich in alkali metal cations tend to be much better at nucleating ice than those rich in calcium. First, we introduce the feldspar group of minerals.

4.2. The feldspar group of minerals

The feldspars are tectosilicates (also called framework silicates) with a general formula of $XAl(Si,Al)Si_2O_8$, where X is usually potassium, sodium or calcium (Deer et al., 1992). Unlike clays, which are phyllosilicates (or sheet silicates), tectosilicates are made up of three dimensional frameworks of silica tetrahedra. Substitution of Si with Al in the structure is charge balanced by cation addition or replacement within the cavities in the framework. This leads to a large variability of composition in the feldspars and means that most feldspars in rocks have compositions between end-members of sodium-, calcium- or potassium-feldspars (Wenk and Bulakh, 2004; Deer et al., 1992). A ternary representation of feldspar compositions is shown in Figure 4.1. All feldspars have very similar crystal structures, but the presence of different ions and degrees of disorder related

to the conditions under which they crystallised from the melt (lava or magma) yields subtle differences which can result in differing symmetry.

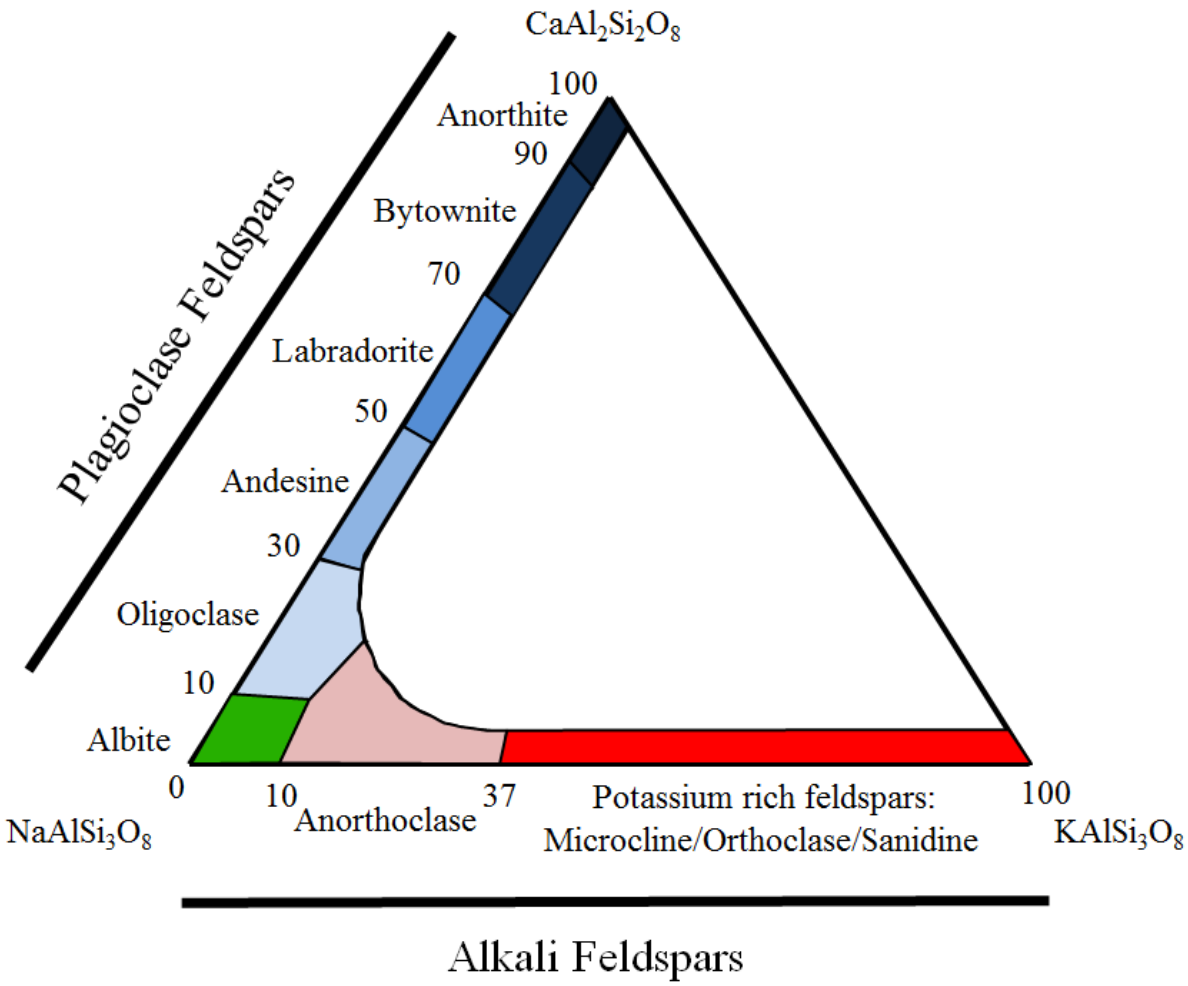

Figure 4.1: The ternary composition diagram for the feldspars group based on similar figures in the literature (Wittke and Sykes, 1990;Deer et al., 1992).

There are three polymorphs (minerals with the same composition, but different crystal structure) of the potassium end-member, which are microcline, orthoclase and sanidine. The polymorphs become more disordered in terms of Al placement in the tetrahedra from microcline to sanidine, respectively. The structures of feldspars which form from a melt vary according to their cooling rate. If cooling is fast (volcanic), sanidine is preserved. If cooling is slow, in some granites for example, microcline may be formed. Feldspars formed in metamorphic rocks have high degrees of Al/Si order. The sodium end-member of the feldspars is albite and the calcium end-member is anorthite. Feldspars with compositions between sodium and calcium form a solid solution and are collectively termed the plagioclase feldspars with specific names for different composition ranges. Feldspars between sodium and potassium end-members are collectively termed the alkali

feldspars and can be structurally complex. A solid solution series exists between high albite and sanidine ('high' refers to high temperature character which is preserved on fast cooling), but not between low albite and microcline ('low' refers to low temperature character which is indicative of slow cooling rates). In contrast to the series between sodium and calcium, and sodium and potassium, there are no feldspars between calcium and potassium end-members because calcium and potassium ions do not actively substitute for one another within the framework lattice due their difference in size and ionic charge (Wenk and Bulakh, 2004; Deer et al., 1992).

There is limited information about the composition of airborne atmospheric mineral dusts and where mineralogy is reported the breakdown of the feldspar family has only been done in a limited way. Atkinson et al. (2013) compiled the available measurements and grouped them into K-feldspars and plagioclase feldspars (see the Supplementary Table 1 in Atkinson et al. (2013)). This compilation indicates that the feldspar type is highly variable in atmospheric dusts, with K-feldspars ranging from 1 to 25% by mass (with a mean of 5%) and plagioclase feldspars ranging from 1 to 14% (with a mean of 7%). The feldspar component of airborne soil dusts is highly variable and the nucleating ability of the various components needs to be investigated.

In order to aid the discussion and representation of the data we have grouped the feldspars into three groups: the plagioclase feldspars (not including albite), albite (the sodium rich corner of the ternary diagram) and potassium (K-) feldspars (microcline, sanidine and orthoclase). The K-feldspars contain varying amounts of sodium, but their naming is determined by their crystal structure. We also collectively refer to albite and potassium feldspars as alkali feldspars.

4.3. Samples and sample preparation

A total of 15 feldspars were sourced for this study. Details of the plagioclase feldspars tested are in Table 4.1 and details of the alkali feldspars are in Table 4.2. We have made use of a series of well characterised plagioclase feldspars which were assembled for previous studies (Carpenter, 1991; Carpenter, 1986; Carpenter et al., 1985). The other samples were sourced from a range of repositories, detailed in Tables 4.1 and 4.2. The naming convention we have used in this paper is to state the identifier of the specific sample followed by the mineral name. For example, BCS 376 microcline is a microcline sample from the Bureau of Analysed Samples with sample code 376. In other cases, such as Amelia Albite, the sample is from a traceable source and is commonly referred to with

this name and when a code is used, such as 97490 plagioclase, the code links to the cited publications.

Table 4.1: Plagioclase feldspars used in this study.

Sample	BET Surface area (m^2/g)	Composition *	Source of composition/phase data
Anorthite glass	1.18 ± 0.01 m²/g	An_{100}	(Carpenter, 1991)
ANC 68	4.25 ± 0.02 m²/g	An_{100}	(Carpenter, 1991) describes similar feldspars
148559	3.07 ± 0.02 m²/g	$An_{99.5}Ab_{0.5}$	-----
21704a	3.07 ± 0.03 m²/g	$An_{86}Ab_{14}$	(Carpenter et al., 1985
Surt M	3.00 ± 0.05 m²/g	$An_{64}Ab_{36}$	(Carpenter, 1986)
67796b	2.80 ± 0.03 m²/g	$An_{60}Or_1Ab_{39}$	(Carpenter et al., 1985)
97490	5.63 ± 0.03 m²/g	$An_{27}Or_1Ab_{71}$	(Carpenter et al., 1985)

*This refers to the chemical makeup of the feldspars. An stands for anorthite, the calcium end-member, Ab stands for albite, the sodium end-member and Or stands for orthoclase, the potassium end-member.

The anorthite glass tested was produced by Carpenter (1991) by melting natural calcite with reagent grade SiO_2 and Al_2O_3 at 1680°C for 3 hours. The melt was then stirred before air cooling. The resulting glass was then annealed at 800°C to relieve internal stresses. The composition of the resulting glass was shown to be stoichiometric $CaAl_2Si_2O_8$. Synthetic anorthite ANC 68 was produced by heating a sample of this glass to 1400°C for 170 hours.

Feldspars 148559, 21704a, 67796b and 97490 plagioclase and Amelia albite are natural samples that form a solid solution series covering the plagioclase series from nearly pure anorthite to nearly pure albite as seen in Table 4.1.

Table 4.2: Alkali feldspars used in this study.

Sample	BET Surface area (m^2/g)	Dominant feldspar phase	Source of composition/phase data
LD1 microcline	1.99 ± 0.05m^2/g	microcline	XRD
LD2 sanidine	3.77 ± 0.03 m^2/g	sanidine	XRD
LD3 microcline	1.78 ± 0.01 m^2/g	microcline	XRD
BCS 376 microcline	2.03 ± 0.01 m^2/g	microcline	Reference sample/XRD (Atkinson et al., 2013)
Amelia Albite (un-ground)	0.73 ± 0.02 m^2/g	albite	(Carpenter et al., 1985)
Amelia Albite ground	3.94 ± 0.02 m^2/g	albite	(Carpenter et al., 1985)
TUD#1 microcline	1.23 ± 0.03 m^2/g	microcline	XRD
TUD#2 albite	1.39 ± 0.03 m^2/g	albite*	XRD
TUD#3 microcline	2.84 ± 0.03 m^2/g	microcline	XRD
BCS 375 albite	5.8 ± 0.03 m^2/g	albite	Reference sample/XRD (Atkinson et al., 2013)

* We note that the XRD pattern was also consistent with oligoclase, which is close to albite in composition. The identification of albite is consistent with that of Alexei Kiselev (Personal communication).

The alkali feldspars used here have not previously been characterised. Rietveld refinement of powder XRD patterns was carried out using TOtal Pattern Analysis Solutions (TOPAS) to determine the phase of the feldspar present. The results of this process are presented in Table 4.2. The surface areas of all the feldspars were measured by Brunauer-Emmett-Teller (BET) nitrogen gas adsorption. All samples, unless otherwise stated, were ground to reduce the particle size and increase the specific surface area using a mortar and pestle which was scrubbed with pure quartz then cleaned with deionised water and methanol before use. Grinding of most samples was necessary in order to make the particles small enough for our experiments. Amelia albite was the only material tested both in an unground state (or at least not a freshly ground state) and a freshly ground state. Suspensions of known concentration were made up gravimetrically

using Milli-Q water (18.2 MΩ.cm). Except where stated otherwise the suspensions were then mixed for a few minutes using magnetic stirrers prior to use in ice nucleation experiments.

Three samples, the BCS 376 microcline, ground Amelia albite and TUD #3 microcline, were tested for changes in ice nucleating efficiency with time, when left in suspension at room temperature. Ice nucleation efficiency was quantified at intervals over 11 days. Between experiments the suspensions were left at room temperature without stirring and then stirred to re-suspend the particulates for the ice nucleation experiments. Suspensions of the three dusts were also tested 16 months after initial experiments were performed to determine the long term impact of contact with water on ice nucleation efficiency.

4.4. Experimental method and data analysis

In order to quantify the efficiency with which a range of feldspar dusts nucleate ice we made use of the microliter Nucleation by Immersed Particle Instrument (µl-NIPI). This system has been used to make numerous ice nucleation measurements in the past (O′Sullivan et al., 2015; Hiranuma et al., 2015; Whale et al., 2015b; Herbert et al., 2014; O'Sullivan et al., 2014; Atkinson et al., 2013; Umo et al., 2015; Wilson et al., 2015) and has been described in detail by Whale et al. (2015a). Briefly, droplets of an aqueous suspension, containing a known quantity of feldspar particles are pipetted onto a hydrophobic coated glass slide. This slide is placed on a temperature controlled stage and cooled from room temperature at a rate of 5 °Cmin^{-1} to 0 °C and then at 1 °Cmin^{-1} until all droplets are frozen. Dry nitrogen is flowed over the droplets at 0.2 l min^{-1} to prevent frozen droplets from affecting neighbouring liquid droplets. Freezing is observed with a digital camera, allowing determination of the fraction of droplets frozen as a function of temperature. Multiple experiments have been combined to produce single sets of data for each mineral. Suspensions of the feldspars were made up gravimetrically and specific surface areas of the samples were measured using the Brunauer–Emmett–Teller (BET) N_2 adsorption method using a Micromeritics TriStar 3000.

To normalise to surface area and allow comparison of different nucleators $n_s(T)$ values are calculated. $n_s(T)$ is the number of ice nucleating sites that become active per surface area on cooling from 0°C to temperature *T*. $n_s(T)$ can be calculated using (Connolly et al., 2009):

$$\frac{n(T)}{N} = 1 - \exp(-n_s(T)A) \qquad 4.1$$

Where $n(T)$ is the number of droplets frozen at temperature T, N is the total number of droplets in the experiment and A is the surface area of nucleator per droplet. This description is site specific and does not include time dependence. The role of time dependence in ice nucleation has recently been extensively discussed (Herbert et al., 2014; Vali, 2014). For feldspar it is thought that the time dependence of nucleation is relatively weak (at least for BCS 376 microcline) and that the particle to particle, or active site to active site, variability is much more important.

In order to estimate the uncertainty in $n_s(T)$ due to the randomness of the distribution of the active sites in droplet freezing experiments, we conducted Monte Carlo simulations. In these simulations, we generate a list of possible values for the number of active sites per droplet (k). The theoretical relationship between the fraction of droplets frozen and k can be derived from the Poisson distribution:

$$\frac{n(T)}{N} = 1 - \exp(-k) \qquad 4.2$$

and we can calculate $n_s(T)$ using the following:

$$n_s = \frac{k}{A} \qquad 4.3$$

The simulation works in the following manner. First, we take a value of k and we simulate a corresponding random distribution of active sites through the droplet population for an experiment. Every droplet containing one or more active sites is then considered to be frozen. In this way, we can obtain a simulated value of the fraction frozen for a certain value of k. Repeating this process many times and for all the possible values of k, we obtain a distribution of possible values of k that can explain every value of the observed fraction frozen. This resulting distribution is neither Gaussian nor symmetric, so in order to propagate the uncertainty in Equation 3, we take the following steps. First, we generate random values of k following the corresponding previously simulated distribution for every value of the fraction frozen. Then, we simulate random values of A following a Gaussian distribution centred on the value derived from the specific surface area per droplet with the standard deviation derived from the uncertainty in droplet volume and specific surface area. We assume that each droplet contains a representative surface area distribution. By combining these two distributions of simulated values, we calculate the distribution of $n_s(T)$values, and from that distribution, we obtain the 95% confidence interval.

4.5. Results and discussion

4.5.1. Ice nucleation efficiencies of plagioclase and alkali feldspars

The values of $n_s(T)$ derived from the freezing experiments of the 15 feldspar samples are shown in Figure 4.2 along with the $n_s(T)$ parameterisation from Atkinson et al. (2013) for BCS 376 microcline. The various groups of feldspars are indicated by colour which corresponds to the regions of the phase diagram in Figure 4.1. We define potassium (K-) feldspars (red) as those rich in K including microcline, orthoclase and sanidine; the Na end-member is albite (green); and plagioclase series feldspars (blue) are a solid solution between albite and the calcium end-member, anorthite.

Out of the six K-feldspars studied, five fall on or near the line defined by Atkinson et al. (2013). These include three microcline samples and one sanidine sample, which have different crystal structures. Sanidine has disordered Al atoms, microcline has ordered Al atoms and orthoclase has intermediate order; these differences result in differences in symmetry and hence space group. The freezing results indicate that Al disordering does not play an important role in nucleation. However, one K-feldspar sample, TUD#3 microcline, was substantially more active. This indicates that crystal structure and composition are not the only factors dictating the ice nucleating ability of K-feldspars.

All plagioclase feldspars tested were less active ice nucleators than the K-feldspars which were tested. There was relatively little variation in the ice nucleation activities of the plagioclase solid solution series characterised by Carpenter (1986) and Carpenter et al. (1985). For instance, of those feldspars that possess the plagioclase structure, greater sodium content does not systematically increase effectiveness of ice nucleation. Overall, the results for plagioclase feldspars indicate that they have an ice nucleating ability much smaller than that of the K-feldspars.

It is also interesting to note that the ANC 68 synthetic anorthite had different nucleating properties to the anorthite glass from which it was crystallised (and had the same composition). The ANC 68 synthetic anorthite sample has a much more shallow $n_s(T)$ curve than the glass. This is noteworthy, because the composition of these two materials is identical, but the phase of the material is different. It demonstrates that crystallinity is not required to cause nucleation, but the presence of crystallinity can provide rare sites which can trigger nucleation at much warmer temperatures. In a future study it would be interesting to attempt to probe the nature of these sites.

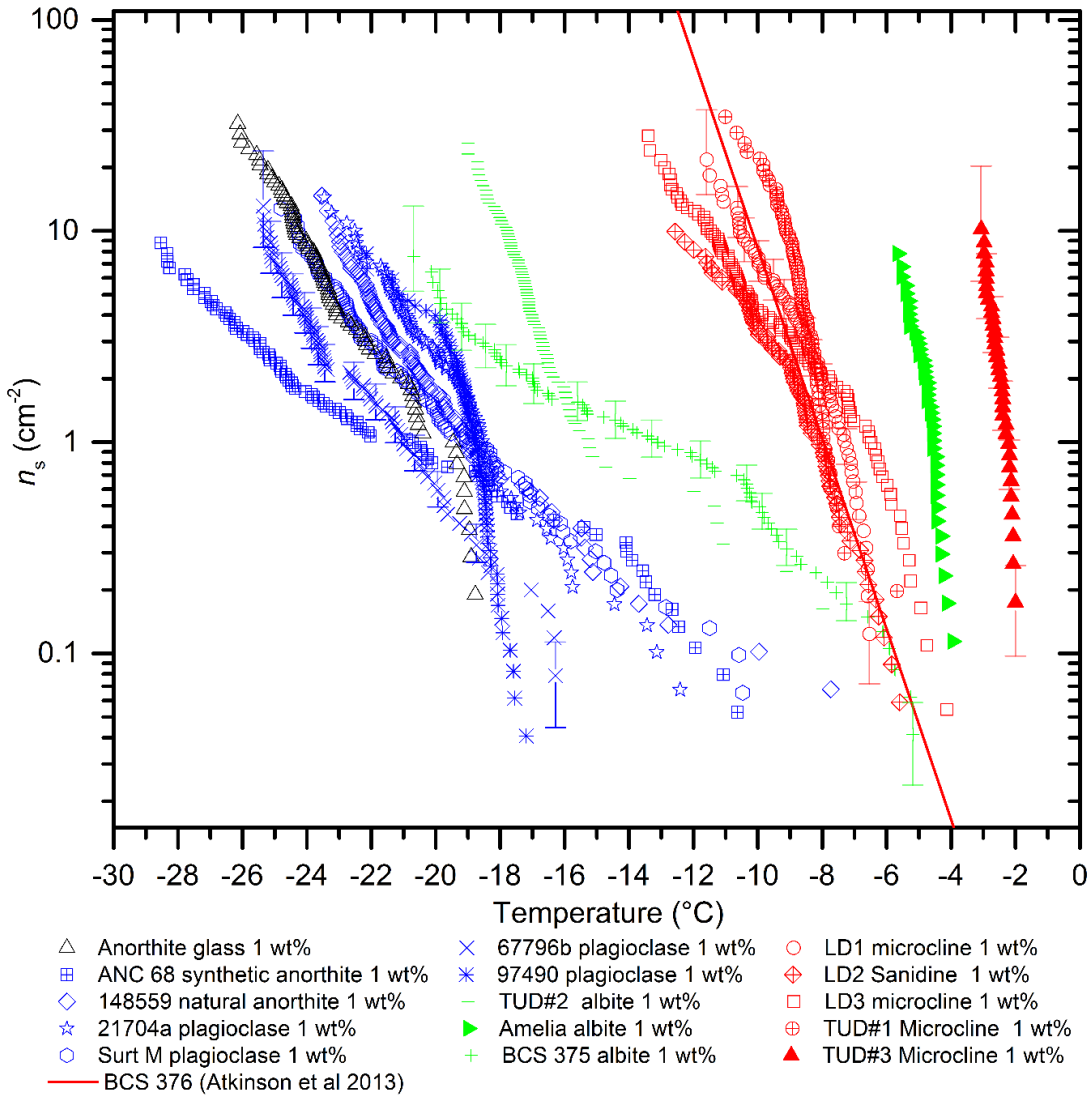

Figure 4.2: Ice nucleation efficiency expressed as $n_s(T)$ for the various feldspars tested in this study. The K-feldspars are coloured red, the plagioclase feldspars are coloured blue, the albites are coloured green and the feldspar glass is coloured black. Except for Amelia albite and TUD#1 microcline all samples were tested twice and the data from the two runs combined. Sample information can be found in tables 4.1 and 4.2. Temperature uncertainty is ±0.4°C. Y-Error bars calculated using the Poisson Monte Carlo procedure described in Sect. 4. Data points with large uncertainties greater than an order of magnitude have been removed, these are invariably the first one or two freezing events of a given experiment. For clarity error bars have only been included on a selection of datasets (TUD#3 microcline, LD1 microcline, BCS 375 albite and 67796b plagioclase). The error bars shown are typical. Background subtraction of the type conducted by O'Sullivan et al. (2015) made insignificant difference to the reported $n_s(T)$ values.

We tested three predominantly Na-feldspars (albites). Amelia albite was found to be highly active, approaching that of TUD#3 microcline. The others, BCS 375 albite, and

TUD#2 albite were less active, intermediate between the K-feldspars and plagioclase feldspars.

To ensure that the high activity of Amelia albite and microcline TUD#3 was not caused by contamination from biological INPs the samples were heated to 100°C in Milli-Q water for 15 minutes. This treatment will disrupt any protein based nucleators present (O′Sullivan et al., 2015). No significant reduction in freezing temperatures (beyond what would be expected from the activity decay described in Sect. 4.5.2) was observed suggesting that the highly active INPs present are associated with the feldspars rather than biological contamination.

It has been noted by Vali (2014) that there is an indication that nucleators which are more active at higher temperatures tend to have steeper slopes of ln *J* (nucleation rate) vs. We have observed this trend here in the data shown in Figure 4.2 ($n_s(T)$ is proportional to *J*). The slopes of experiments where freezing occurred at colder temperatures (plagioclases) generally being flatter than those where freezing took place at warmer temperatures (alkali feldspars). Vali (2014) suggests that this maybe the result of different observational methods. In this study we have used a single method for all experiments so the trend is unlikely to be due to an instrument artefact. The implication is that sites with lower activity tend to be more diverse in nature. This may indicate that there are fewer possible ways to compose a site that is efficient at nucleating ice and that there will be less variation in these sites as a result. The active sites of lower activity may take a greater range of forms and so encompass a greater diversity of activation temperatures.

To summarise, plagioclase feldspars tend to have relatively poor ice nucleating abilities, all K-feldspars we tested are relatively good at nucleating ice and the albites are variable in their nucleating activity. Out of the six K-feldspars tested, five have very similar activities and are well approximated by the parameterisation of Atkinson et al. (2013) in the temperature-n_s regime we investigated here. However, we have identified two alkali feldspar samples, one K-feldspar and one albite, which are much more active than the others indicating that a factor or factors other than the polymorph or composition determines the efficiency of alkali feldspars as ice nucleators.

4.5.2. The stability of active sites

It was observed that the ice nucleation activity of ground Amelia albite and ground TUD #3 microcline declined over the course of ~30 minutes, the time between successive runs. Only the initial run is shown in Figure 4.2 where the feldspar had spent only about 10 minutes in suspension. This decay in activity over the course of ~30 mins was not seen in

the other feldspars. To investigate this effect samples of BCS 376 microcline, Amelia albite and TUD #3 microcline were left in water within a sealed vial and tested at intervals over the course of 16 months, with a focus on the first 11 days. The results of these experiments are shown in Figure 4.3 and Figure 4.4. The median freezing temperature of the Amelia albite sample was most sensitive to time spent in water, decreasing by 8 ^{o}C in 11 days and by 16 ^{o}C in 16 months. The TUD#3 microcline sample decreased by about 2 ^{o}C in 16 months, but the freezing temperatures of the BCS 376 did not change significantly over 16 months (within the temperature uncertainty of ±0.4°C). Clearly, the stability of the active sites responsible for ice nucleation in these samples is highly variable.

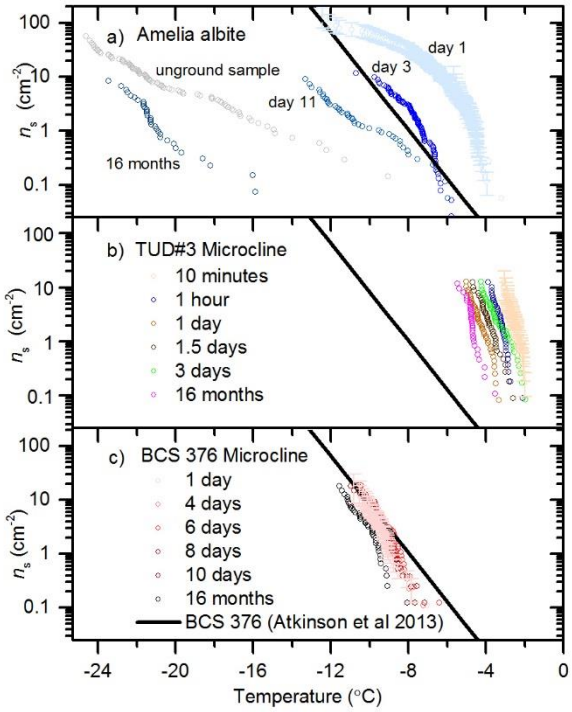

Figure 4.3: The dependence of n_s on time spent in water for three feldspar samples. The time periods indicate how long samples were left in contact with water. Fresh samples were tested minutes after preparation of suspensions. Note that ice nucleation temperatures of BCS 376 are almost the same after 16 months in water while those of Amelia albite decreases by around 16°C. TUD #3 microcline loses activity quickly in the first couple of days of exposure to water but total decrease in nucleation temperatures after 16 months is only around 2°C.

Amelia albite is a particularly interesting case, where the highly active sites are also highly unstable. For Amelia albite we observed that the ice nucleation ability of the powder directly as supplied (the sample had been ground many years prior to

experiments) was much lower than the freshly ground sample. The n_s values for the 'as-supplied' Amelia albite are shown in Figure 4.3. This suggests that the sites on Amelia albite are unstable and in general are sensitive to the history of the sample. We note that from previous work that BCS 376 feldspar ground to varied extents nucleates ice similarly (Whale et al., 2015a) and we have not observed a decay of active sites of the BCS 376 microcline sample when stored in a dry vial over the course of two years. It is also worth noting that freshly ground BCS 376 microcline did not nucleate ice as efficiently as Amelia albite or TUD#3 microcline. These results indicate that BCS 376 microcline contains very active sites, but that these sites are much more stable than those found in Amelia albite.

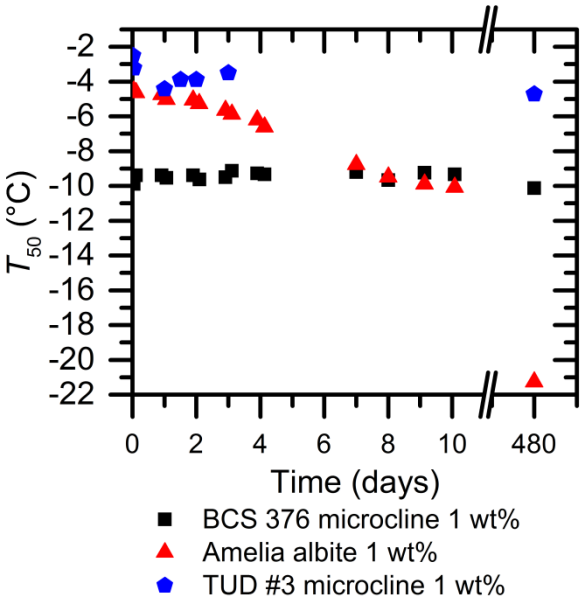

Figure 4.4: Median freezing temperature against time left in suspension for BCS 376 microcline, TUD#3 microcline and Amelia albite.

It is evident that highly active sites in Amelia albite are generated by grinding but lose activity when exposed to liquid water, and probably lose activity during exposure to (presumably wet) air, returning to an activity level comparable to that of the plagioclase feldspars. TUD#3 microcline also possesses a highly active site type sensitive to water exposure but falls back to a level of activity higher than the other K-feldspars we have tested. This second, less active site type is shown to be stable in water over the course of 16 months. TUD#3 must possess populations of both more active, unstable sites and less active (although still relatively active compared to the sites on other K-feldspars) stable

sites. Amelia albite possesses only unstable sites and much less active sites similar to those found on the plagioclase feldspars we have tested.

These results indicate something of the nature of the active sites on feldspars. Throughout this paper we refer to nucleation occurring on active sites, or specific sites, on the surface of feldspar. It is thought that nucleation by most ice active minerals is consistent with nucleation on active sites with a broad spectrum of activities (Herbert et al., 2014; Wheeler et al., 2015; Niedermeier et al., 2015; Hiranuma et al., 2015; Wex et al., 2014; Augustin-Bauditz et al., 2014; Niedermeier et al., 2010; Lüönd et al., 2010; Vali, 2014). However, the nature of these sites is not known. It is postulated that active sites are related to defects in the structure and therefore that each site has a characteristic nucleation ability, producing a spectrum of sites. Defects are inherently less stable than the bulk of the crystal and we might expect these sites to be affected by dissolution processes, or otherwise altered, in preference to the bulk of the crystal (Parsons et al.;2015). The fact that we observe ice nucleation by populations of active sites with different stabilities in water implies that these sites have different physical or chemical characteristics. Furthermore, the fact that some populations of active sites are sensitive to exposure to water suggests that the history of particles can be critical in determining the ice nucleating ability of mineral dusts. This raises the question of whether differences in ice nucleation efficiency observed by different instruments (Emersic et al., 2015; Hiranuma et al., 2015), could be related to the different conditions particles experience prior to nucleation.

4.5.3. Comparison to literature data

We have compared the $n_s(T)$ values for various feldspars from a range of literature sources with data from this study in Figure 4.5. Inspection of this plot confirms that K-feldspars nucleate ice more efficiently than the plagioclase feldspars. Also, with the exception of the hyper-active Amelia albite sample, the K-feldspars are more active than the albites.

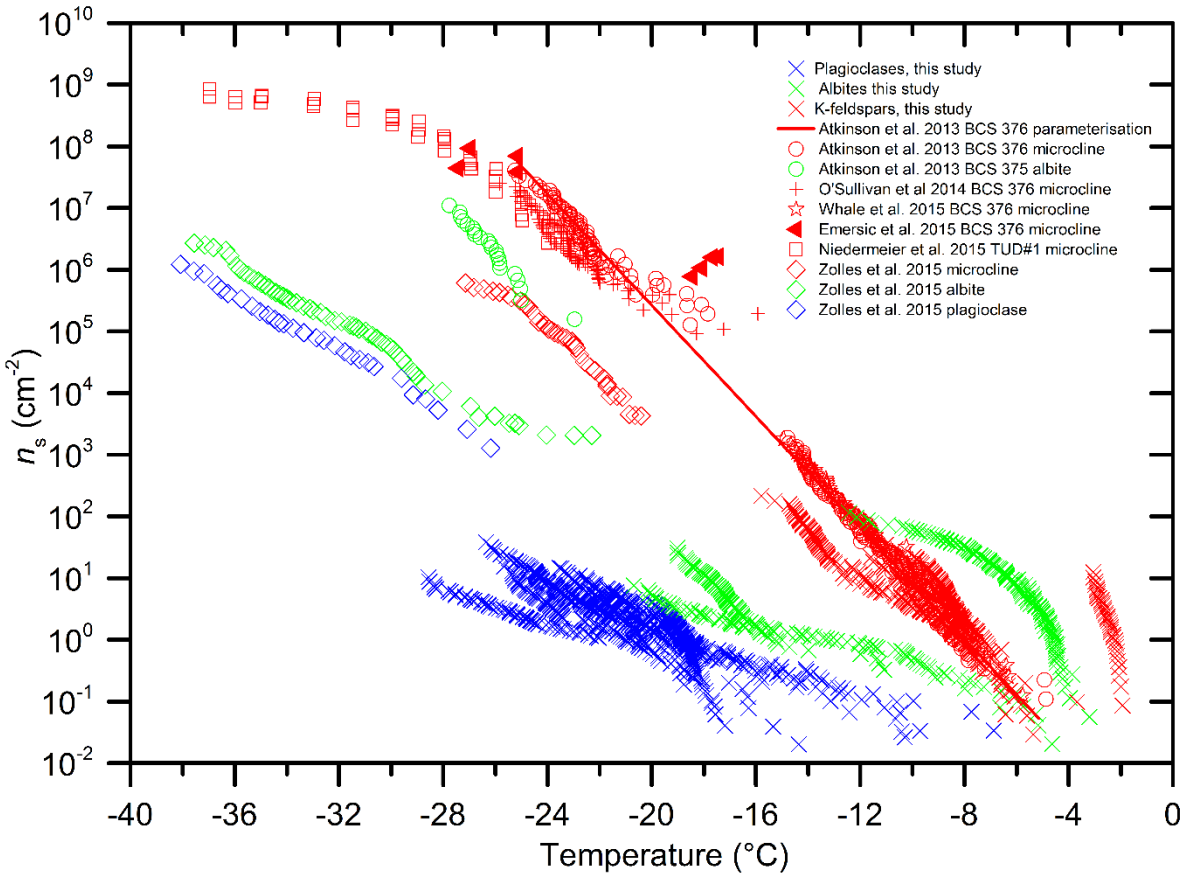

Figure 4.5: Comparison of literature data from Atkinson et al. (2013), Emersic et al. (2015), Niedermeier et al. (2015) and Zolles et al. (2015) with data from this study. Feldspars are coloured according to their composition, as in Figure 4.2. 0.1 wt% data for Amelia albite and LD1 microcline, which is not shown in figure 4.2, has been included. Where samples are known to lose activity with time the most active runs have been shown. Note that data from Niedermeier et al. (2015) includes some data from Augustin-Bauditz et al. (2014).

Results for BCS 376 microcline have been reported in several papers (Whale et al., 2015a; Emersic et al., 2015; O'Sullivan et al., 2014; Atkinson et al., 2013). There is a discrepancy between the cloud chamber data from Emersic et al. (2015) and the picolitre droplet cold stage experiments at around -18°C, whereas the data at about -25°C are in agreement. Emersic et al. (2015) attribute this discrepancy to aggregation of feldspar particles in microlitre scale droplet freezing experiments reducing the surface area of feldspar exposed to water leading to a lower $n_s(T)$ value. It is unlikely that this effect can account for the discrepancy because in the temperature range of the Emersic et al. (2015) data the comparison is being made to results from picolitre droplet freezing experiments which Emersic et al. (2015) argue should not be affected by aggregation because there are not enough particles present in each droplet to result in significant aggregation. Atkinson et

al. (2013) estimated that on average even the largest droplets only contained a few 10s of particles. We also note that our microscope images of droplets show many individual particles moving independently around in the picolitre droplets in those experiments, indicating that the feldspar grains do not aggregate substantially. Hence, the discrepancy between the data of Emersic et al. (2015) and Atkinson et al. (2013) at around -18ºC cannot be accounted for by aggregation. Furthermore, Atkinson et al. (2013) report that the surface area determined from the laser diffraction size distribution of BCS 376 microcline in suspension is 3.5 times smaller than that derived by the gas adsorption measurements (see supplementary Figure 5 in Atkinson et al. (2013) and the corresponding discussion). This difference in surface area can be accounted for by the fact that feldspar grains are not smooth spheres, as assumed in the analysis of the laser diffraction data. Feldspar grains are well-known to be rough and aspherical (Hodson et al., 1997). Atkinson et al. (2013) also note that the laser diffraction technique lacks sensitivity to the smallest particles in the distribution which will also lead to an underestimate in surface area. Nevertheless, the data presented by Atkinson et al. (2013) suggests that aggregation of feldspar particles leading to reduced surface area is at most a minor effect. As such the discrepancy between different instruments remains unexplained and more work is needed on this topic.

Ice nucleation by single size-selected particles of TUD#1 microcline has been investigated by Niedermeier et al. (2015) at temperatures below -23°C. We found that TUD#1 microcline was in good agreement with K-feldspar parameterisation from Atkinson et al. (2013) between about -6 and -11°C. Between -23 and -25°C, the $n_s(T)$ values produced by Niedermeier et al. (2015) are similar (lower by a factor of roughly 4) to that of the Atkinson et al. (2013) parameterisation, despite the different sample types. Niedermeier et al. (2015) used the Leipzig Aerosol Cloud Interaction Simulator (LACIS), in which they size selected particles, activated them to cloud droplets and then quantified the probability of freezing at a particular temperature. It is interesting that the Niedermeier et al. (2015) $n_s(T)$ values curve off at lower temperatures to a limiting value which they term n_s^*, indicating that nucleation by K-feldspars may hit a maximum value and emphasises why we need to be cautious in extrapolating $n_s(T)$ parameterisations beyond the range of experimental data.

The data for a microcline, a plagioclase (andesine) and albite from Zolles et al. (2015) is consistent with our finding that plagioclase feldspars are less effective nucleators than K-feldspars. It is also consistent with Atkinson et al. (2013) who found that albite is less

efficient at nucleating ice than microcline. However, the data for K-feldspar from Zolles et al. (2015) sits below the line from Atkinson et al. (2013) for BCS 376 microcline and are lower than the points from Niedermeier et al. (2015) for TUD#1 microcline. Their measurements involved making up concentrated suspensions (19.6-4.8 wt%) suspensions and then creating a water-in-oil emulsion where droplets were between 10-40 µm. They quote their particle sizes as being between 1-10 µm for the feldspars. Atkinson et al. (2013) worked with 0.8 wt% suspensions, with droplets of 9 to 19 µm where the mode particle size was ~700 nm. Hence, Zolles et al. (2015) worked with a significantly more concentrated suspensions and larger particles than used by Atkinson et al. (2013). However, it is not possible to determine whether the observed difference in n_s is due to differences in the sample or the techniques used, but may mean that certain K-feldspars nucleate ice less well than those defined by the Atkinson et al. (2013) line in this temperature regime. This would be a very interesting result as it may provide a point of difference that could provide insight into why K-feldspar nucleate ice efficiently.

There has been relatively little work on what makes feldspar a good nucleator of ice. Zolles et al. (2015) suggest that only K-feldspars will nucleate ice well on the basis that Ca^{2+} and Na^{+} are chaotropic (structure breaking in water) while K^{+} is kosmotropic (structure making in water). We have only observed one feldspar that contains little K^{+} but nucleates ice relatively efficiently, Amelia albite. This feldspar loses its activity quickly in water and eventually becomes more comparable to the plagioclase feldspars. It may be that the strong nucleation observed is associated with the small amount of K^{+} it contains and that once this dissolves away the feldspar behaves like a plagioclase.

Augustin-Bauditz et al. (2014) tentatively concluded that microcline may nucleate ice more efficiently than orthoclase at $n_s(T)$ values above about 10^6 cm^{-2} and at temperatures below -23ºC, the conditions where they performed their measurements. They arrived at this conclusion by noting that NX-illite and Arizona test dust both contain orthoclase (8 and 20%, respectively), but the $n_s(T)$ values they report for these materials are more than one order less than microcline. In the microliter regimen this study we have observed some variability amongst the K-feldspars (see Figure 4.2), but no difference between sanidine and the 4 out of 5 microclines which fall around the line defined by Atkinson et al. (2013). As discussed above, the Al in sanidine is the least ordered, with microcline the most ordered and orthoclase at an intermediate order, hence we observe no clear dependency on the ordering of Al in K-feldspars. Further investigations of the ice nucleating ability of the various K-feldspar phases at low temperature would be valuable.

We could not do this in the present study with the samples used here because we did not have sufficient quantities of the samples.

4.6. Conclusions

In this study we have analysed the ice nucleating ability of 15 well characterised feldspar samples. These minerals include plagioclase feldspars (in the solid solution series between Ca and Na end-members), the K-feldspars (sanidine, orthoclase and microcline) and albite (the Na end-member). The results indicate that the alkali feldspars, including albite and K-feldspars, tend to nucleate ice more efficiently than plagioclase feldspars. The plagioclase feldspars nucleate ice at the lowest temperatures with no obvious dependence on the Ca-Na ratio. The albites have a wide variety of nucleating abilities, with one sample nucleating ice much more efficiently than the microcline sample Atkinson et al. (2013) studied. This hyper-active albite lost its activity over time while suspended in water. Five out of six of the K-feldspar samples we studied nucleated ice with a similar efficiency to the 'generic' microcline studied by Atkinson et al. (2013). A single K-feldspar we studied had a very high activity, nucleating ice as warm as -2°C in our microliter droplet assay. The striking activity of this hyperactive microcline decayed with time spent in water, but not to the same extent as the hyper-active albite sample. While the hyperactive sites are sensitive, to varying degrees, to time spent in water, the activity of the 'generic' microcline sample used by Atkinson et al. (2013) did not change significantly.

In light of these findings, we suggest that there are at least three classes of site present in the feldspars studied here: i) relatively inactive sites associated with plagioclase feldspars; ii) more active sites associated with K-feldspars that is stable in water over the course of many months; iii) hyper-active sites associated with one albite and one K-feldspar that we studied that loses activity when exposed to water.

The specific details of these active sites continue to elude us, although it appears that they are only present in alkali feldspars and in particular, the K-feldspars. Unlike the plagioclase feldspars which form a solid solution, the Na and K feldspars in alkali feldspars are often exsolved, possessing intergrowths of the Na and K feldspars referred to as microtexture (Parsons et al., 2015). It is possible that the boundaries between the two phases in the intergrowth provide sites for nucleation that are not present in plagioclase feldspars. More work is needed to explore this possibility.

In a previous study Atkinson et al. (2013) used an $n_s(T)$ parameterisation of a single K-feldspar (BCS 376 microcline) to approximate the ice nucleating properties of desert dust in a global aerosol model. Given that four out of five of the K-feldspars we studied here have very similar ice nucleating abilities, this approximation seems reasonable. However, we have identified two hyper-active feldspars and do not know how representative these samples are of natural feldspars in dust emission regions. We also note that the active sites on these feldspars are less stable than those of BCS 376 microcline. Nevertheless, there is the possibility that the parameterisation used by Atkinson et al. (2013) underestimates the contribution of feldspars at warmer temperatures above about -15°C.

In the longer term it may be possible to identify what it is that leads to the variation in ice nucleation activity between the different feldspar classes. In particular, the nature of the active sites in the hyper-active feldspars and the reason plagioclase is so much poorer at nucleating ice are subjects of interest. The instability of the sites in the hyperactive feldspars may be related to dissolution of feldspar in water and investigation of this process may allow progress towards understanding of nucleation by feldspars. The results presented here are empirical in nature and do not provide a thorough underpinning understanding of the nature of the active sites. Nevertheless, the fact that the feldspar group of minerals have vastly different ice nucleating properties despite possessing very similar crystal structures may provide us with a means of gaining a fundamental insight to heterogeneous ice nucleation.

References

Atkinson, J. D., Murray, B. J., Woodhouse, M. T., Whale, T. F., Baustian, K. J., Carslaw, K. S., Dobbie, S., O'Sullivan, D., and Malkin, T. L.: The importance of feldspar for ice nucleation by mineral dust in mixed-phase clouds, Nature, 498, 355-358, 10.1038/nature12278, 2013.

Augustin-Bauditz, S., Wex, H., Kanter, S., Ebert, M., Niedermeier, D., Stolz, F., Prager, A., and Stratmann, F.: The immersion mode ice nucleation behavior of mineral dusts: A comparison of different pure and surface modified dusts, Geophys. Res. Lett., 41, 7375-7382, 10.1002/2014gl061317, 2014.

Carpenter, M.: Experimental delineation of the “e” ⇌ i\bar 1 and “e” ⇌ c\bar 1 transformations in intermediate plagioclase feldspars, Phys. Chem. Minerals., 13, 119-139, 10.1007/bf00311902, 1986.

Carpenter, M. A., McConnell, J. D. C., and Navrotsky, A.: Enthalpies of ordering in the plagioclase feldspar solid solution, Geochim. Cosmochim. Acta, 49, 947-966, http://dx.doi.org/10.1016/0016-7037(85)90310-2, 1985.

Carpenter, M. A.: Mechanisms and kinetics of al-si ordering in anorthite; I, Incommensurate structure and domain coarsening, Am. Mineral., 76, 1110-1119, 1991.

Connolly, P. J., Möhler, O., Field, P. R., Saathoff, H., Burgess, R., Choularton, T., and Gallagher, M.: Studies of heterogeneous freezing by three different desert dust samples, Atmos. Chem. Phys., 9, 2805-2824, 10.5194/acp-9-2805-2009, 2009.

Cox, S. J., Kathmann, S. M., Purton, J. A., Gillan, M. J., and Michaelides, A.: Non-hexagonal ice at hexagonal surfaces: The role of lattice mismatch, Phys. Chem. Chem. Phys., 14, 7944-7949, 10.1039/c2cp23438f, 2012.

Cox, S. J., Kathmann, S. M., Slater, B., and Michaelides, A.: Molecular simulations of heterogeneous ice nucleation. I. Controlling ice nucleation through surface hydrophilicity, J. Chem. Phys, 142, 184704, doi:http://dx.doi.org/10.1063/1.4919714, 2015a.

Cox, S. J., Kathmann, S. M., Slater, B., and Michaelides, A.: Molecular simulations of heterogeneous ice nucleation. II. Peeling back the layers, J. Chem. Phys, 142, 184705, doi:http://dx.doi.org/10.1063/1.4919715, 2015b.

Deer, W. A., Howie, R. A., and Zussman, J.: An introduction to the rock forming minerals, 2nd ed., Addison Wesley Longman, Harlow, UK, 1992.

DeMott, P. J., Sassen, K., Poellot, M. R., Baumgardner, D., Rogers, D. C., Brooks, S. D., Prenni, A. J., and Kreidenweis, S. M.: African dust aerosols as atmospheric ice nuclei, Geophys. Res. Lett., 30, 1732, 10.1029/2003GL017410, 2003.

Emersic, C., Connolly, P. J., Boult, S., Campana, M., and Li, Z.: Investigating the discrepancy between wet-suspension- and dry-dispersion-derived ice nucleation efficiency of mineral particles, Atmos. Chem. Phys., 15, 11311-11326, 10.5194/acp-15-11311-2015, 2015.

Fitzner, M., Sosso, G. C., Cox, S. J., and Michaelides, A.: The many faces of heterogeneous ice nucleation: Interplay between surface morphology and hydrophobicity, J. Am. Chem. Soc., 137, 13658-13669, 10.1021/jacs.5b08748, 2015.

Freedman, M. A.: Potential sites for ice nucleation on aluminosilicate clay minerals and related materials, J. Phys. Chem. Lett., 6, 3850-3858, 10.1021/acs.jpclett.5b01326, 2015.

Ginoux, P., Prospero, J. M., Gill, T. E., Hsu, N. C., and Zhao, M.: Global-scale attribution of anthropogenic and natural dust sources and their emission rates based on modis deep blue aerosol products, Rev. Geophys., 50, RG3005, 10.1029/2012rg000388, 2012.

Herbert, R. J., Murray, B. J., Whale, T. F., Dobbie, S. J., and Atkinson, J. D.: Representing time-dependent freezing behaviour in immersion mode ice nucleation, Atmos. Chem. Phys., 14, 8501-8520, 10.5194/acp-14-8501-2014, 2014.

Herbert, R. J., Murray, B. J., Dobbie, S. J., and Koop, T.: Sensitivity of liquid clouds to homogenous freezing parameterizations, Geophys. Res. Lett., 42, 1599-1605, 10.1002/2014gl062729, 2015.

Hiranuma, N., Augustin-Bauditz, S., Bingemer, H., Budke, C., Curtius, J., Danielczok, A., Diehl, K., Dreischmeier, K., Ebert, M., Frank, F., Hoffmann, N., Kandler, K., Kiselev, A., Koop, T., Leisner, T., Möhler, O., Nillius, B., Peckhaus, A., Rose, D., Weinbruch, S., Wex, H., Boose, Y., DeMott, P. J., Hader, J. D., Hill, T. C. J., Kanji, Z. A., Kulkarni, G., Levin, E. J. T., McCluskey, C. S., Murakami, M., Murray, B. J., Niedermeier, D., Petters, M. D., O'Sullivan, D., Saito, A., Schill, G. P., Tajiri, T., Tolbert, M. A., Welti, A., Whale, T. F., Wright, T. P., and Yamashita, K.: A comprehensive laboratory study on the immersion freezing behavior of illite nx particles: A comparison of 17 ice nucleation measurement techniques, Atmos. Chem. Phys., 15, 2489-2518, 10.5194/acp-15-2489-2015, 2015.

Hodson, M. E., Lee, M. R., and Parsons, I.: Origins of the surface roughness of unweathered alkali feldspar grains, Geochim. Cosmochim. Acta, 61, 3885-3896, 10.1016/s0016-7037(97)00197-x, 1997.

Hoose, C., Lohmann, U., Erdin, R., and Tegen, I.: The global influence of dust mineralogical composition on heterogeneous ice nucleation in mixed-phase clouds, Environ. Res. Lett., 3, 10.1088/1748-9326/3/2/025003, 2008.

Hoose, C., Kristjánsson, J. E., Chen, J.-P., and Hazra, A.: A classical-theory-based parameterization of heterogeneous ice nucleation by mineral dust, soot, and biological particles in a global climate model, J. Atmos. Sci., 67, 2483-2503, 10.1175/2010jas3425.1, 2010.

Hoose, C., and Möhler, O.: Heterogeneous ice nucleation on atmospheric aerosols: A review of results from laboratory experiments, Atmos. Chem. Phys., 12, 9817-9854, 10.5194/acp-12-9817-2012, 2012.

Hu, X. L., and Michaelides, A.: Ice formation on kaolinite: Lattice match or amphoterism?, Surf. Sci., 601, 5378-5381, 10.1016/j.susc.2007.09.012, 2007.

Lüönd, F., Stetzer, O., Welti, A., and Lohmann, U.: Experimental study on the ice nucleation ability of size-selected kaolinite particles in the immersion mode, J. Geophys. Res., 115, D14201, 10.1029/2009jd012959, 2010.

Lupi, L., Hudait, A., and Molinero, V.: Heterogeneous nucleation of ice on carbon surfaces, J. Am. Chem. Soc., 136, 3156-3164, 10.1021/ja411507a, 2014.

Lupi, L., and Molinero, V.: Does hydrophilicity of carbon particles improve their ice nucleation ability?, J. Phys. Chem. A, 118, 7330-7337, 10.1021/jp4118375, 2014.

Murray, B. J., O'Sullivan, D., Atkinson, J. D., and Webb, M. E.: Ice nucleation by particles immersed in supercooled cloud droplets, Chem. Soc. Rev., 41, 6519-6554, 10.1039/C2CS35200A, 2012.

Niedermeier, D., Hartmann, S., Shaw, R. A., Covert, D., Mentel, T. F., Schneider, J., Poulain, L., Reitz, P., Spindler, C., Clauss, T., Kiselev, A., Hallbauer, E., Wex, H., Mildenberger, K., and Stratmann, F.: Heterogeneous freezing of droplets with immersed mineral dust particles - measurements and parameterization, Atmos. Chem. Phys., 10, 3601-3614, 10.5194/acp-10-3601-2010, 2010.

Niedermeier, D., Augustin-Bauditz, S., Hartmann, S., Wex, H., Ignatius, K., and Stratmann, F.: Can we define an asymptotic value for the ice active surface site density for heterogeneous ice nucleation?, J. Geophy. Res.: Atmos., 120, 5036-5046, 10.1002/2014jd022814, 2015.

Niemand, M., Möhler, O., Vogel, B., Vogel, H., Hoose, C., Connolly, P., Klein, H., Bingemer, H., DeMott, P. J., Skrotzki, J., and Leisner, T.: A particle-surface-area-based parameterization of immersion freezing on desert dust particles, J. Atmos. Sci., 69, 10.1175/jas-d-11-0249.1, 2012.

O'Sullivan, D., Murray, B. J., Malkin, T. L., Whale, T. F., Umo, N. S., Atkinson, J. D., Price, H. C., Baustian, K. J., Browse, J., and Webb, M. E.: Ice nucleation by fertile soil dusts: Relative importance of mineral and biogenic components, Atmos. Chem. Phys., 14, 1853-1867, 10.5194/acp-14-1853-2014, 2014.

O′Sullivan, D., Murray, B. J., Ross, J. F., Whale, T. F., Price, H. C., Atkinson, J. D., Umo, N. S., and Webb, M. E.: The relevance of nanoscale biological fragments for ice nucleation in clouds, Sci. Rep., 5, 10.1038/srep08082, 2015.

Parsons, I., Fitz Gerald, J. D., and Lee, M. R.: Routine characterization and interpretation of complex alkali feldspar intergrowths, Am. Mineral., 100, 1277-1303, 10.2138/am-2015-5094, 2015.

Reinhardt, A., and Doye, J. P. K.: Effects of surface interactions on heterogeneous ice nucleation for a monatomic water model, J. Chem. Phys., 141, 10.1063/1.4892804, 2014.

Riechers, B., Wittbracht, F., Hütten, A., and Koop, T.: The homogeneous ice nucleation rate of water droplets produced in a microfluidic device and the role of temperature uncertainty, Phys. Chem. Chem. Phys., 15, 5873-5887, 10.1039/C3CP42437E, 2013.

Slater, B., Michaelides, A., Salzmann, C. G., and Lohmann, U.: A blue-sky approach to understanding cloud formation, B. Am. Meteorol. Soc., 10.1175/bams-d-15-00131.1, 2015.

Umo, N. S., Murray, B. J., Baeza-Romero, M. T., Jones, J. M., Lea-Langton, A. R., Malkin, T. L., O'Sullivan, D., Neve, L., Plane, J. M. C., and Williams, A.: Ice nucleation by combustion ash particles at conditions relevant to mixed-phase clouds, Atmos. Chem. Phys., 15, 5195-5210, 10.5194/acp-15-5195-2015, 2015.

Vali, G.: Interpretation of freezing nucleation experiments: Singular and stochastic; sites and surfaces, Atmos. Chem. Phys., 14, 5271-5294, 10.5194/acp-14-5271-2014, 2014.

Wenk, H.-R., and Bulakh, A.: Minerals: Their constitution and origin, Cambridge University Press, Cambridge, UK, 2004.

Wex, H., DeMott, P. J., Tobo, Y., Hartmann, S., Rösch, M., Clauss, T., Tomsche, L., Niedermeier, D., and Stratmann, F.: Kaolinite particles as ice nuclei: Learning from the use of different kaolinite samples and different coatings, Atmos. Chem. Phys., 14, 5529-5546, 10.5194/acp-14-5529-2014, 2014.

Whale, T. F., Murray, B. J., O'Sullivan, D., Wilson, T. W., Umo, N. S., Baustian, K. J., Atkinson, J. D., Workneh, D. A., and Morris, G. J.: A technique for quantifying heterogeneous ice nucleation in microlitre supercooled water droplets, Atmos. Meas. Tech., 8, 2437-2447, 10.5194/amt-8-2437-2015, 2015a.

Whale, T. F., Rosillo-Lopez, M., Murray, B. J., and Salzmann, C. G.: Ice nucleation properties of oxidized carbon nanomaterials, J. Phy. Chem. Lett., 3012-3016, 10.1021/acs.jpclett.5b01096, 2015b.

Wheeler, M. J., Mason, R. H., Steunenberg, K., Wagstaff, M., Chou, C., and Bertram, A. K.: Immersion freezing of supermicron mineral dust particles: Freezing results, testing different schemes for describing ice nucleation, and ice nucleation active site densities, J. Phys. Chem. A, 119, 4358-4372, 10.1021/jp507875q, 2015.

Wilson, T. W., Ladino, L. A., Alpert, P. A., Breckels, M. N., Brooks, I. M., Browse, J., Burrows, S. M., Carslaw, K. S., Huffman, J. A., Judd, C., Kilthau, W. P., Mason, R. H., McFiggans, G., Miller, L. A., Najera, J. J., Polishchuk, E., Rae, S., Schiller, C. L., Si, M., Temprado, J. V., Whale, T. F., Wong, J. P. S., Wurl, O., Yakobi-Hancock, J. D., Abbatt, J. P. D., Aller, J. Y., Bertram, A. K., Knopf, D. A., and Murray, B. J.: A marine biogenic source of atmospheric ice-nucleating particles, Nature, 525, 234-238, 10.1038/nature14986, 2015.

Wittke, W., and Sykes, R.: Rock mechanics, Springer Berlin, 1990.

Zielke, S. A., Bertram, A. K., and Patey, G. N.: Simulations of ice nucleation by kaolinite (001) with rigid and flexible surfaces, J. Phys. Chem. B, 10.1021/acs.jpcb.5b09052, 2015.

Zolles, T., Burkart, J., Häusler, T., Pummer, B., Hitzenberger, R., and Grothe, H.: Identification of ice nucleation active sites on feldspar dust particles, J. Phys. Chem. A, 119, 2692-2700, 10.1021/jp509839x, 2015.

5. The microtexture of alkali feldspar is important for its ice nucleating ability

This chapter is in preparation for submission to *Physical Chemistry Chemical Physics as:*

Whale, T. F., Holden M. A., O'Sullivan, D., Wilson, T.W., Harrison A. D., Murray B. J. 'The microtexture of alkali feldspar is important for its ice nucleating ability'.

Abstract

Heterogeneous ice nucleation is important in diverse fields, ranging from the atmospheric sciences to cryobiology. Currently, little is known about the relationship between the physical and chemical properties of substances and their efficiency as ice nucleators. Improved knowledge of this relationship could help to improve understanding of the role of ice nucleation in the atmosphere and other real-world situations. It has been previously established that alkali feldspars nucleate ice more efficiently than plagioclase feldspars and they are thought to be important ice nucleators in mixed-phase clouds. A key difference between plagioclase feldspars and alkali feldspars is that most natural alkali feldspars possess complex microtexture. Microtexture is the name given to a wide range of microscopic inhomogeneities resulting from the mutual insolubility of potassium and sodium in the feldspar structure. In contrast, plagioclase feldspars form solid solutions and do not possess microtextures. In order to test if microtexture is important in ice nucleation we have tested the immersion mode ice nucleation efficiency of eight alkali feldspars of known microtextural composition, surface roughness, microporosity and chemical composition using a microlitre droplet freezing experiment. One alkali feldspar, Eifel sanidine, nucleated ice far less efficiently than the other alkali feldspars tested; this was notable because it has no microtexture, lacking the exsolution lamellae common to the majority of other alkali feldspars. Given the similarity in chemical and crystallographic properties of these feldspars, the impact of the features associated with microtexture is significant.

5.1. Introduction

Immersion mode heterogeneous ice nucleation is of interest and importance in a number of fields including cryobiology,(Morris and Acton, 2013) freeze drying, (Kasper and Friess, 2011) food science and atmospheric science (Murray et al., 2012;Hoose and Möhler, 2012;Lohmann and Feichter, 2005). Without heterogeneous nucleation liquid water can supercool to temperatures below -35°C (Herbert et al., 2015;Murray et al., 2010;Riechers et al., 2013). Much effort has been devoted to the quantification of the ice nucleating efficiency of the many species of atmospheric aerosol that may be responsible for glaciation of those clouds which contain a mixture of supercooled water droplets and ice crystals, known as mixed phase clouds. The state of these clouds impacts significantly upon both weather and climate, but the identity of ice nucleating particles (INPs) in the atmosphere is still poorly resolved (Murray et al., 2012).

In pursuit of the identity of ice nucleating species in the atmosphere Atkinson et al. (2013) found that 'K-feldspar' is the most efficient ice nucleating mineral of those common in the atmosphere. It was also found by global modelling of aerosol species that it may account for a large proportion of observed atmospheric INP concentrations. Alkali feldspars, those containing mostly potassium and sodium cations, nucleate ice more efficiently than all other mineral dusts tested to date (Atkinson et al., 2013;Augustin-Bauditz et al., 2014;Zolles et al., 2015;Emersic et al., 2015;Niedermeier et al., 2015). Recently, Harrison et al. (2016) confirmed that plagioclase feldspars nucleate ice less well than alkali feldspars and that the nucleating activity was not simply related to crystal structure. It was concluded that there is another factor controlling ice nucleation by feldspars and that there are at least three broad types of ice nucleating site present on different varieties of feldspar (Harrison et al., 2016). These are 'hyper-active sites' that nucleate ice at temperatures as warm as -2°C in the experimental apparatus used and lose activity when exposed to water, 'typical' sites that nucleate ice in approximately the manner described by the parameterisation for BCS 376 microcline from Atkinson et al. (2013) that do not decay in water, and much less active sites associated with plagioclase feldspars. Here we present new data that provides some insight into the likely nature ice nucleation on feldspars.

One of the key differences between alkali feldspars and plagioclase feldspars is the presence of a range of features collectively referred to as 'microtexture' in many alkali feldspars. These features mostly result from exsolution caused by the lack of mutual

solubility of sodium and potassium feldspars at colder temperatures during formation (below about 700°C). Plagioclase feldspars form solid solutions and therefore lack microtexture. In this study we have sought out feldspars of known microtexture and tested and compared their ice nucleation efficiencies. These feldspars were previously characterised by Hodson et al. (1997) for the purpose of investigating surface roughness. In addition, we have also sourced an alkali feldspar which is in many respects the same as the other alkali feldspars, but lacks microtexture.

5.2. Feldspar structure and phase relationships

Feldspar structure is a complex topic which has been extensively studied. For example, alkali feldspar microtextures can be used as geothermometers, allowing the thermal histories of the rocks containing them to be determined. Similarly, surface roughness and microporosity can have a strong impact on dissolution rates of feldspars and therefore on various aspects of soil and environmental science (Lee et al., 1998;Hodson et al., 1997;Lee and Parsons, 1995). It is likely that much of the readership of this article will have little familiarity with the topic. Hence, we include a brief discussion of the relevant properties. The subject of microtexture has recently been extensively reviewed, (Parsons et al., 2015) and descriptions are available in standard textbooks (Deer et al., 1992).

A Feldspar is a mineral that has the composition MT_4O_8 where T stands for atoms which are capable of tetrahedral coordination to oxygen (Al, Si) and M is a larger metal cation. The tetrahedra formed share corners in a 3-D continuous framework with the larger cations filling the cavities in this structure. There are three common endmember chemical compositions. These are $KAlSi_3O_8$, $NaAlSi_3O_8$, and $CaAl_2Si_2O_8$. Within these endmember compositions multiple crystal structures are known to exist. The potassium feldspar endmember can adopt three separate crystal structures; sanidine, orthoclase and microcline, while sodium feldspar endmembers can adopt two crystal structures; high and low albite. The difference between these phases is the level of aluminium ordering. In sanidine and high albite the aluminium is fully disordered. The other polymorphs have a greater degree of aluminium ordering, up to full ordering in the case of microcline and low albite and intermediate ordering in orthoclase. Low albite and microcline have triclinic symmetry while the remaining polymorphs have monoclinic symmetry. Formation temperature broadly dictates the polymorph that forms, with the series sanidine-orthoclase-microcline and high albite-low albite corresponding to decreasing

crystallization temperatures. Higher crystallization temperatures lead to greater degrees of aluminium ordering. Members of the K-Na series are known as alkali feldspars while members of the Na-Ca series are known as plagioclase feldspars.

When describing the composition of a given feldspar sample it is usual to refer to the percentage of K^+ , Na^+ and Ca^{2+} cations by reference to the feldspar endmembers, albite, orthoclase and anorthite, abbreviated to Ab, Or and An respectively. Note that in this commonly used convention, reference to the Or endmember is a reference to K-feldspars rather than specifically Orthoclase. Only small amounts of Ca^{2+} can dissolve into alkali feldspars and only small amounts of K^+ can dissolve into plagioclase feldspars. The wide variety of bulk structure is further complicated by variation in the finer structure of the feldspars, particular the alkali feldspars. The structure occurs, in the first instance, because solid solutions containing both K^+ and Na^+ cations are not stable below certain temperatures. As a result exsolution, a separation of the feldspar phases, occurs giving zones enriched in one of the cations and corresponding zones enriched in the other. Figure 5.1 is an approximate equilibrium phase diagram for alkali feldspars and helps to illustrate exsolution in alkali feldspars. In nature the structure can be altered further by hydrothermal processes and so called ‘deuteric alteration’ which occurs during the cooling of the magma from which rocks form (Parsons et al., 2015;Lee et al., 1995). The inhomogeneities resulting from exsolution and fluid mediated alteration are typically referred to as ‘microtexture’ (see Figure 5.3 for visual representations of microtexture). The scale of this microtexture can range from a few nanometers to centimetres. Microtextures on multiple scales and of multiple origins are often found in a single sample and examples containing up to eight chemically distinct phases have been identified (Parsons et al., 2013).

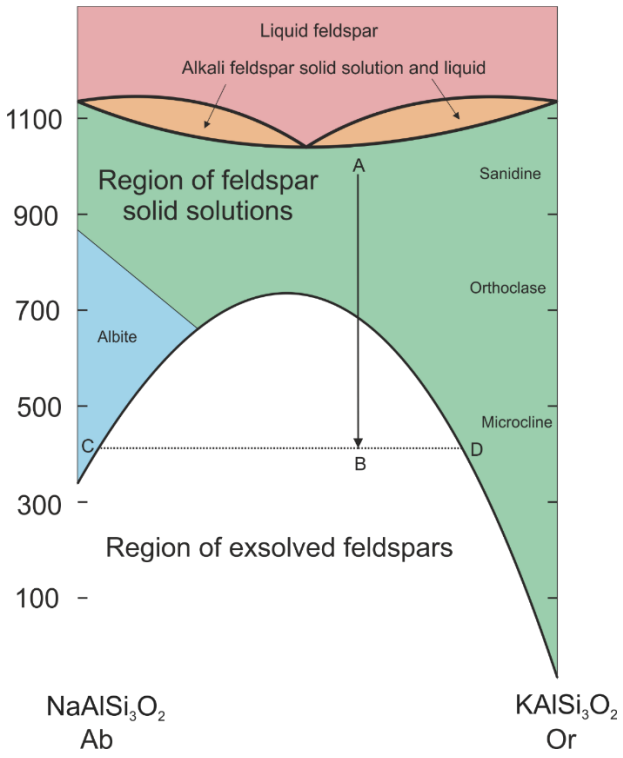

Figure 5.1: Simplified, approximate phase diagram for alkali feldspars adapted from Parsons (2010). Mineral names indicate regions where the various phases of feldspar are stable. Sanidine, orthoclase and microcline are K-feldspar polymorphs that differ in the level of ordering of their alumino-silicate frameworks. Albites are Na-feldspars. Below around 700°C, feldspar containing mixtures of Na^+ and K^+ decompose from a single solid solution phase into mixture of feldspar phases. The arrows indicates a possible pathway. On cooling a feldspar of composition A through the green region any crystallization will result in a single feldspar phase. On further cooling to point B the solid solution is no longer stable, instead the feldspar will tend to exsolve to produce a feldspar richer in Na^+ at point C and a feldspar richer in K^+ at point D.

As the different feldspar phases possess slightly different unit-cell dimensions the interfaces between phases in microtextured feldspars must accommodate strain. The phase boundaries may be fully coherent, semi-coherent or incoherent (Figure 5.2). In the fully coherent case the Si-Al-O framework remains unbroken across the phase boundary. Semi-coherent boundaries possess periodic misfit dislocations which give a lower overall coherency strain energy. Incoherent boundaries involve neighboring discrete sub-grains which do not share any connection of their Si-Al-O frameworks. In general, coherent and semi-coherent intergrowths are the result of ex-solution during magmatic cooling while incoherent intergrowths result from replacement reactions involving magmatic fluid or hydrothermal processes; dissolution of the mineral in an aqueous liquid followed by re-precipitation of an altered mineral. Such microtextures are referred to as ‘alteration

microtextures' whereas coherent and semi-coherent microtextures resulting from exsolution during cooling are referred to as 'pristine microtextures'. During rock formation exsolution and formation of microtextures with coherent grain boundaries begins at around 600°C while misfit dislocations begin to form between 410°C and 370°C (Parsons et al., 2015).

Hodson et al. (1997) determined the microporosity of the samples we have investigated using scanning electron microscopy. Microporosity is a characteristic property of many alkali feldspars and results from the same sort of fluid-feldspar interactions that lead to alteration microtextures. The dissolution processes that precede re-precipitation of altered microtextures often leave a network of micropores throughout the altered feldspar (Worden et al. 1990) As such, alteration microtextures tend to be associated with high densities of micropores.

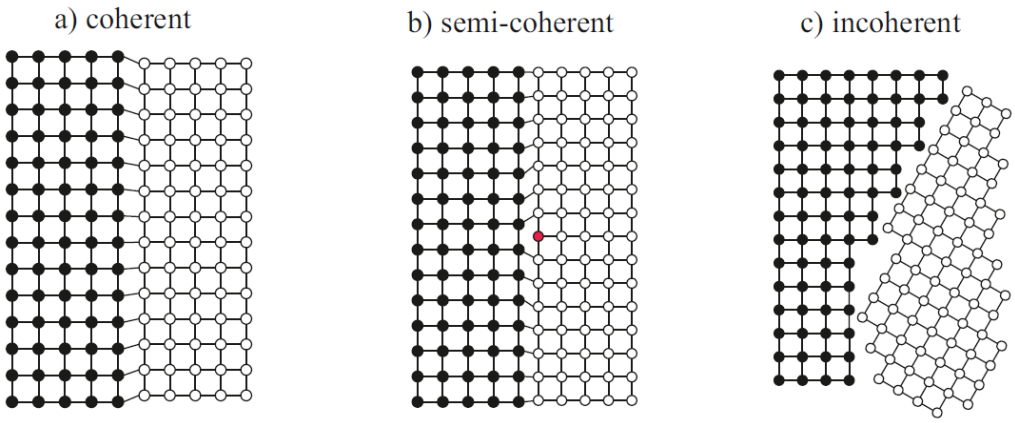

Figure 5.2: Conceptual diagrams of the three possible types of phase boundary. Coherent boundaries maintain the integrity of the alumino-silicate framework. Chemical bonds near to the interface will be somewhat strained from ideality in order to accommodate the differences in lattice parameters. In the semi-coherent boundaries strain is accommodated by periodic dislocations in the otherwise shared alumino-silicate framework. In the incoherent case the alumino-silicate framework is not shared and boundaries have many dislocations (Parsons et al., 2015;Lee et al., 1998).

Hodson et al. (1997) investigated the relationship between microtexture and surface roughness for the feldspars tested here. Surface roughness was characterized as A_{BET}/A_{GEOM} where A_{BET} is the specific surface area of a samples as determined by BET and A_{GEOM} is the specific surface area as calculated by assuming all particles have regular geometric shapes. Larger ratios therefore indicate larger deviations from a geometric

approximation of surface area and therefore a rougher surface. Feldspars of greater microtextural complexity tend break in a less clean manner on grinding and therefore have higher A_{BET}/A_{GEOM} ratios. Values for the feldspars we have tested range from 4.16 to 7.10. It had been thought that these pores accounted for a large proportion of the BET surface area of alkali feldspars (Blum, 1994). However, Hodson et al. (1997) showed that this is not the case and that surface roughness is responsible for most of the difference geometric and gas adsorption surface areas observed.

5.3. Samples

The samples used in this study have previously been characterized by Hodson et al. (1997) with the goal of examining surface roughness and microporosity in unweathered powdered alkali feldspars. They characterized bulk chemical composition, microtexture, and collected information about the microporosity and roughness of the feldspars. Table 1 lists these feldspars together with some of their properties. All the samples tested, except Eifel sanidine, are 'perthites'. This means they are exsolved and possess microtexture, with regions rich in K^+ and regions rich in Na^+. Most of the feldspars we have tested possess alteration microtextures as well as pristine microtextures. Figure 5.3 and Figure 5.4 are schematics showing the form of the various microtextures present in these feldspars.

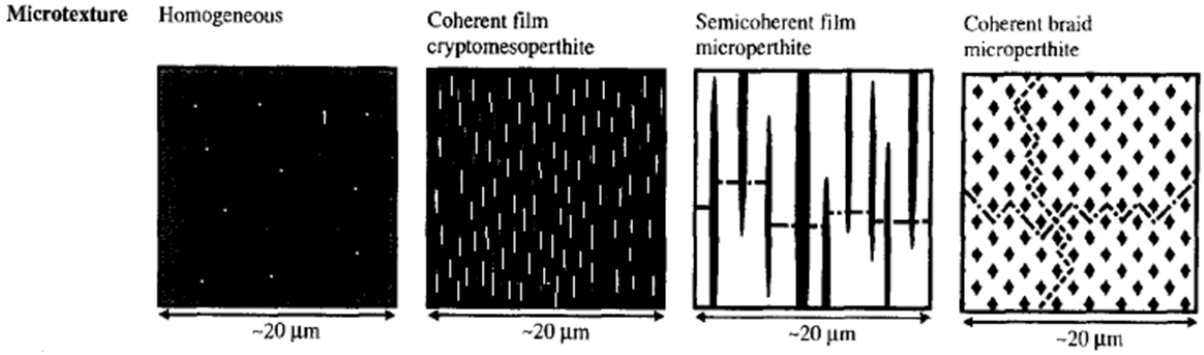

Figure 5.3: Schematic representations of the pristine microtexture of the various forms of alkali feldspar microtexture used in this study. The figure has been adapted from Hodson et al. (1997). K^+ rich regions of the diagrams are black while Na^+ rich regions are white. Of the samples tested here Eifel sanidine is homogenous, larvikite is a coherent film cryptomesoperthite, 43738 and KB14 are coherent braid microperthites while the light and dark Shaps, Keystone microcline and Perth perthite are semi coherent film microperthites. All of the samples except Eifel sanidine and larvikite also have alteration microtexture of the type shown in Figure 5.4. This wide range variation in pristine microtexture stems from differences in temperature and cooling rates during formation (Parsons et al. 2015).

Eifel sanidine is found as large crystals which are optically transparent and microtexturally homogenous, containing no exsolution lamellae. Such homogenous feldspars are rare and are referred to as ‘gem quality’. Most alkali feldspars possess microtextures. Larvikite is a crypto-mesoperthite; ‘crypto’ indicates very fine microtexture, fine enough that lamellae can’t be seen by light microscopy, while ‘meso’ means it contains roughly equal amounts of sodium and potassium. Larvikite is composed of relatively long and narrow lamella of orthoclase in oligoclase (plagioclase containing mostly Na^+ with some Ca^{2+}; see the phase diagram in Harrison et al. (2016)), with coherent grain boundaries. Light and dark Shap are from the same geological formation. Dark Shap has undergone more hydrothermal alteration than light shap after formation. The pristine microtexture of both Shaps is comprised of semi-coherent albite films in tweed orthoclase. Tweed microtexture (cross-hatched regions) is characteristic of orthoclase and develops as a result of the transition from monoclinic to triclinic symmetry (sanidine to orthoclase) on cooling, the microtexture is on the scale of a few unit cells. Perth perthite and Keystone microcline are macroperthites (microtexture is visible to the naked eye) with veins on the millimeter scale. Both consists of veins of albite separated by veins of a dominantly microcline microperthite consisting of semicoherent albite films in microcline. For 43738 and KB14 the pristine texture is a coherent braid microperthite. Diamond shaped columns of low albite are enclosed by intersecting microcline lamellae. The altered microtexture is made up of incoherent patches of low albite and microcline which are 200-300 μm across. Patch perthites, (see Figure 5.4) make up ~70% of KB14 and ~90% of 43738. Details of the properties of the feldspars are in table 5.1.

All the samples, except Eifel Sanidine, were the smallest particles separated from powders by the size selection procedures used by Hodson et al. (1997). The larger particles were used in that study, leaving the smaller material for our study. The surface areas of the samples were measured by Brunauer-Emmett-Teller nitrogen gas adsorption using a Micromeritics TriStar 3000. The Eifel sanidine sample was sourced separately and ground using an agate mortar and pestle prior to BET measurements and ice nucleation testing. The identity of this mineral was confirmed using powder X-ray diffraction.

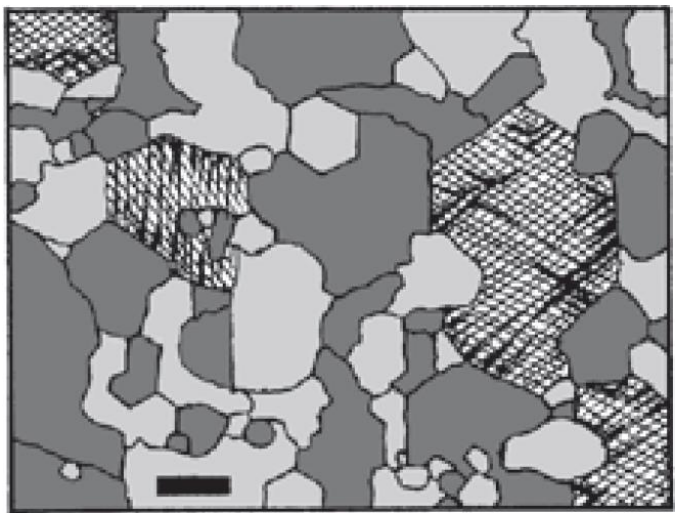

Figure 5.4: Schematic showing replacement microtexture in a alkali feldspar. The figure has been adapted from Parsons (2013). The scale bar is 50 µm long, although other scales of replacement also occur (Parsons et al., 2015).The figure shows patch perthite formed as a result of 'deuteric coarsening'. This is a dissolution- reprecipitation reaction that leads to replacement of the native perthite, in this case braid perthite of the sort shown in the right hand panel of Figure 5.3 with grains of low albite and microcline with incoherent grain boundaries. These are represented by lighter and darker colours respectively. The crosshatched regions represent the pristine braid microperthite. All the samples we have tested apart from Eifel Sanidine and larvikite possess replacement microtexture of this type. The incoherent grain boundaries possess many dislocations.

5.4. Methods

The µl-NIPI droplet freezing assay has been used for all ice nucleation experiments conducted in this study. It has been thoroughly described previously (Whale et al., 2015). Briefly, approximately 50, 1 µl droplets of MilliQ water containing the ice nucleator under investigation are pipetted onto a silanised glass slide (Hampton Research) using an electronic pipette (Picus Biohit). The slide is supported by an Asymptote EF600 Stirling Cryocooler which is used to control the temperature of the droplets. The slide and droplets are covered by a Perspex shield and a flow of dry nitrogen over the droplets is used to prevent condensation from forming on the slide which prevents communication of ice between droplets. Freezing is monitored using a camera. In this study droplets were always cooled at 1°C min^{-1}. This process allows the fraction of droplets frozen at a given temperature to be determined. Suspensions of the feldspars tested were made up

gravimetrically and stirred using a magnetic follower for a few minutes prior to use. In this study we have used 1 wt% and 0.1 wt% suspensions.

Table 5.1: Alkali feldspars samples used in this study. Or, Ab and An are abbreviations for orthoclase, albite and anorthite respectively, which are potassium, sodium and calcium feldspar endmembers respectively. The ratios indicate the molar proportions of these components.

Sample name	**Bulk chemical composition**	**Main mineral phases**	**Pristine microtexture**	**Pristine grain boundary type**	**Alteration microtextures**	**BET surface area (m^2g^{-1})**
Light Shap	$Or_{71}Ab_{28}An_{<1}$	orthoclase	lamellar microperthite	semi-coherent	Yes	0.70 ± 0.01
Eifel sanidine	$Or_{84.1}Ab_{15.9}An_{0.1}$	sanidine	none	none	No	2.05 ± 0.02
Larvikite	$Or_{30.4}Ab_{58.1}An_{11.5}$	orthoclase	lamellar crypto-mesoperthite	coherent	No	0.77 ± 0.02
Dark Shap	$Or_{71}Ab_{28}An_{<1}$	orthoclase	lamellar microperthite	semi-coherent	Yes	0.84 ± 0.01
Perth perthite	$Or_{57.4}Ab_{42}An_{0.6}$	microcline	vein macroperthite	semi-coherent	Yes	0.70 ± 0.01
Keystone microcline	$Or_{78.3}Ab_{20.7}An_{1.0}$	microcline	vein macroperthite	semi-coherent	Yes	0.77± 0.01
43738	$Or_{50.3}Ab_{44.0}An_{5.6}$	low albite/microcline	braid microperthite	coherent	Yes	0.84 ± 0.03
KB14	≈ $Or_{40}Ab_{60}$	low albite/microcline	braid microperthite	coherent	Yes	1.09 ± 0.01

$n_s(T)$ is the number of ice nucleating sites that become active per surface area on cooling from 0°C to temperature *T*. $n_s(T)$ can be calculated using (Connolly et al., 2009):

$$\frac{n(T)}{N} = 1 - \exp(-n_s(T)A) \qquad 5.1$$

Where $n(T)$ is the number of droplets frozen at temperature (T), N is the total number of droplets in the experiment and A is the surface area of nucleant per droplet. $n_s(T)$ is a site specific measure of ice nucleation efficiency which does not account for the effects of time dependence. It has been shown that ice nucleation by several feldspars is minimally

time dependent (Herbert et al., 2014). Error bars were calculated using errors calculated from simulations of possible site distributions propagated with the uncertainty in surface area of nucleator per droplet as described in Harrison et al. (2016). Temperature uncertainty for µl-NIPI has been estimated to be ±0.4 °C (Whale et al. 2015).

5.5. Results and discussion

We have determined $n_s(T)$ values for the nine new feldspar we have tested, which are presented in Figure 5.5. We compare the efficiencies of our feldspar samples to that of BCS 376 (Atkinson et al., 2013). Light Shap and KB14 nucleate ice similarly with 1 wt% suspensions starting to freeze at ~-4°C. The shape of the freezing curves for these feldspars is flatter than that of BCS 376 with the result that at $n_s(T)$ = 50 the curves cross the BCS 376 line and nucleate ice less efficiently at colder temperatures. Dark Shap is similar but freezing starts at slightly warmer temperatures of ~-4°C. Perthite is similar but with a colder freezing onset of ~-5°C. Keystone microcline behaves more like BCS 376 and has a similar slope. 43738 feldspar nucleates ice with a similar slope to BCS 376 and Keystone microcline but at lower temperatures, although the first few events of the 1 wt% dispersion occur at relatively high temperature. Larvikite nucleates less efficiently than BCS 376 save for a few events at higher temperatures - the slope of the freezing curve is much flatter. Eifel sanidine nucleates ice far less efficiently than the other feldspars at equivalent $n_s(T)$, nucleating at temperatures around 14°C colder than BCS 376 with a slope similar to BCS 376.

Eifel sanidine, which lacks microtexture, nucleates ice with similar efficiency to the plagioclase feldspars tested in Harrison et al.(Harrison et al., 2016) as can be seen clearly in Figure 5.5. All other alkali feldspars we have tested to date nucleate ice more efficiently. We therefore suggest that features associated with microtexture are responsible for the enhanced ice nucleation observed in the majority of alkali feldspars compared to Eifel sanidine and plagioclase feldspars. We note that the dislocations associated with incoherent and semi-coherent microtextures serve as sites of attack during the early stages of weathering.(Hodson, 1998;Lee et al., 1998;Parsons and Lee, 2005;Holdren and Speyer, 1987;Lee and Parsons, 1997) Such features might also serve as ice nucleation sites. It is known that ‘coarseness and dislocation density differ in the order patch perthite > microperthite > cryptoperthite’.(Lee et al., 1998) Feldspars with incoherent microtextures have more dislocations than semi-coherent microtextures which

in turn have more dislocations than feldspars with coherent microtextures. Eifel Sanidine and plagioclase feldspars, which lack these microtextural features, have lower dislocation densities still. Broadly, the results we have obtained suggest that ice nucleation activity follows the same trend. Eifel sanidine nucleates relatively poorly and larvikite, which possesses only coherent grain boundaries and so will have fewer dislocations and associated features, nucleates ice less efficiently than the other feldspars we have tested, all of which possess alteration microtextures.

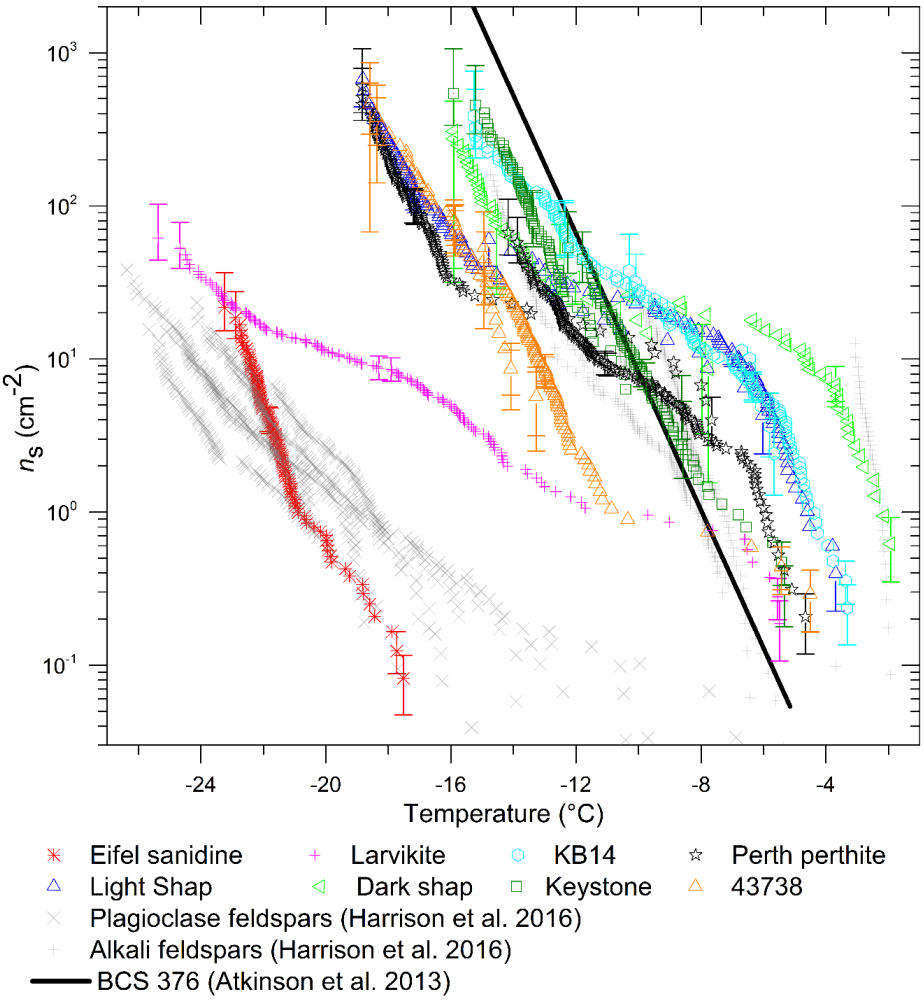

Figure 5.5: Plot of $n_s(T)$ values for the alkali feldspars described in Table 5.1. Experiments were conducted on both 1 wt% suspensions and 0.1 wt% suspensions. 0.1 wt% suspensions have dots in the symbols to differentiate them. Each line consists of between two and four experiments. Data for alkali and plagioclase feldspars from Harrison et al. (2016) are plotted as grey crosses. It can be seen that Eifel sanidine nucleates ice much less well than other alkali feldspars and similarly to plagioclase feldspar. Larvikite is also nucleates ice less efficiently than most other alkali feldspars.

While the results are consistent with the hypothesis that microtexture plays a role in ice nucleation by feldspars it is unclear which microtextural feature or related property

enhances ice nucleation. In Harrison et al. (2016) it was shown that there are at least two distinct classes of site found in alkali feldspars. Unfortunately we do not know the nature of the microtexture of the alkali feldspars studied in that work so it is not possible to relate those results to microtexture. We are not able to distinguish the impact of semi-coherent and incoherent grain boundaries in this work as all the feldspars with a semi-coherent pristine microtexture which we have tested here also have alteration microtextures and therefore fail to provide a point of contrast.

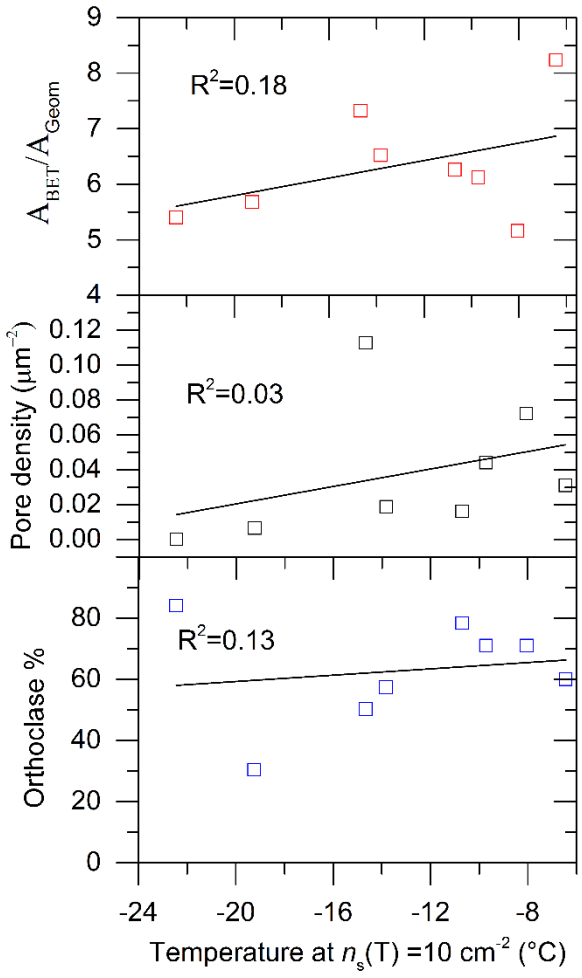

Figure 5.6: Plots of temperature at $n_s(T)$ = 10 cm-2 against surface roughness, λ, pore density and orthoclase percentage for the alkali feldspars detailed in table 5.1.

Other properties measured by Hodson et al. (1997) might also have a bearing on ice nucleation efficiency. In Figure 5.6 we have plotted the temperature at $n_s(T)$ = 10, hereafter referred to as $T_{ns=10}$ n_{s10}, as a simple single number proxy for ice nucleation activity. We do not find any meaningful correlations between the values for surface

roughness, micropore density and Or (potassium feldspar) percentage with ns_{10}. From this, we conclude that rougher feldspar and more microporous feldspars do not obviously nucleate ice better than less rough and less microporous feldspars. Similarly, it does not appear that greater potassium content leads to more efficient ice nucleation. This is consistent with previous work that has shown that Amelia albite which only contains 1% Or can nucleate ice very efficiently (Harrison et al., 2016).

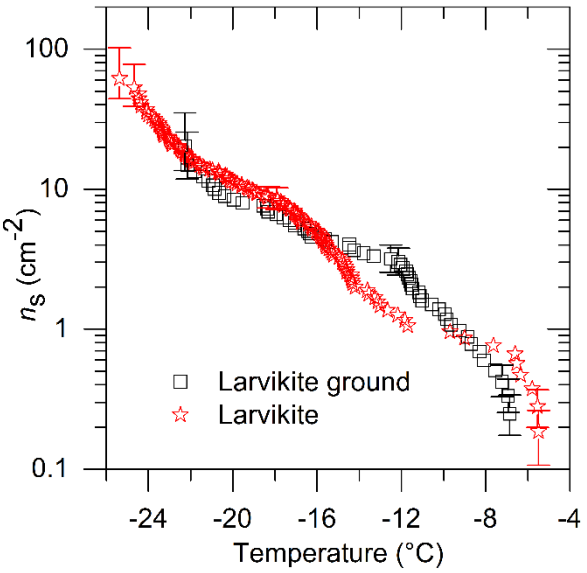

Figure 5.7: Comparison of $n_s(T)$ values for ground and unground larvikite. The data for larvikite is the same as that in Figure 5.5: Plot of $n_s(T)$ values for the alkali feldspars described in Table 5.1. Experiments were conducted on both 1 wt% suspensions and 0.1 wt% suspensions. 0.1 wt% suspensions have dots in the symbols to differentiate them. Each line consists of between two and four experiments. Data for alkali and plagioclase feldspars from Harrison et al. (2016) are plotted as grey crosses. It can be seen that Eifel sanidine nucleates ice much less well than other alkali feldspars and similarly to plagioclase feldspar. Larvikite is also nucleates ice less efficiently than most other alkali feldspars.Figure 5.5. This larvikite had a surface area of 0.77 ± 0.02 m^2g^{-1} while the ground larvikite sample had a specific surface area of 1.94±0.01 m^2g^{-1}. The ice nucleation activity of both is similar so we conclude that grinding has not affected the ice nucleation activity of the sample.

A striking result from Harrison et al. (2016) was that grinding greatly increased the ice nucleation activity of Amelia albite. The Amelia Albite sample used by Harrison et al. (2016) had been ground many years previously when we first received it and the nucleating ability increased dramatically when we freshly ground it. This indicated that Amelia Albite aged with time when exposed to air, which was consistent with measurements showing that its activity decreased dramatically when suspended in water.

To test if extra grinding influences the ice nucleating ability of the less active feldspars we tested here we reground the sample of larvikite, which had last been ground 20 years ago, to give a surface area of 1.94 ± 0.01 m^2g^{-1}. This process did not have a significant impact on its ice nucleation efficiency as can be seen in Figure 5.7. Eifel Sanidine as we have tested it here was freshly ground to a relatively high surface area shortly before ice nucleation experiments. As such we do not think that grinding of Eifel sanidine and larvikite exposes or creates sites in the manner that it does for Amelia albite. This is consistent with the hypothesis that a lack of microtextural features in these samples reduces their ice nucleating abilities relative to other alkali feldspars.

5.6. The nature of sites on alkali feldspars

In most cases a site specific description of immersion mode ice nucleation fits experimental data better than single time dependent models (Vali, 2014, 2008). It has been shown that this is the case for BCS 376 feldspar in the temperature regime we have investigated here.(Herbert et al., 2014) If, as we think, features associated with microtextural grain boundaries are responsible for enhancing ice nucleation rates this marks progress towards identification of the sites in question. Also, as grain boundaries will not be spread across the surface of the feldspar evenly the reason for the uneven distribution of sites observed on BCS 376 by Herbert et al. (2014) is apparent.

Dislocations are the primary defect type associated with microtextures. Ice nucleation sites are much rarer than dislocations. In this study we have investigated ice active site densities between about 0.1 and 100 sites per cm^2. Even Eifel sanidine has on the order of 10^6 dislocations cm^{-2} and the other feldspars we have tested will likely have dislocation densities orders of magnitude higher.(Hodson et al., 1997) As such it is not reasonable to suggest that a single dislocation serves as a site for ice nucleation. Additionally, Classical nucleation theory suggests that critical nuclei in the temperature range we have investigated are likely to be 1-3 nm across (Pummer et al., 2015) while dislocations are angstrom scale features. Other features form through chemical attack of dislocations during and after formation of feldspar rocks. These include etch pits (Parsons and Lee, 2005), which are formed by chemical attack of dislocations, nano-tunnels, which appear during the fluid-feldspar reactions that lead to alteration microtextures and are located the sites of dislocations (Fitzgerald and Cayzer, 2006) and so called ‘pull aparts’ which are tiny nanoscale cracks found crossing albite lamellae (Fitzgerald and Cayzer, 2006). Etch

pits, nanotunnels and pull-aparts are typically nanoscaled and therefore much closer in scale to the likely critical nucleus size (Fitzgerald and Cayzer, 2006). They are also significantly rarer than dislocations meaning they may be better candidates as the surface feature responsible for ice nucleation. Nano-tunnels and pull-aparts were discovered in Shap granites of the type we have studied here (light and dark Shap) so these features are most-likely present in the alkali feldspars that are known to nucleate ice efficiently. Interestingly, It has been shown recently that nanoscaled features on silicon surfaces can influence immersion mode ice nucleation while micrometer scaled features on chemically similar surfaces do not have an influence (Gurganus et al., 2014). In summary, we suggest that nucleation occurs on nanoscale features associated with microtexture rather than crystallographic dislocations.

5.7. Conclusions

We have tested the hypothesis that differences in microtexture can account for the differences in ice nucleation activity between alkali and plagioclase feldspars found by Harrison et al. (2016) by obtaining alkali feldspars of varied microtextural composition and testing their ice nucleation activities. We have shown that for alkali feldspars ice nucleation efficiency is not driven solely by chemical composition or crystal structure. Eifel Sanidine, which is very similar to the other feldspars we have tested in terms of chemical composition and crystal structure does not nucleate ice nearly as well. Indeed, its ice nucleation efficiency is similar to that of the plagioclase feldspars tested by Harrison et al.(2016). Eifel sanidine is microtexturally pristine, lacking the exsolution lamellae and alteration microtextures common to the vast majority of natural feldspars. As whatever feature is responsible for ice nucleation will be spread across the surface of the feldspars in a non-uniform fashion this hypothesis is consistent with, and might go some way to explaining, the ‘site specific’ nature of most heterogeneous ice nucleation. We suggest that these sites are likely to be nanoscale features associated with chemical modification of dislocations which may be consistent with recent work showing that nanoscale features can influence ice nucleation (Gurganus et al., 2014).

Further work will be needed to establish the activity of these real world feldspars for atmospheric purposes. Looking forward, work should be conducted to resolve which features specifically are responsible for efficient ice nucleation. For instance, it should be possible to obtain specimens where the dislocation density is known and relate this to ice

nucleation efficiency. It is reasonable to think that other minerals, and other inorganic ice nucleators generally, might also exhibit more variable ice nucleation than has been previously assumed. It is clear from this work that feldspars that are very similar in terms of chemical composition and crystal structure can nucleate ice quite differently due to topographical features. It is known that different quartzes can exhibit different dislocation densities for instance (Blum et al., 1990). While this means that care should be applied when attempting to generalize the ice nucleation activity of such minerals, and even more care taken when trying to apply such information to studies of the atmosphere it is clear that there is much scope for useful investigation building towards a more comprehensive understanding of heterogeneous ice nucleation.

References

Alex D. Harrison, T. F. W., Michael J. Carpenter, Mark A. Holden, G. J. Morris, Lesley Neve, Daniel O'Sullivan, Jesus Vergara Temprado, Benjamin J. Murray: Not all feldspar is equal: A survey of ice nucleating properties across the feldspar group of minerals, 2016.

Atkinson, J. D., Murray, B. J., Woodhouse, M. T., Whale, T. F., Baustian, K. J., Carslaw, K. S., Dobbie, S., O'Sullivan, D., and Malkin, T. L.: The importance of feldspar for ice nucleation by mineral dust in mixed-phase clouds, Nature, 498, 355-358, 10.1038/nature12278, 2013.

Augustin-Bauditz, S., Wex, H., Kanter, S., Ebert, M., Niedermeier, D., Stolz, F., Prager, A., and Stratmann, F.: The immersion mode ice nucleation behavior of mineral dusts: A comparison of different pure and surface modified dusts, Geophys. Res. Lett., 41, 7375-7382, 10.1002/2014gl061317, 2014.

Blum, A. E., Yund, R. A., and Lasaga, A. C.: The effect of dislocation density on the dissolution rate of quartz, Geochim. Cosmochim. Acta, 54, 283-297, http://dx.doi.org/10.1016/0016-7037(90)90318-F, 1990.

Blum, A. E.: Feldspars in weathering, in: Feldspars and their reactions, Springer, 595-630, 1994.

Connolly, P. J., Möhler, O., Field, P. R., Saathoff, H., Burgess, R., Choularton, T., and Gallagher, M.: Studies of heterogeneous freezing by three different desert dust samples, Atmos. Chem. Phys., 9, 2805-2824, 10.5194/acp-9-2805-2009, 2009.

Deer, W. A., Howie, R. A., and Zussman, J.: An introduction to the rock forming minerals, 2nd ed., Addison Wesley Longman, Harlow, UK, 1992.

Emersic, C., Connolly, P. J., Boult, S., Campana, M., and Li, Z.: Investigating the discrepancy between wet-suspension- and dry-dispersion-derived ice nucleation efficiency of mineral particles, Atmos. Chem. Phys., 15, 11311-11326, 10.5194/acp-15-11311-2015, 2015.

Fitzgerald, J. D., and Cayzer, N.: Nanotunnels and pull-aparts: Defects of exsolution lamellae in alkali feldspars, Am. Mineral., 91, 772-783, 2006.

Gurganus, C. W., Charnawskas, J. C., Kostinski, A. B., and Shaw, R. A.: Nucleation at the contact line observed on nanotextured surfaces, Phys. Rev. Lett., 113, 235701, 2014.

Harrison, A. D., Whale, T. F., Carpenter, M. A., Holden, M. A., Neve, L., O'Sullivan, D., Vergara Temprado, J., and Murray, B. J.: Not all feldspar is equal: A survey of ice nucleating properties across the feldspar group of minerals, Atmos. Chem. Phys. Discuss., 2016, 1-26, 10.5194/acp-2016-136, 2016.

Herbert, R. J., Murray, B. J., Whale, T. F., Dobbie, S. J., and Atkinson, J. D.: Representing time-dependent freezing behaviour in immersion mode ice nucleation, Atmos. Chem. Phys., 14, 8501-8520, 10.5194/acp-14-8501-2014, 2014.

Herbert, R. J., Murray, B. J., Dobbie, S. J., and Koop, T.: Sensitivity of liquid clouds to homogenous freezing parameterizations, Geophys. Res. Lett., 42, 1599-1605, 10.1002/2014gl062729, 2015.

Hodson, M. E., Lee, M. R., and Parsons, I.: Origins of the surface roughness of unweathered alkali feldspar grains, Geochim. Cosmochim. Acta, 61, 3885-3896, 10.1016/s0016-7037(97)00197-x, 1997.

Hodson, M. E.: Micropore surface area variation with grain size in unweathered alkali feldspars: Implications for surface roughness and dissolution studies, Geochim. Cosmochim. Acta, 62, 3429-3435, 1998.

Holdren, G. R., and Speyer, P. M.: Reaction rate-surface area relationships during the early stages of weathering. Ii. Data on eight additional feldspars, Geochim. Cosmochim. Acta, 51, 2311-2318, http://dx.doi.org/10.1016/0016-7037(87)90284-5, 1987.

Hoose, C., and Möhler, O.: Heterogeneous ice nucleation on atmospheric aerosols: A review of results from laboratory experiments, Atmos. Chem. Phys., 12, 9817-9854, 10.5194/acp-12-9817-2012, 2012.

Kasper, J. C., and Friess, W.: The freezing step in lyophilization: Physico-chemical fundamentals, freezing methods and consequences on process performance and quality attributes of biopharmaceuticals, Eur. J. Pharm. Biopharm., 78, 248-263, 2011.

Lee, M. R., and Parsons, I.: Microtextural controls of weathering of perthitic alkali feldspars, Geochim. Cosmochim. Acta, 59, 4465-4488, http://dx.doi.org/10.1016/0016-7037(95)00255-X, 1995.

Lee, M. R., Waldron, K., and Parsons, I.: Exsolution and alteration microtextures feldspar phenocrysts from the shap granite, Min. Mag., 59, 63-78, 1995.

Lee, M. R., and Parsons, I.: Dislocation formation and albitization in alkali feldspars from the shap granite, Am. Mineral., 82, 557-570, 1997.

Lee, M. R., Hodson, M. E., and Parsons, I.: The role of intragranular microtextures and microstructures in chemical and mechanical weathering: Direct comparisons of experimentally and naturally weathered alkali feldspars, Geochim. Cosmochim. Acta, 62, 2771-2788, http://dx.doi.org/10.1016/S0016-7037(98)00200-2, 1998.

Lohmann, U., and Feichter, J.: Global indirect aerosol effects: A review, Atmos. Chem. Phys., 5, 715-737, 10.5194/acp-5-715-2005, 2005.

Morris, G. J., and Acton, E.: Controlled ice nucleation in cryopreservation - a review, Cryobiology, 66, 85-92, 10.1016/j.cryobiol.2012.11.007, 2013.

Murray, B. J., Broadley, S. L., Wilson, T. W., Bull, S. J., Wills, R. H., Christenson, H. K., and Murray, E. J.: Kinetics of the homogeneous freezing of water, Phys. Chem. Chem. Phys., 12, 10380-10387, 10.1039/c003297b, 2010.

Murray, B. J., O'Sullivan, D., Atkinson, J. D., and Webb, M. E.: Ice nucleation by particles immersed in supercooled cloud droplets, Chem. Soc. Rev., 41, 6519-6554, 10.1039/C2CS35200A, 2012.

Niedermeier, D., Augustin-Bauditz, S., Hartmann, S., Wex, H., Ignatius, K., and Stratmann, F.: Can we define an asymptotic value for the ice active surface site density for heterogeneous ice nucleation?, J. Geophys. Res.: Atmos., 120, 5036-5046, 10.1002/2014jd022814, 2015.

Parsons, I., and Lee, M. R.: Minerals are not just chemical compounds, Can. Mineral., 43, 1959-1992, 2005.

Parsons, I.: Feldspars defined and described: A pair of posters published by the mineralogical society. Sources and supporting information, Min. Mag., 74, 529-551, 10.1180/minmag.2010.074.3.529, 2010.

Parsons, I., Fitz Gerald, J., Heizler, M., Heizler, L., Ivanic, T., and Lee, M.: Eight-phase alkali feldspars: Low-temperature cryptoperthite, peristerite and multiple replacement reactions in the klokken intrusion, Contrib. Mineral. Petrol., 165, 931-960, 10.1007/s00410-012-0842-5, 2013.

Parsons, I., Fitz Gerald, J. D., and Lee, M. R.: Routine characterization and interpretation of complex alkali feldspar intergrowths, Am. Mineral., 100, 1277-1303, 10.2138/am-2015-5094, 2015.

Pummer, B. G., Budke, C., Augustin-Bauditz, S., Niedermeier, D., Felgitsch, L., Kampf, C. J., Huber, R. G., Liedl, K. R., Loerting, T., Moschen, T., Schauperl, M., Tollinger, M., Morris, C. E., Wex, H., Grothe, H., Pöschl, U., Koop, T., and Fröhlich-Nowoisky, J.: Ice nucleation by water-soluble macromolecules, Atmos. Chem. Phys., 15, 4077-4091, 10.5194/acp-15-4077-2015, 2015.

Riechers, B., Wittbracht, F., Hütten, A., and Koop, T.: The homogeneous ice nucleation rate of water droplets produced in a microfluidic device and the role of temperature uncertainty, Phys. Chem. Chem. Phys., 15, 5873-5887, 10.1039/C3CP42437E, 2013.

Vali, G.: Repeatability and randomness in heterogeneous freezing nucleation, Atmos. Chem. Phys., 8, 5017-5031, 10.5194/acp-8-5017-2008, 2008.

Vali, G.: Interpretation of freezing nucleation experiments: Singular and stochastic; sites and surfaces, Atmos. Chem. Phys., 14, 5271-5294, 10.5194/acp-14-5271-2014, 2014.

Whale, T. F., Murray, B. J., O'Sullivan, D., Wilson, T. W., Umo, N. S., Baustian, K. J., Atkinson, J. D., Workneh, D. A., and Morris, G. J.: A technique for quantifying heterogeneous ice nucleation in microlitre supercooled water droplets, Atmos. Meas. Tech., 8, 2437-2447, 10.5194/amt-8-2437-2015, 2015.

Worden, R. H., Walker, F. D. L., Parsons, I., and Brown, W. L.: Development of microporosity, diffusion channels and deuteric coarsening in perthitic alkali feldspars, Contrib. Mineral. Petrol., 104, 507-515, 10.1007/bf00306660, 1990.

Zolles, T., Burkart, J., Häusler, T., Pummer, B., Hitzenberger, R., and Grothe, H.: Identification of ice nucleation active sites on feldspar dust particles, J. Phys. Chem. A, 119, 2692-2700, 10.1021/jp509839x, 2015.

6. The enhancement and suppression of immersion mode heterogeneous ice nucleation by solutes

This chapter is in preparation for submission to *Chemical Communications as:*

Whale, T. F., Wilson, T.W., Murray B. J. 'The enhancement and suppression of immersion mode heterogeneous ice nucleation by solutes'

ABSTRACT

Heterogeneous nucleation of ice from aqueous solutions is important in atmospheric science and cryobiology, but the influence of solutes on heterogeneous ice nucleation is poorly understood. In the atmospheric community the current paradigm is that a dilute solution droplet will tend to freeze at a temperature very close to that at which a pure water droplet would freeze and at higher solute concentrations the freezing temperature for a given nucleator is determined by the water activity of the solution, rather than the identity of the solute. By testing combinations of nucleators and solute molecules we have demonstrated that 0.015 M solutions of certain ammonium salts can cause suspended particles of feldspars and quartz to nucleate ice up to around 3°C warmer. Similar solutions of certain alkali metal halides can depress freezing points for the same nucleators to a far greater extent than would be expected from the change in water activity alone. Other nucleators, silica, humic acid and Arizona Test Dust, are unaffected, to within experimental uncertainty. This split in response to solutes may indicate that different mechanisms of ice nucleation are occurring on the different nucleators or that surface modification of relevance to ice nucleation proceeds in different ways for different nucleators. The solute effect may be of importance in the atmosphere as sea salt and ammonium sulphate are common condensation nuclei for cloud droplets.

6.1. Introduction

Ice nucleation is an important process in several fields. It has relevance to the atmosphere, (Murray et al., 2012) cryopreservation of biological samples, (Morris and Acton, 2013) freeze drying (Searles et al., 2001) and freezing of foodstuffs (Kiani and Sun, 2011). Ice nucleation in the 'real world' will very often take place in aqueous solutions rather than pure water. It is known that this is the case in the atmosphere, for example cloud droplets in mixed-phase clouds are always composed of dilute solutions of a range of solutes. Each supermicron cloud droplet typically forms on a much smaller particle containing soluble hygroscopic material. A small proportion of these cloud droplets also contain ice nucleating particles (INPs) and may go on to freeze if they become sufficiently cold. In contrast, ice clouds which form in the upper troposphere can form through the freezing of very concentrated submicron solution droplets called haze particles. Similarly, aqueous solutions used for cryopreservation will usually contain a mixture of solutes to prevent damage to cells (Fuller, 2004).

As such, the role of solute molecules in the freezing of liquid water is a process of fundamental interest. In the case of homogenous ice nucleation (ice nucleation in the absence of any heterogeneous ice nucleating particles (INPs)), it is generally accepted that the 'water activity criterion' (Koop et al., 2000) describes the change in nucleation temperature observed with the addition of solute molecules. That is to say, the shift in nucleation temperature observed with the addition of solute molecules can be calculated solely from the difference between the water activity of the solution in equilibrium with ice (the water activity at the melting point) and the water activity of the solution at the freezing temperature, this value was named Δa_w (Koop et al., 2000). This result was surprising when it was published in the year 2000 as it might be expected the interfacial tension between solution and the critical nuclei, and the diffusion activation energy for a water molecule to cross the solution/ice interface are influenced by the nature of the solute molecules. Nevertheless, Koop et al. demonstrated that homogeneous freezing in 18 different aqueous solutions, ranging from inorganic salts like NaCl to organic solute like glucose, is determined by water activity.

Much of the ice nucleation in the troposphere and all ice nucleation in cryopreservation systems is heterogeneous; i.e. induced at a surface. The current paradigm for the impact of solutes on immersion mode heterogeneous ice nucleation was established by Zobrist et al (2008). They conducted droplet freezing experiments using nonadecanol monolayers

and dispersions of nanometer sized silica spheres, Arizona Test Dust (ATD) and AgI as ice nucleators. These nucleants were dispersed in various concentrations of a wide range of solute molecules. These included salts such as LiCl, NaCl and $(NH_4)_2SO_4$, organic compounds such as ethylene glycol and glycerol, organic acids and the polymer polyethylene glycol 300, among others. They found that an adapted form of the water activity criterion gave a satisfactory description of the shift between experiments conducted in pure water and experiments conducted in the presence of solutes. Essentially, the freezing behavior of each nucleator could be described by a constant offset in water activity from the melting temperature with the size of the offset dictated by the nucleator. A characteristic shift in water activity could then be calculated for each of the four nucleators. For comparison, $\Delta a_w = 0.305$ for homogenous nucleation whereas $\Delta a_{w,het}$ for heterogeneous nucleation ranged from 0.100 for the nondecanol monolayers used to 0.195 for ATD. Several other studies with non-reactive solutes are consistent with the conclusion that heterogeneous freezing can be described by Δa_w (Knopf and Alpert, 2013;Rigg et al., 2013;Knopf and Forrester, 2011;Alpert et al., 2011;Cantrell and Robinson, 2006). There is evidence of acids causing reductions in the ice nucleation activity of certain mineral dusts that is greater than would be expected from the water activity of the acid solutions and these reductions are attributed to the destruction of ice nucleating sites by the acid (Cziczo et al., 2009;Sullivan et al., 2010;Chernoff and Bertram, 2010).

Reischel and Vali (1975) performed a study of the effects of 0.01 M, 0.1 M and 1M solutions of 22 different salts on four different nucleators. The nucleators were kaolin, leaf-derived nuclei (LDN), AgI and CuS. LDN (known to be the ice nucleation active bacteria *Pseudomonas Syringae* (Maki et al., 1974)) was little impacted by any solutes. For all other nucleators responses were complicated with enhancements and suppressions of ice nucleation much larger than would be expected from the water activity criterion observed. Remarkably, they observed that for CuS, AgI and kaolin the presence of ammonium salts usually led to higher nucleation temperatures. Other nucleator/solute combinations, particularly the combination of LiI and kaolin, were also observed to lead to large enhancements in ice nucleation efficiency. Gobinathan, and Ramasamy (1981) demonstrated that dissolved NH_4I can enhance the ice nucleation activity of PbI_2. Zobrist et al. (2008) also observed that in the presence of $(NH_4)_2SO_4$, AgI exhibited enhanced nucleation properties. As their experimental technique involved synthesis of AgI in the presence of solute molecules they attributed this to changes in crystal habit caused by

changes in concentration of Ag^+ in the presence of $(NH_4)_2SO_4$. Overall, there are enough exceptions to the water activity criterion approach to warrant further investigation.

6.2. Materials and methods

To this end, we have tested the ice nucleation activities of various combinations of nucleators and solutes using the microlitre Nucleation by Immersed Particles Instrument (µl-NIPI). This instrument has been described in detail previously (Whale et al., 2015a) and used for a number of studies of immersion mode heterogeneous ice nucleation (Whale et al., 2015a;Whale et al., 2015b;Atkinson et al., 2013). Briefly, 40 to 50 droplets with a volume of one microlitre are placed on a silanised glass coverslip and cooled using a Grant-Asymptote EF600 Stirling cryocooler. For this study the solutes we used were KCl, NaCl, NaI, $(NH_4)Cl$, $(NH_4)_2SO_4$ and $(NH_4)OH$. These salts were purchased from Sigma-Aldrich. A range of nucleators have been used for this study. BCS376 microcline, which was characterized by Atkinson et al. (2013) was obtained from the Bureau of Analysed Samples. It contains 76.6% alkali feldspar, 16.7% plagioclase feldspar and 3.9% quartz. The Eifel Sanidine was first tested by Whale et al. (2016) and is pure alkali feldspar. Humic acid (leonardite) was purchased from the International Humic Substances Society. It's ice nucleating activity has been tested previously previously (O'Sullivan et al., 2014). Quartz was purchased from Sigma Aldrich. The sample used was found to be 98.4% pure by Atkinson et al. (2013). Nanoporous amorphous silica gel was purchased from Sigma-Aldrich (214396) and Arizona Test Dust (ATD) was purchased from Powder Technology inc. Solutions and suspensions of nucleators were made up gravimetrically. In this study we have used a solute concentration of 0.015 M for most experiments, for which we would expect a homogeneous freezing depression of less than 0.1°C for all solutes. Other experiments have been conducted with weaker concentrations, for which freezing point depressions, according to the water activity criterion, will be smaller still.

In order to facilitate comparison of data presented here with other studies we have calculated the ice nucleation active surface-site density, $n_s(T)$, where possible. Specific surface areas were not known for humic acid and ATD. $n_s(T)$ can be calculated using (Connolly et al., 2009):

$$\frac{n(T)}{N} = 1 - \exp(-n_s(T)A) \qquad 6.1$$

Where $n(T)$ is the number of droplets frozen at temperature (T), N is the total number of droplets in the experiment and A is the surface area of nucleant per droplet. $n_s(T)$ is a site specific measure of ice nucleation efficiency which does not account for the effects of time dependence (Herbert et al., 2014). All experiments here were done with the same cooling rate (1 °C min^{-1}). Uncertainty in n_s was calculated using simulations of possible site distributions propagated with the uncertainty in surface area of nucleator per droplet as described in Harrison et al. (2016). Temperature uncertainty for µl-NIPI has been estimated to be ±0.4 °C (Whale et al. 2015a).

6.3. Results and discussion

We froze 0.1 wt% suspensions of BCS 376 microcline in 0.015 M solutions of potassium chloride, sodium iodide, sodium chloride, ammonium hydroxide, ammonium chloride and ammonium sulphate. The results of these experiments are presented in Figure 6.1. All three ammonium compounds enhanced ice nucleation, leading to warmer freezing temperatures. The extent of enhancement (≈3°C) was identical in all cases. The presence of the alkali halides led to colder freezing temperatures. The deactivation in all cases was greater than would be expected from the water activity criterion, which would be around less than 0.1°C as mentioned previously. Clearly then, ice nucleation by BCS 376 microcline does not follow the water activity criterion at the solute concentration investigated here. The variation in freezing point depressions caused by the alkali metal halides has the order KCl>NaCl>NaI.

We have also examined the effect of varying concentration of $(NH_4)_2SO_4$ and NaCl on nucleation by BCS 376 feldspar, the results are presented in Figure 6.2. For these experiments we reduced concentrations of the solutes by factors of 10 and 100. The magnitude of the fall in freezing temperature was reduced for NaCl with reducing salt concentration. For $(NH_4)_2SO_4$ there was little difference in the level of enhancement between the 1.5 x 10^{-2} M and 1.5 x 10^{-3} M solution while the enhancement in freezing activity was smaller for the 1.5 x 10^{-3} M solution, around 1.5°C rather than 3°C. This hints at a saturation effect, particularly in combination with the data in figure 6.1 showing that all ammonium salts lead to an equal enhancement of ice nucleation.

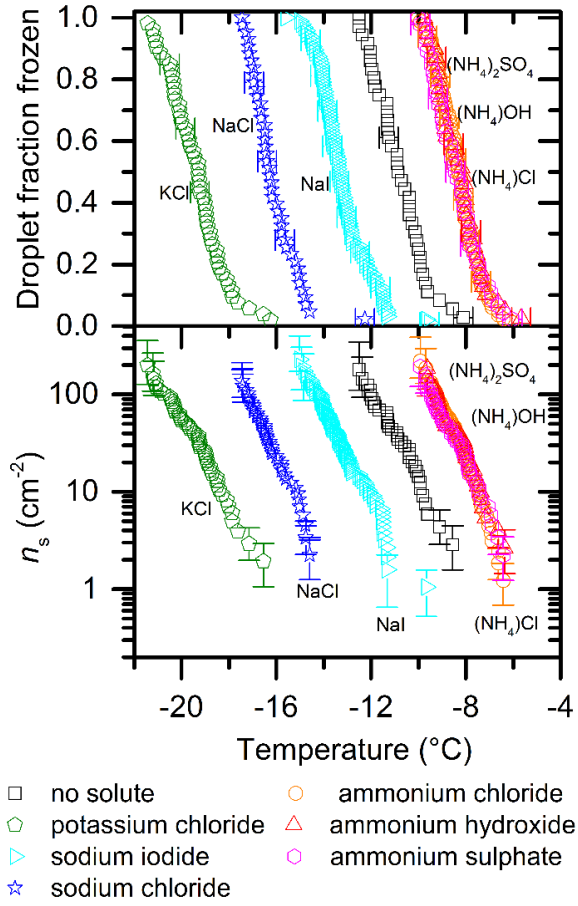

Figure 6.1: Fraction frozen curves and $n_s(T)$ values for 0.1 wt% of BCS 376 K-feldspar suspended in 0.015 M solutions of various solutes. The concentration of solute used produces a freezing point depression of less than 0.1°C. The water activity of these solutions is very close to 1 so no significant depression in nucleation temperature would be expected given our experimental temperature uncertainty is ± 0.4 °C. All three ammonium compounds cause ice to nucleate 3°C warmer while the three alkali halides produced freezing point depressions ranging from 2.5°C for NaI to 8.5°C for KCl.

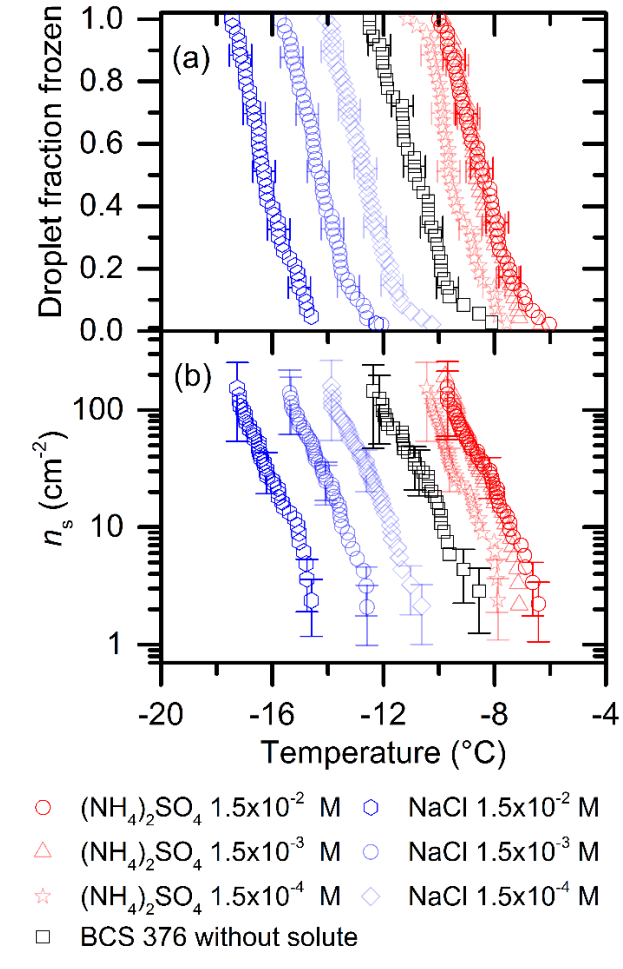

Figure 6.2: (a) Droplet fraction frozen against temperature for BCS 376 feldspar with various concentrations of $(NH_4)_2SO_4$ and NaCl. (b) $n_s(T)$ values for the fraction frozen data in panel. Reduced concentrations of $(NH_4)_2SO_4$ and NaCl lead to a lessening of the effects that those salts have on nucleation by BCS 376 feldspar.

We tested five other nucleators with 0.015 M solutions of $(NH_4)_2SO_4$, KCl and NaCl. Figure 6.3 and Figure 6.4 show the results of these experiments. Eifel sanidine and quartz qualitatively showed the same response as BCS376, i.e. $(NH_4)_2SO_4$ increased ice nucleation temperatures while NaCl and KCl reduced them (Figure 6.3) whereas Humic acid, silica gel and ATD were unaffected by the presence of solutes (Figure 6.4).

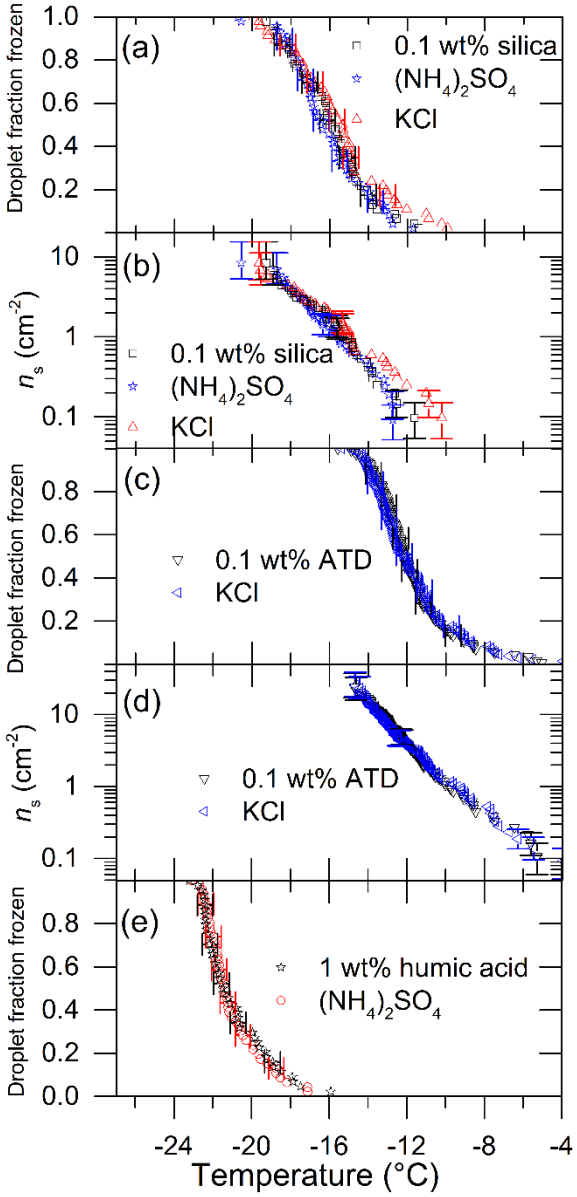

Figure 6.3: The impact of 0.015 M KCl and $(NH4)_2SO_4$ on ice nucleation by silica, humic acid and ATD. (a) Droplet fraction frozen against temperature for a 0.1 wt% silica suspension with data showing the impact on freezing temperature of 0.015M NaCl and 0.015M $(NH_4)_2SO4$. (b) $n_s(T)$ values for the fraction frozen data in panel (a). (c) Droplet fraction frozen against temperature for a 0.1 wt% ATD suspension with data showing the impact on freezing temperature of 0.015M KCl. (d) $n_s(T)$ values for the fraction frozen data in panel (c). (e) Droplet fraction frozen against temperature for a 1 wt% humic acid suspension with data showing the impact on freezing temperature of 0.015M KCl. At the concentrations investigated these solutes do not impact ice nucleation temperatures for these nucleators

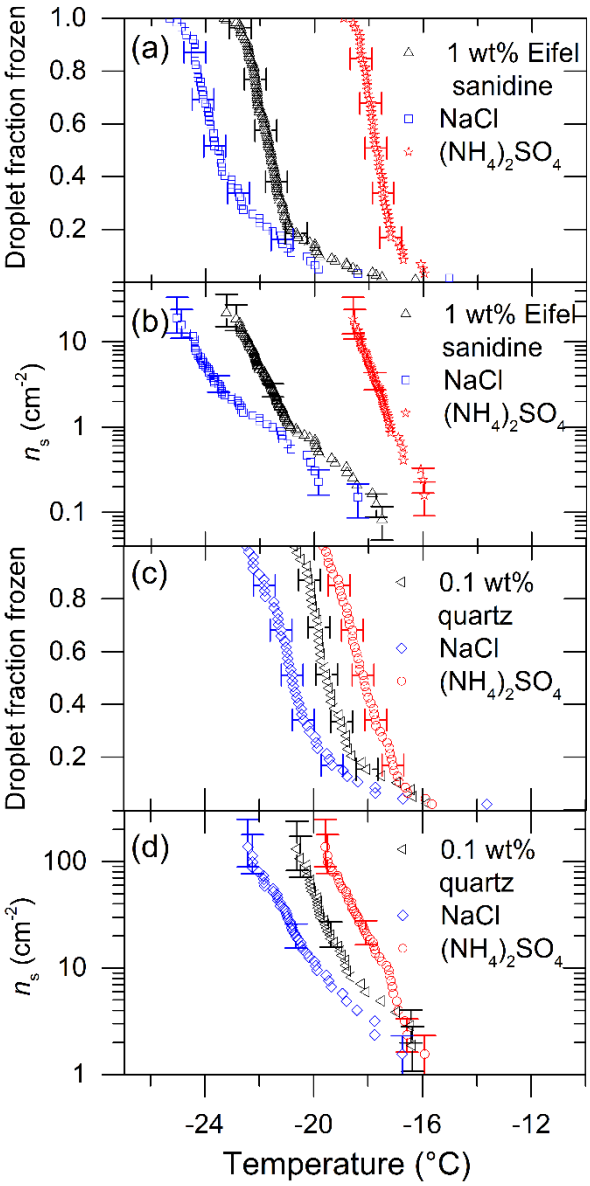

Figure 6.4: The impact of 0.015 M NaCl and $(NH4)_2SO_4$ on ice nucleation by quartz and Eifel sanidine. (a) Droplet fraction frozen against temperature for a 1 wt% Eifel sanidine suspension with data showing the impact on freezing temperature of 0.015M NaCl and 0.015M $(NH_4)_2SO_4$. (b) $n_s(T)$ values for the fraction frozen data in panel (a). (c) Droplet fraction frozen against temperature for a 0.1 wt% quartz suspension with data showing the impact on freezing temperature of 0.015M NaCl and 0.015M $(NH4)_2SO_4$. (d) $n_s(T)$ values for the fraction frozen data in panel (c). For these nucleators the presence of NaCl reduces nucleation temperatures while the presence of $(NH4)_2SO_4$ increases nucleation temperatures.

The impact of solutes on ice nucleation by ATD, silica and humic acid have been tested previously so some comparison to literature data is possible. Droplets containing ATD were frozen with various solutes by Zobrist et al. (2008) The silica gel we have tested is likely to have similar ice nucleation properties to the silica balls tested by Zobrist et al.(2008) and the humic acid we have tested is similar to humic substances tested by Knopf and Alpert (2013) and Rigg et al.(2013) These studies showed that the water activity criterion described ice nucleation at lower water activities and our results do not contradict this- we saw no difference in freezing temperatures for these nucleators and would not expect to with the weak solute concentrations used. These recent studies did not look at quartz or feldspars.

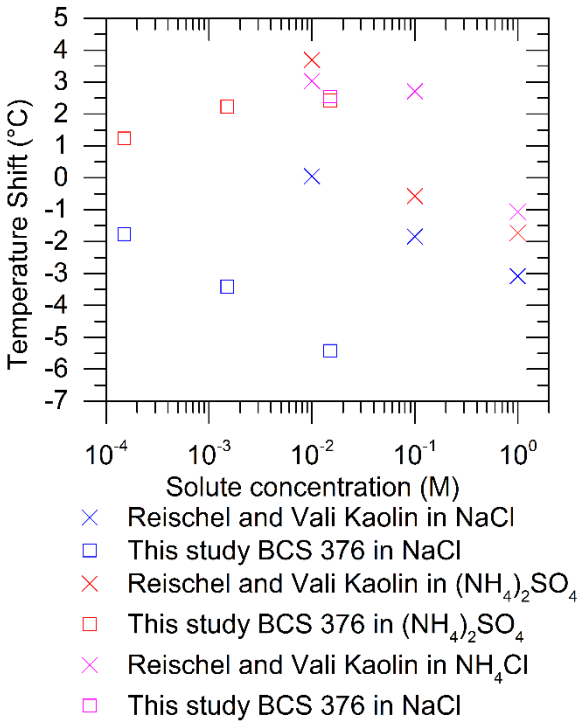

Figure 6.5 : Comparison of shifts in true supercooling induced by $(NH4)_2SO_4$, NH4Cl and NaCl in droplets containing kaolin from Reischel and Vali (1975) with shifts for BCS 376 feldspar from this study. Shifts for this study were calculated from the difference in T50 between the pure water experiment and the experiment with the solute. 0.01 M solutions of the ammonium salts lead to similar enhancements in both studies. We obtained a different temperature shift for 0.01 M NaCl, although it should be noted that the nucleators are different.

Reischel and Vali (1975) observed enhancement of ice nucleation by kaolin in the presence of ammonium salts. It is possible that this material contained some feldspar as clays such as kaolinite are very often produced from weathering of feldspars (Wenk and Bulakh, 2004). Hence, we have compared the impacts of $(NH_4)_2SO_4$, NH_4Cl and NaCl on kaolin from Reischel and Vali (1975) and BCS 376 from this study in Figure 6.5. Interestingly, similar shifts to warmer freezing temperatures (about 2.5°C to 3.5°C) were observed in both studies for concentrations of $(NH_4)_2SO_4$ and NH_4Cl of approximately 0.01 M. The other direct point of comparison, 0.01 M NaCl, does not agree well. We observed a shift of 5.5°C to colder temperatures while Reischel and Vali (1975) observed very little shift. It is difficult to compare to any other literature data as there is no commonality in the nucleators used. Nevertheless, it is clear that at the concentrations we have investigated here some solutes, particularly ammonium salts, can enhance ice nucleation and others can inhibit it. Our work suggests that some nucleators are not

affected by solutes however it is clear from Reischel and Vali(Reischel and Vali, 1975) that varying concentrations of solutes can have unpredictable impacts on nucleation temperatures so it is possible that higher or lower concentrations of solutes would alter freezing temperatures. Equally, as most data supporting the water activity criterion comes from more concentrated solutions it is conceivable that at higher concentrations than those we have investigated the unsystematic enhancements and deactivations we and Reischel and Vali (1975) have observed would not occur. Overall, we conclude that at solute concentrations lower than 1 M the water activity criterion approach is not valid for some nucleators and that the approach should also be examined at higher concentrations for a greater range of nucleators. Next, we discuss possible reasons for the effects we have observed.

Recently it has been suggested that aggregation of particles in droplet freezing experiments, leading to a loss of particles from suspension and a reduction of surface area within aggregates of particles, may be responsible for discrepancies between different instruments for used measuring ice nucleation (Emersic et al., 2015;Hiranuma et al., 2015). It is well known that aqueous salts can change the rate at which particles aggregate and the size of aggregates, hence it is conceivable that aggregation could be enhanced or inhibited on adding salts leading to changes in ice nucleating activity. To test this we took individual chips of a feldspar rich rock of approximately 1 mm diameter and placed them onto a hydrophobic slide. We then pipetted 1 µl MilliQ water droplets onto them and conducted a freezing experiment using µl-NIPI as usual. The median freezing temperature was -16.4 ± 0.4 °C. We removed the rock chips from the water droplets, dried them and repeated the experiment in a 0.015 M solution of $(NH_4)_2SO_4$. Median freezing temperature shifted to -11.8 ± 0.4 °C. This demonstrates that the ice nucleation enhancing effect of $(NH_4)_2SO_4$ on feldspar does not depend on the nucleator being in powder form and that the solute effect on ice nucleation is not related to particle aggregation. Figure 6.6 shows the layout of and droplet fraction frozen measurements for the experiment.

It is interesting that the solute effect is observed for both Eifel sanidine and BCS 376 microcline. It has been shown that BCS 376 microcline nucleates ice more efficiently than Eifel sanidine and that this may be due to features associated with grain boundaries, which Eifel Sandine lacks, despite having broadly similar crystallographic structure and chemical composition to other alkali feldspars. This suggests that the sites on the two

kinds of feldspar have a similar nature, even though they nucleate ice at different temperatures.

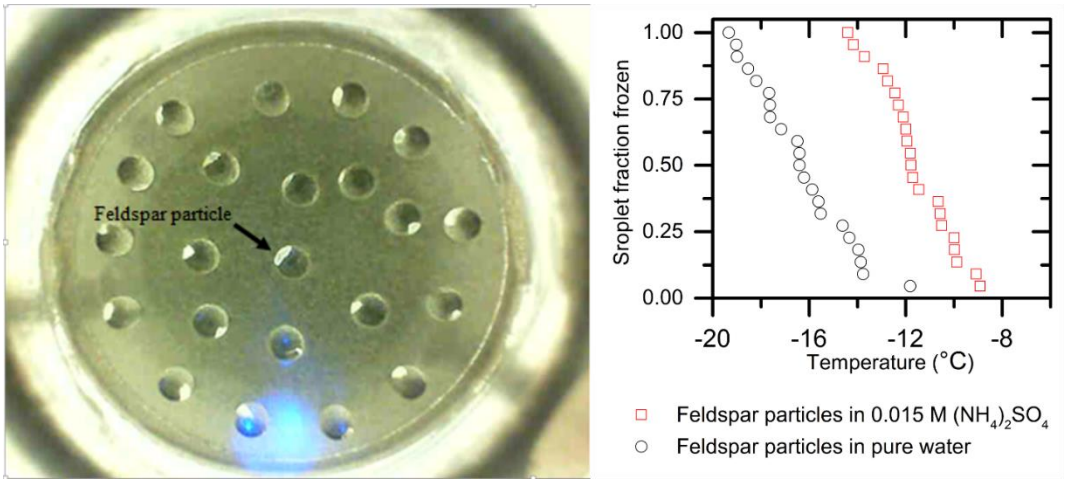

Figure 6.6: Photograph of chips of feldspar immersed in water droplets in the µl-NIPI system. The white parts of the droplets are the immersed chips. When these water droplets were replaced by a 0.015 M ammonium sulphate solution ice nucleation was enhanced. The right hand panel shows the fraction of droplets frozen against temperature with and without ammonium sulphate.

We can see three broad categories of mechanism by which ammonium salts and alkali metal halides might influence ice nucleation by certain nucleators:

1) Replacement of cations with NH_4^+ in, or insertion of NH_4^+ into, the nucleator surface enhances ice nucleation by altering surface properties in a way conducive to efficient ice nucleation. Conversely, insertion of alkali metal cations into surfaces does the reverse, inhibiting ice nucleation. Nucleators that cannot incorporate cations into their structures are not affected in the same way.
2) Adsorption of NH_4^+ onto the nucleator surface changes the strength of the interaction of water with the surface in a way favorable to ice nucleation. Conversely, adsorption of alkali metal cations to the surface inhibits ice nucleation or else metal cations fail to adsorb to the surface
3) The interaction of NH_4^+ with water alters the nature of the critical nucleus in a way that encourages ice nucleation. Conversely, alkali metal cations disrupt critical nucleus formation. Different nucleators nucleate ice via different mechanisms, which are impacted differently by solutes.

So which of these three scenarios is more likely? It is known that NH_4^+ can substitute for the cations in feldspars to form ammonium feldspar (Voncken et al., 1993;Erd et al., 1964). The chemical composition of silica is identical to that of quartz so it is interesting that quartz is apparently influenced by solute effects while silica is not. It may be that the regular crystal structure of quartz is more susceptible to inclusion of solute ions than the amorphous structure of silica. This leaves the question of why ammonium ions should improve ice nucleation and alkali metals should do the opposite. Possibly, different cations will lead to different strengths of interaction of the nucleator surface with water molecules which might alter nucleation rates. It has recently been shown computationally that varying interaction strength of surface with water can have complex effects on nucleation rates (Cox et al., 2015a, b;Fitzner et al., 2015;Bi et al., 2016). Surface adsorption of NH_4^+ or alkali metal cations may have a similar impact on interaction strength of the surface with water. Sum-frequency vibrational spectroscopy has been used to show that ammonium can promote ordering of water at the surface of sapphire crystal (Anim-Danso et al., 2016) and silica (Wei et al., 2002). These studies show that this occurs due to interaction with aluminol and silanol groups on the surfaces of the sapphire and silica, respectively. Such groups are likely to occur on the surfaces of most of the nucleators we have studied here so adsorption of this type provides a plausible explanation for the effects we have observed.

It has been shown that in computational models different surfaces can nucleate ice in different ways (Bi et al., 2016;Fitzner et al., 2015). Fitzner et al.(Fitzner et al., 2015) identified three different ways in which different surfaces could nucleate ice. These are: a typical lattice match scenario where the surface creates an in-plane template for an ice face, a mechanism whereby ice like structure is induced by appropriate structuring of the first two overlayers of a relatively rough nucleator surface and a mechanism where strong interaction between the nucleator surface and water induces structure several water layers above the surface. It is quite possible that different ice nucleators in experimental systems nucleate ice in different ways. Possibly, certain of these routes are influenced by solutes while others aren't. While the ability of certain ions to encourage or discourage structuring of water may be relevant to ice nucleation (Zolles et al., 2015) our results do not fit this picture. All the cations and anions we have looked at are classified as structure breaking in water, apart from Na^+ which is intermediate (Marcus, 2009). The solutes clearly have different effects on ice nucleation so we conclude that any influence that solutes have on the structure and ease of assembly of the critical nuclei must be related to

other properties of the solutes. This does not rule out the possibility that the effect is based in the solution rather than on the surface of the nucleator.

Overall, we do not have sufficient evidence to conclusively differentiate between the three possible mechanism outlines above. It is possible that more than one of these mechanisms is at play. Regardless, the solute effect on ice nucleation provides a potential route to differentiating mechanisms of immersion mode ice nucleation and therefore a route to understanding them. Further work looking at different solutes, different nucleators and concentration dependences may help to unpick the puzzle. Sum frequency vibrational spectroscopy of surfaces which are differently impacted by the solute effect on ice nucleation may be a useful tool. Additionally, these effects are of potential importance for atmospheric science as solute concentrations similar to those we have used are can occur in cloud droplets. Clearly, a great deal more work is needed to understand the concentration dependence of these effects and their interaction with the water activity criterion, both of which will be vital for application to the atmosphere. Equally, establishing which of the many potential atmospheric INPs are impacted by these solute effects will be of importance in the future.

References

Alpert, P. A., Aller, J. Y., and Knopf, D. A.: Ice nucleation from aqueous NaCl droplets with and without marine diatoms, Atmos. Chem. Phys., 11, 5539-5555, 10.5194/acp-11-5539-2011, 2011.

Anim-Danso, E., Zhang, Y., and Dhinojwala, A.: Surface charge affects the structure of interfacial ice, J. Phys. Chem. C, 120, 3741-3748, 10.1021/acs.jpcc.5b08371, 2016.

Atkinson, J. D., Murray, B. J., Woodhouse, M. T., Whale, T. F., Baustian, K. J., Carslaw, K. S., Dobbie, S., O'Sullivan, D., and Malkin, T. L.: The importance of feldspar for ice nucleation by mineral dust in mixed-phase clouds, Nature, 498, 355-358, 10.1038/nature12278, 2013.

Bi, Y., Cabriolu, R., and Li, T.: Heterogeneous ice nucleation controlled by the coupling of surface crystallinity and surface hydrophilicity, J. Phys. Chem. C, 120, 1507-1514, 10.1021/acs.jpcc.5b09740, 2016.

Cantrell, W., and Robinson, C.: Heterogeneous freezing of ammonium sulfate and sodium chloride solutions by long chain alcohols, Geophys. Res. Lett., 33, 2006.

Chernoff, D. I., and Bertram, A. K.: Effects of sulfate coatings on the ice nucleation properties of a biological ice nucleus and several types of minerals, J. Geophys. Res.: Atmos., 115, 2010.

Connolly, P. J., Möhler, O., Field, P. R., Saathoff, H., Burgess, R., Choularton, T., and Gallagher, M.: Studies of heterogeneous freezing by three different desert dust samples, Atmos. Chem. Phys., 9, 2805-2824, 10.5194/acp-9-2805-2009, 2009.

Cox, S. J., Kathmann, S. M., Slater, B., and Michaelides, A.: Molecular simulations of heterogeneous ice nucleation. I. Controlling ice nucleation through surface hydrophilicity, J. Chem. Phys., 142, 184704, doi:http://dx.doi.org/10.1063/1.4919714, 2015a.

Cox, S. J., Kathmann, S. M., Slater, B., and Michaelides, A.: Molecular simulations of heterogeneous ice nucleation. Ii. Peeling back the layers, J. Chem. Phys., 142, 184705, doi:http://dx.doi.org/10.1063/1.4919715, 2015b.

Cziczo, D. J., Froyd, K. D., Gallavardin, S. J., Moehler, O., Benz, S., Saathoff, H., and Murphy, D. M.: Deactivation of ice nuclei due to atmospherically relevant surface coatings, Environ. Res. Lett., 4, 044013, 2009.

Emersic, C., J. Connolly, P., Boult, S., Campana, M., and Li, Z.: Investigating the discrepancy between wet-suspension and dry-dispersion derived ice nucleation efficiency of mineral particles, Atmos. Chem. Phys. Discuss., 15, 887-929, 10.5194/acpd-15-887-2015, 2015.

Erd, R. C., Lee, D. E., White, D. E., and Fahey, J. J.: Buddingtonite ammonium feldspar with zeolitic water, Am.Mineral., 49, 831-&, 1964.

Fitzner, M., Sosso, G. C., Cox, S. J., and Michaelides, A.: The many faces of heterogeneous ice nucleation: Interplay between surface morphology and hydrophobicity, J. Am. Chem. Soc., 137, 13658-13669, 10.1021/jacs.5b08748, 2015.

Fuller, B. J.: Cryoprotectants: The essential antifreezes to protect life in the frozen state, Cryo Letters, 25, 375-388, 2004.

Gobinathan, R., and Ramasamy, P.: Ice nucleating behaviour of pbi2 in the presence of soluble salts, Mater. Res. Bull., 16, 1527-1533, http://dx.doi.org/10.1016/0025-5408(81)90024-6, 1981.

Herbert, R. J., Murray, B. J., Whale, T. F., Dobbie, S. J., and Atkinson, J. D.: Representing time-dependent freezing behaviour in immersion mode ice nucleation, Atmos. Chem. Phys., 14, 8501-8520, 10.5194/acp-14-8501-2014, 2014.

Hiranuma, N., Augustin-Bauditz, S., Bingemer, H., Budke, C., Curtius, J., Danielczok, A., Diehl, K., Dreischmeier, K., Ebert, M., Frank, F., Hoffmann, N., Kandler, K., Kiselev, A., Koop, T., Leisner, T., Möhler, O., Nillius, B., Peckhaus, A., Rose, D., Weinbruch, S., Wex, H., Boose, Y., DeMott, P. J., Hader, J. D., Hill, T. C. J., Kanji, Z. A., Kulkarni, G., Levin, E. J. T., McCluskey, C. S., Murakami, M., Murray, B. J., Niedermeier, D., Petters, M. D., O'Sullivan, D., Saito, A., Schill, G. P., Tajiri, T., Tolbert, M. A., Welti, A., Whale, T. F., Wright, T. P., and Yamashita, K.: A comprehensive laboratory study on the immersion freezing behavior of illite nx particles: A comparison of 17 ice nucleation measurement techniques, Atmos. Chem. Phys., 15, 2489-2518, 10.5194/acp-15-2489-2015, 2015.

Kiani, H., and Sun, D. W.: Water crystallization and its importance to freezing of foods: A review, Trends Food Sci. Technol., 22, 407-426, 10.1016/j.tifs.2011.04.011, 2011.

Knopf, D. A., and Forrester, S. M.: Freezing of water and aqueous nacl droplets coated by organic monolayers as a function of surfactant properties and water activity, J. Phys. Chem. A, 115, 5579-5591, 10.1021/jp2014644, 2011.

Knopf, D. A., and Alpert, P. A.: A water activity based model of heterogeneous ice nucleation kinetics for freezing of water and aqueous solution droplets, Faraday Discuss., 165, 513-534, 10.1039/c3fd00035d, 2013.

Koop, T., Luo, B. P., Tsias, A., and Peter, T.: Water activity as the determinant for homogeneous ice nucleation in aqueous solutions, Nature, 406, 611-614, 2000.

Maki, L. R., Galyan, E. L., Chang-Chien, M.-M., and Caldwell, D. R.: Ice nucleation induced by pseudomonas syringae, J. Appl. Microbiol., 28, 456-459, 1974.

Marcus, Y.: Effect of ions on the structure of water: Structure making and breaking, Chem. Rev., 109, 1346-1370, 10.1021/cr8003828, 2009.

Morris, G. J., and Acton, E.: Controlled ice nucleation in cryopreservation - a review, Cryobiology, 66, 85-92, 10.1016/j.cryobiol.2012.11.007, 2013.

Murray, B. J., O'Sullivan, D., Atkinson, J. D., and Webb, M. E.: Ice nucleation by particles immersed in supercooled cloud droplets, Chem. Soc. Rev., 41, 6519-6554, 10.1039/C2CS35200A, 2012.

O'Sullivan, D., Murray, B. J., Malkin, T. L., Whale, T. F., Umo, N. S., Atkinson, J. D., Price, H. C., Baustian, K. J., Browse, J., and Webb, M. E.: Ice nucleation by fertile soil dusts: Relative importance of mineral and biogenic components, Atmos. Chem. Phys., 14, 1853-1867, 10.5194/acp-14-1853-2014, 2014.

Reischel, M. T., and Vali, G.: Freezing nucleation in aqueous electrolytes, Tellus, 27, 414-427, 10.1111/j.2153-3490.1975.tb01692.x, 1975.

Rigg, Y. J., Alpert, P. A., and Knopf, D. A.: Immersion freezing of water and aqueous ammonium sulfate droplets initiated by humic-like substances as a function of water activity, Atmos. Chem. Phys., 13, 6603-6622, 10.5194/acp-13-6603-2013, 2013.

Searles, J. A., Carpenter, J. F., and Randolph, T. W.: The ice nucleation temperature determines the primary drying rate of lyophilization for samples frozen on a temperature-controlled shelf, J. Pharm. Sci., 90, 860-871, 10.1002/jps.1039, 2001.

Sullivan, R. C., Petters, M. D., DeMott, P. J., Kreidenweis, S. M., Wex, H., Niedermeier, D., Hartmann, S., Clauss, T., Stratmann, F., Reitz, P., Schneider, J., and Sierau, B.: Irreversible loss of ice nucleation active sites in mineral dust particles caused by sulphuric acid condensation, Atmos. Chem. Phys., 10, 11471-11487, 10.5194/acp-10-11471-2010, 2010.

Voncken, J., Van Roermund, H., Van der Eerden, A., Jansen, J., and Erd, R.: Holotype buddingtonite: An ammonium feldspar without zeolitic H_2O, Am. Mineral., 78, 204-204, 1993.

Wei, X., Miranda, P. B., Zhang, C., and Shen, Y. R.: Sum-frequency spectroscopic studies of ice interfaces, Phys. Rev. B, 66, 085401, 2002.

Wenk, H.-R., and Bulakh, A.: Minerals: Their constitution and origin, Cambridge University Press, 2004.

Whale, T. F., Murray, B. J., O'Sullivan, D., Wilson, T. W., Umo, N. S., Baustian, K. J., Atkinson, J. D., Workneh, D. A., and Morris, G. J.: A technique for quantifying heterogeneous ice nucleation in microlitre supercooled water droplets, Atmos. Meas. Tech., 8, 2437-2447, 10.5194/amt-8-2437-2015, 2015a.

Whale, T. F., Rosillo-Lopez, M., Murray, B. J., and Salzmann, C. G.: Ice nucleation properties of oxidized carbon nanomaterials, J. Phys. Chem. Lett., 3012-3016, 10.1021/acs.jpclett.5b01096, 2015b.

Whale, T. F., Murray, B. J., Holden, M. A., Wilson, T. W., and Carpenter, M. A.: A study of the ice nucleation activity of alkali feldspars, 2016.

Zobrist, B., Marcolli, C., Peter, T., and Koop, T.: Heterogeneous ice nucleation in aqueous solutions: The role of water activity, J. Phys. Chem A, 112, 3965-3975, 10.1021/jp7112208, 2008.

Zolles, T., Burkart, J., Häusler, T., Pummer, B., Hitzenberger, R., and Grothe, H.: Identification of ice nucleation active sites on feldspar dust particles.: J. Phys. Chem A, 119, 2692-2700, 10.1021/jp509839x, 2015.

7. Conclusions

7.1. Overview of thesis

In the introduction to this study two main objectives were outlined. The first was to produce an instrument for quantitatively measuring low concentrations of INPs at high temperatures. The second objective was to contribute towards understanding of the relationship between the physical and chemical properties of ice nucleators and their efficiency as ice nucleators. This section reviews how these objectives have been addressed before discussion of potential future work following on from the project and concluding remarks.

7.1.1. Objective one: A high temperature droplet freezing experiment

The first objective of this project was to develop a system for measuring immersion mode ice nucleation by relatively rare INPs at relatively warm temperatures. The µl-NIPI droplet freezing experiment that was developed to meet this objective is described in *Chapter two*; published as '*A technique for quantifying heterogeneous ice nucleation in microlitre supercooled water droplets*' (Whale et al., 2015a). µl-NIPI uses larger water droplets than many other ice nucleation experiments to sample larger surface area of nucleators and therefore to sample the rare particles or ice nucleating sites that induce freezing at warmer temperatures. To date, this facility has been used in several papers looking at atmospherically relevant INPs including feldspars, biological INPs and nucleators in the sea surface microlayer.

The simplicity of µl-NIPI makes it much faster at generating droplet freezing results than most instruments, so it is suited to conducting relatively large numbers of experiments on multiple different nucleators. This facility has been used to address the second goal of this project, improving understanding of the impact of physical and chemical properties on the efficacy of ice nucleators.

7.1.2. Objective two: Examining the fundamental aspects of ice nucleation

As discussed in *Chapter one*, the strength of interaction between the surface of a nucleator and the water molecule must play a role in the ice nucleation process. Past experimental work on soot found that more hydrophilic soots nucleated ice more efficiently more hydrophobic soots (Gorbunov et al., 2001), although the mode of ice nucleation in these experiments was not clear. These experimental results were consistent with the usual view that greater strength of interaction between a nucleator surface and water molecules must

improve ice nucleation efficiency (Pruppacher and Klett, 1997). Lupi and Molinero (Lupi and Molinero, 2014) performed a computational study suggesting that the opposite was true and that less hydrophilic carbon species would likely nucleate ice more efficiently than more hydrophilic species. *Chapter three*, published as '*Ice nucleation properties of oxidized carbon nanomaterials'* (Whale et al., 2015b) sought to test this finding experimentally. The ice nucleation activities of suspensions of carboxylated graphene nanoflakes, graphene oxide, oxidized single walled carbon nanotubes and oxidized multiwalled carbon nanotubes were determined. The GNFs are small, effectively 2-dimensional flakes of graphene which are among the smallest entities observed to have nucleated ice. The carbon nanotube species were found to nucleate ice more efficiently than flat graphene species, and less oxidized materials nucleated ice more efficiently than more oxidized species overall. It was demonstrated using the FROST framework of Herbert et al. (2014), which is described in *Chapter one*, that ice nucleation by carboxylated graphene nanoflakes is site specific. This implies that specific locations on the surface of the GNFs nucleate ice more efficiently than the bulk of the surface. The results are more consistent with the findings of Lupi and Molinero (2014) than the usual view that more oxidised species will nucleate ice more efficiently than less oxidised species. The comparison is not direct as the structure of carbon nanotubes and flat graphene species is different. Computational work by Lupi et al. (2014) showed that curvature and molecular roughness of carbon surfaces also impacted ice nucleation efficiency. Nevertheless this chapter gives tentative experimental corroboration of the computational finding (Lupi and Molinero, 2014) that lower hydrophilicity improves ice nucleating efficiency of carbon species. Computational studies published subsequent to *Chapter three* have found complex relationships between the hydrophilicity, surface structure and the ice nucleating efficiency of model surfaces (Fitzner et al., 2015) and carbon surfaces (Bi et al., 2016). It is more difficult to place the results of *Chapter three* in the context of these subsequent studies. Possible future work that might be able to resolve this is discussed in section 7.2.2.

Following the discovery of the relatively high ice nucleating efficiency of 'K-feldspar' compared to other mineral dusts (Atkinson et al., 2013) and non-biological ice nucleating species (see *Chapter one*) I realised that the rich phase diagram of the feldspar family made it a good candidate for testing the impact of small changes in composition and structure on ice nucleating efficiency. Feldspars can be classified into three broad structural families. These are plagioclase feldspars, alkali feldspars and albites. In *Chapter four*, currently under review but publicly available as '*Not all feldspar is equal:*

a survey of ice nucleating properties across the feldspar group of minerals' (Harrison et al., 2016) it was found that all alkali feldspars nucleate ice much more efficiently than plagioclase feldspars while albite feldspars are intermediate in activity. There is little difference in crystal structure between alkali and plagioclase feldspars, and neither provides an obvious lattice match to crystalline ice. A major difference between the two families is that the Na^+ and K^+ ions in alkali feldspars almost invariably exsolve during formation while the Ca^{2+} and Na^+ ions of plagioclase feldspars do not exsolve, meaning that these feldspars remain as solid solutions. This leads to a wide variety of microtextural features in alkali feldspars. I hypothesised that these features played a role in ice nucleation by alkali feldspars. In *Chapter four* it was also found that two feldspars, one an alkali feldspar and the other an albite, nucleated ice more efficiently than the majority of other feldspars tested. The activity of these feldspars also decayed substantially when they were left in water. After 16 months the temperature at which a suspension of Amelia albite nucleated ice had reduced by 16 °C. It seems likely that this decay is related to chemical alteration or dissolution of ice nucleating sites, although why this should affect some highly active sites but not less active sites is not known.

In *Chapter five*, the unpublished paper '*The microtexture of alkali feldspars is important for its ice nucleating ability'* the hypothesis that microtexture impacts the ice nucleating efficiency of feldspars was tested by determining the ice nucleating efficiency of a range of alkali feldspars with known microtexture, sourced from a previous study on the surface roughness of alkali feldspars (Hodson et al., 1997). It was found that a rare alkali feldspar which lacked microtexture nucleated ice similarly to plagioclase feldspars, while another alkali feldspar which possessed only coherent grain boundaries, and therefore likely has a lower number of dislocations and nanoscale features than most alkali feldspars was less efficient at nucleating ice than those feldspars possessing more complex microtexture. On this basis we concluded that features related to microtexture are indeed important for the efficient ice nucleation exhibited by alkali feldspars. Such features are spread unevenly across the surface of a nucleator, meaning some parts of the surface of feldspar are better at nucleating ice than others. This provides an explanation for why ice nucleation by BCS 376 feldspar has been observed to be site-specific (Herbert et al., 2014).

Finally, *Chapter six*, the unpublished paper *'The enhancement and suppression of immersion mode heterogeneous ice nucleation by solutes'* looked at ice nucleation induced by a range of nucleators in dilute solutions of ammonium salts and alkali halides. It was found that ice nucleation by quartz and feldspars was substantially enhanced in the

presence of ammonium salts and suppressed in the presence of alkali halides. Other nucleators, including amorphous silica gel were not affected by the solutes. These results contrast with contemporary understanding of the impact of solutes on immersion mode ice nucleation, which suggest that temperature shift induced by solutes can be entirely accounted for by the change in water activity they induce (Zobrist et al., 2008). However, earlier studies had reported highly variable impacts of solutes on different ice nucleators (Reischel and Vali, 1975). This conflicts with the water activity based approach and appears to have been forgotten more recently. The results of *Chapter 6* do not directly conflict with any previous experimental results but do show that the simple water activity based model is not valid for certain systems at water activities close to 1. The split in response to the presence of solutes might suggest that (at least) two different mechanism of ice nucleation occur on different nucleators.

7.2. Future Work

This work presented in this thesis points towards many potential routes for future research. While µl-NIPI has proved to be a very useful instrument, numerous improvements are possible, the following section discusses these. Additionally, there are several more experiments following on from work in this thesis that might help to improve understanding of ice nucleation.

7.2.1. Improvement of droplet freezing experiments

Automatic detection of freezing would allow data to be generated much more quickly. Other groups have done this with video analysis software (Budke and Koop, 2015). An infra-red camera would make this easier as the latent heat released on droplet freezing would make the events easy to distinguish.

The freezing baseline of µl-NIPI is inconvenient as it limits the temperature range over which the instrument can be used. There are many situations where the ability to test less active INPs is desirable. Ideally an ice nucleation instrument should ideally be capable of nucleating ice homogenously, if it can do this then activity of any ice nucleating entity can in principle be quantified. There is only one report of the homogenous ice nucleation occurring reproducibly at temperatures predicted by CNT (Fornea et al., 2009). It may be possible to make progress by purifying the water used. MilliQ water is only filtered to 0.2 µm so smaller particles will remain, which may nucleate ice. Also, relatively little effort was made at optimising the surface in chapter 2. The silanised glass slides used are convenient but other surfaces may nucleate ice less efficiently and thereby push the

background freezing observed towards homogenous nucleation temperatures. Candidate surfaces might be silicon wafers and superhydrophobic polymer coatings.

µl-NIPI has been used for isothermal experiments, but the use of a dry flow to prevent the spread of ice on the glass slide limits the length of time for which droplets can be left on the surface before they evaporate. Ideally, a droplet freezing experiment would use separate cells and no dry flow so droplets could be left for much longer periods. Similarly, experiments where the same droplets are frozen and thawed repeatedly have the potential to provide much useful information on the stochasticity and site specific nature of ice nucleation, as well as ageing processes.

7.2.2. Future work on understanding the mechanism of heterogeneous ice nucleation

As discussed, this project has achieved some progress towards understanding of immersion mode heterogeneous ice nucleation. *Chapter five* links immersion mode ice nucleation activity to surface features related to microtexture. The actual nature of the ice-active sites within these features is not currently known. I have hypothesised that nano-tunnels or pull-aparts (Fitzgerald and Cayzer, 2006) may be the relevant features, on the basis of their scale and likely rarity. Work by Campbell et al. (2013) looking at deposition of organic vapours on mica suggests a possible method for testing this. By making thin sections of feldspar and freezing liquid water droplets on them, then identifying the location of origin of freezing individual features that nucleate ice might be identified. These features might then be identified using microscopy. In a similar vein, further work on suspended particles of different feldspars might be productive. For instance, it is possible to obtain alkali and plagioclase feldspars with known defect densities to test if greater defect densities lead to more efficient ice nucleation. Similarly, droplet freezing experiments on variously functionalised carbon surfaces would provide another interesting point of comparison, as long as the surfaces were sufficiently hydrophobic to support droplets. It may also be possible to characterise the sites that nucleate ice on carbon surfaces, assuming that such sites exist, in a similar fashion to that described above for feldspar thin sections. Similarly, it is possible to functionalise carbon nanomaterials in various ways (Georgakilas et al., 2012). This would alter hydrophilicity and might make it possible to better understand the relationship between hydrophilicity and ice nucleation efficiency.

While we have shown that the ice nucleation efficiency of certain feldspars (particularly Amelia Albite) can decrease drastically when left in water, the reason for the decay is not

known. It might be possible to relate the rate of decay to the rate at which the feldspars dissolve, and thereby determine why this discrepancy in behaviour between different feldspars occurs.

It seems very likely that features of the sort that enhance ice nucleation on feldspars will also impact ice nucleation by other nucleators. In *Chapter six* it was shown that chemically similar silica gel and quartz nucleate ice with different efficiencies and respond differently to the presence of solute molecules, indicating that they nucleate ice by different mechanisms. Examination of different polymorphs of SiO_2 may therefore prove to be a useful approach, particularly in combination with characterisation of surfaces via microscopy.

The solute effects discussed in *Chapter six* have the potential to provide much information about the mechanism of ice nucleation. As discussed, a starting point would be to work out which one of the three possible mechanisms (surface adsorption, absorption or interaction with the critical nucleus) is responsible for the effect. A possible experiment to help resolve this would involve freezing solution droplets on surfaces of nucleators or containing nucleator chips, as in *Chapter six.* If the enhancement persists when these droplets are removed (which may be practically difficult) then the effect can probably be attributed to either adsorption of solute molecules to the surface or absorption in the structure of the nucleator rather than an effect above the surface. Surface spectroscopy techniques may also help to improve understanding of the interaction and account for the differences in response to solutes observed with different nucleators (Anim-Danso et al., 2016). Given that ice nucleation by BCS 376 microcline is known to be site-specific (Herbert et al., 2014), and that the sites are probably nanoscale features associated with microtexture (*Chapter 5*), the solutes must interact with these sites to account for the effects observed. By combining surface spectroscopy with techniques for identifying specific sites mentioned above it may be possible to better resolve the nature of this interaction. Also, different combinations of solutes and nucleators should be examined, and the impact of concentration on the effects observed. Some ions, for instance Li^+, are known to be structure making in water (Marcus, 2009). By examining the impact of a range of structure making ions it may be possible to establish if the impacts of these differ from the impacts of the structure breaking ions we have investigated so far. If the reason for the split in response to solutes we have observed is general, it may be possible to use it as a diagnostic test for establishing what is causing ice nucleation in natural samples.

7.2.3. Final remarks

This project has shown that the relationship between physical and chemical properties of substances and ice nucleation efficiency is complex. While this project has shed light on possible reasons for this complexity, a great deal remains to be explained. One message that might be taken from this work is that the ice nucleating efficiency of substances is not necessarily closely associated with the classifications that are typically given to those substances. Clearly, it does not make sense to ascribe a single measurement of ice nucleating efficiency to all feldspars. It would probably be possible to prepare two feldspars of identical chemical composition, which could not be distinguished by powder X-ray diffraction, which would nevertheless nucleate ice with entirely different efficiencies. It seems likely that the same is true of other substances which have not been subjected to such detailed scrutiny. It is also likely that different nucleators nucleate ice in different ways; the solutes results in *Chapter six* hint at this. It may be that there is a relatively small number of overarching mechanisms, or it could be that every nucleator has its own particular mechanism. As such, complete understanding of ice nucleation by one nucleator or class of nucleators may not help improve understanding of other cases.

Overall, this project represents progress in the understanding of immersion mode heterogeneous ice nucleation. It is hoped that the project will lay groundwork for future experimental work that will reveal much more detail about specific features that nucleate ice, and the reasons for this. The discoveries that microtexture impacts immersion ice nucleation, and that solutes can have such profound influence on immersion mode ice nucleation provide potential routes for furthering understanding of the process.

References

Anim-Danso, E., Zhang, Y., and Dhinojwala, A.: Surface charge affects the structure of interfacial ice, J. Phys. Chem. C, 120, 3741-3748, 10.1021/acs.jpcc.5b08371, 2016.

Atkinson, J. D., Murray, B. J., Woodhouse, M. T., Whale, T. F., Baustian, K. J., Carslaw, K. S., Dobbie, S., O'Sullivan, D., and Malkin, T. L.: The importance of feldspar for ice nucleation by mineral dust in mixed-phase clouds, Nature, 498, 355-358, 10.1038/nature12278, 2013.

Bi, Y., Cabriolu, R., and Li, T.: Heterogeneous ice nucleation controlled by the coupling of surface crystallinity and surface hydrophilicity, J. Phys. Chem. C, 120, 1507-1514, 10.1021/acs.jpcc.5b09740, 2016.

Campbell, J. M., Meldrum, F. C., and Christenson, H. K.: Characterization of preferred crystal nucleation sites on mica surfaces, Cryst. Growth Des., 13, 1915-1925, 10.1021/cg301715n, 2013.

Fitzgerald, J. D., and Cayzer, N.: Nanotunnels and pull-aparts: Defects of exsolution lamellae in alkali feldspars, Am. Mineral., 91, 772-783, 2006.

Fitzner, M., Sosso, G. C., Cox, S. J., and Michaelides, A.: The many faces of heterogeneous ice nucleation: Interplay between surface morphology and hydrophobicity, J. Am. Chem. Soc., 137, 13658-13669, 10.1021/jacs.5b08748, 2015.

Fornea, A. P., Brooks, S. D., Dooley, J. B., and Saha, A.: Heterogeneous freezing of ice on atmospheric aerosols containing ash, soot, and soil, J. Geophys. Res.-Atmos., 114, D13201, 10.1029/2009jd011958, 2009.

Georgakilas, V., Otyepka, M., Bourlinos, A. B., Chandra, V., Kim, N., Kemp, K. C., Hobza, P., Zboril, R., and Kim, K. S.: Functionalization of graphene: Covalent and non-covalent approaches, derivatives and applications, Chem. Rev., 112, 6156-6214, 2012.

Gorbunov, B., Baklanov, A., Kakutkina, N., Windsor, H. L., and Toumi, R.: Ice nucleation on soot particles, J. Aerosol Sci., 32, 199-215, 10.1016/s0021-8502(00)00077-x, 2001.

Harrison, A. D., Whale, T. F., Carpenter, M. A., Holden, M. A., Neve, L., O'Sullivan, D., Vergara Temprado, J., and Murray, B. J.: Not all feldspar is equal: A survey of ice nucleating properties across the feldspar group of minerals, Atmos. Chem. Phys. Discuss., 2016, 1-26, 10.5194/acp-2016-136, 2016.

Herbert, R. J., Murray, B. J., Whale, T. F., Dobbie, S. J., and Atkinson, J. D.: Representing time-dependent freezing behaviour in immersion mode ice nucleation, Atmos. Chem. Phys., 14, 8501-8520, 10.5194/acp-14-8501-2014, 2014.

Hodson, M. E., Lee, M. R., and Parsons, I.: Origins of the surface roughness of unweathered alkali feldspar grains, Geochim. Cosmochim. Acta, 61, 3885-3896, 10.1016/s0016-7037(97)00197-x, 1997.

Lupi, L., Hudait, A., and Molinero, V.: Heterogeneous nucleation of ice on carbon surfaces, J. Am. Chem. Soc., 136, 3156-3164, 10.1021/ja411507a, 2014.

Lupi, L., and Molinero, V.: Does hydrophilicity of carbon particles improve their ice nucleation ability?, J. Phys. Chem. A, 118, 7330-7337, 10.1021/jp4118375, 2014.

Marcus, Y.: Effect of ions on the structure of water: Structure making and breaking, Chem. Rev., 109, 1346-1370, 10.1021/cr8003828, 2009.

Pruppacher, H. R., and Klett, J. D.: Microphysics of clouds and precipitation, 2nd ed., Kluwer Academic Publishers, 1997.

Reischel, M. T., and Vali, G.: Freezing nucleation in aqueous electrolytes, Tellus, 27, 414-427, 10.1111/j.2153-3490.1975.tb01692.x, 1975.

Whale, T. F., Murray, B. J., O'Sullivan, D., Wilson, T. W., Umo, N. S., Baustian, K. J., Atkinson, J. D., Workneh, D. A., and Morris, G. J.: A technique for quantifying heterogeneous ice nucleation in microlitre supercooled water droplets, Atmos. Meas. Tech., 8, 2437-2447, 10.5194/amt-8-2437-2015, 2015a.

Whale, T. F., Rosillo-Lopez, M., Murray, B. J., and Salzmann, C. G.: Ice nucleation properties of oxidized carbon nanomaterials, J. Phys. Chem. Lett., 3012-3016, 10.1021/acs.jpclett.5b01096, 2015b.

Zobrist, B., Marcolli, C., Peter, T., and Koop, T.: Heterogeneous ice nucleation in aqueous solutions: The role of water activity, J. Phys. Chem. A, 112, 3965-3975, 10.1021/jp7112208, 2008.